

Hyperfine structures and Landé g_J -factors for $n = 2$ states in beryllium-, boron-, carbon-, and nitrogen-like ions from relativistic configuration interaction calculations

S. Verdebout^a, C. Nazé^a, P. Jönsson^{b,*}, P. Rynkun^c, M. Godefroid^a, G. Gaigalas^c

^a*Chimie Quantique et Photophysique, CP160/09, Université Libre de Bruxelles, B 1050 Brussels, Belgium*

^b*Faculty of Technology and Society, Group for Materials Science and Applied Mathematics, Malmö University, 205-06 Malmö, Sweden*

^c*Institute of Theoretical Physics and Astronomy, Vilnius University, LT-01108 Vilnius, Lithuania*

Abstract

Energy levels, hyperfine interaction constants, and Landé g_J -factors are reported for $n = 2$ states in beryllium-, boron-, carbon-, and nitrogen-like ions from relativistic configuration interaction calculations. Valence, core-valence, and core-core correlation effects are taken into account through single and double-excitations from multireference expansions to increasing sets of active orbitals. A systematic comparison of the calculated hyperfine interaction constants is made with values from the available literature.

*Corresponding author.

Email address: per.jonsson@mah.se (P. Jönsson)

Contents

1. Introduction	3
2. Computational procedure	3
3. Computation of hyperfine structures and Landé g_J -factors	4
3.1. Hyperfine structure	4
3.2. Landé g_J -factor	6
4. Electron correlation effects on the hyperfine structure	6
5. Generation of configurations expansions	7
5.1. Boron-, carbon-, and nitrogen-like systems	7
5.2. Beryllium-like systems	8
6. Results and discussion	9
6.1. Beryllium-like systems	9
6.2. Boron-like systems	11
6.3. Carbon-like systems	12
6.4. Nitrogen-like systems	13
References	14
Explanation of Tables	17
Tables	
1. Total energies (in E_h), excitation energies (in cm^{-1}), hyperfine magnetic dipole constants $A_J(I/\mu_I)$ (MHz per unit of μ_N), electric quadrupole constants B_J/Q (MHz/barn), and Landé g_J -factors for levels in the beryllium isoelectronic sequence ($5 \leq Z \leq 74$). For each of the many-electron wave functions, the leading components are given in the LSJ coupling scheme. The number in square brackets is the power of 10. See page 17 for Explanation of Tables.	19
2. Total energies (in E_h), excitation energies (in cm^{-1}), hyperfine magnetic dipole constants $A_J(I/\mu_I)$ (MHz per unit of μ_N), electric quadrupole constants B_J/Q (MHz/barn), and Landé g_J -factors for levels in the boron isoelectronic sequence ($8 \leq Z \leq 30$ and $Z = 36, 42$). For each of the many-electron wave functions, the leading components are given in the LSJ coupling scheme. The number in square brackets is the power of 10. See page 17 for Explanation of Tables.	28
3. Total energies (in E_h), excitation energies (in cm^{-1}), hyperfine magnetic dipole constants $A_J(I/\mu_I)$ (MHz per unit of μ_N), electric quadrupole constants B_J/Q (MHz/barn), and Landé g_J -factors for levels in the carbon isoelectronic sequence ($7 \leq Z \leq 28$). For each of the many-electron wave functions, the leading components are given in the LSJ coupling scheme. The number in square brackets is the power of 10. See page 18 for Explanation of Tables.	36
4. Total energies (in E_h), excitation energies (in cm^{-1}), hyperfine magnetic dipole constants $A_J(I/\mu_I)$ (MHz per unit of μ_N), electric quadrupole constants B_J/Q (MHz/barn), and Landé g_J -factors for levels in the nitrogen isoelectronic sequence ($7 \leq Z \leq 36$ and $Z = 42, 74$). For each of the many-electron wave functions, the leading components are given in the LSJ coupling scheme. The number in square brackets is the power of 10. See page 18 for Explanation of Tables.	43

1. Introduction

The hyperfine interaction, i.e. the interaction between the electrons and the non-spherical part of the electromagnetic field produced by the nucleus, is important in a number of applications. The hyperfine interaction breaks the J symmetry of the atom and may open forbidden transitions that can be used for diagnostic purposes in plasmas [1, 2]. Combined with accurate measurements of hyperfine structure splittings, calculated atomic parameters can be used to extract nuclear quadrupole moments Q [3]. In a different setting the hyperfine interaction is a key factor in determining excited state nuclear g -factors from recoil-in-vacuum experiments [4]. Hyperfine interaction is also important in astrophysics, high resolution solar, stellar spectra reveal isotope shifts and hyperfine structures of many spectral lines. To correctly interpret the spectra it is necessary to include isotope shifts and hyperfine structures in a theoretical modeling of the line profiles [5, 6]. Hyperfine interaction is also of theoretical interest and is a valuable and sensitive probe of both electron correlation and QED effects [7–9].

Strong magnetic fields have been detected in hot stars of types O, B, and A. Investigations of these magnetic fields require knowledge of accurate Landé g_J -factors [10]. There is also a need for data to support polarization measurements of the coronal magnetic field [11]. Some experimental g_J -factors have been published in successive NIST compilations, but data for many levels are still lacking. From a more theoretical point of view Landé g_J -factors give valuable information about coupling conditions in atomic systems, and they can also be used to identify and label states [12].

A number of computer codes have modules for computing hyperfine structures and Landé g_J -factors, e.g. CIV3 [13], MCHF [14], ATSP2K [15]. The former codes are non-relativistic with relativistic corrections in the Breit-Pauli approximation. Hyperfine interaction is an inner property and is very sensitive to relativistic effects [16]. For this reason the calculations in this work rely instead on the fully relativistic GRASP2K code [17, 18], which has modules both for hyperfine structure [19] and Landé g_J -factors [20]. The purpose of the present work is to complement the data sets on the isotope shift electronic factors [21] along the beryllium, boron, carbon, and nitrogen isoelectronic sequences with hyperfine interaction constants and Landé g_J -factors. The values should also serve as reference for other theoretical work.

2. Computational procedure

The GRASP2K package is based on the well-established multiconfiguration Dirac-Hartree-Fock (MCDHF) method [22]. Here the atomic state functions (ASFs), describing the studied fine-structure states, are obtained as linear combinations of symmetry adapted configuration state functions (CSFs)

$$|\gamma PJM_J\rangle = \sum_{j=1}^{N_{CSFs}} c_j |\gamma_j PJM_J\rangle. \quad (1)$$

In the above expression P , J , and M_J are the parity and the angular quantum numbers, respectively. The γ symbol denotes all the other appropriate labeling of the configuration state function, such as the orbital occupancy and the coupling scheme. The configuration state functions are built from products of one-electron Dirac orbitals

$$|n\kappa m\rangle = \frac{1}{r} \begin{pmatrix} P(n\kappa; r)\chi_{\kappa m}(\Omega) \\ iQ(n\kappa; r)\chi_{-\kappa m}(\Omega) \end{pmatrix}, \quad (2)$$

where we introduce the single electron quantum numbers n and κ . Requiring the energy functional of the ASF with respect to the Dirac-Coulomb N -electron Hamiltonian

$$H_{\text{DC}} = \sum_{i=1}^N (c \boldsymbol{\alpha}_i \cdot \mathbf{p}_i + (\beta_i - 1)c^2 + V_i^N) + \sum_{i < j}^N \frac{1}{r_{ij}}, \quad (3)$$

to be stationary with respect to perturbations in the expansion coefficients $\{c_j\}$ in the multiconfiguration expansion leads to a matrix eigenvalue problem. The stationary condition with respect to variations in the radial functions, in turn, leads to a system of coupled integro-differential equations subject to boundary conditions at the origin and the infinity [22]. In the relativistic self-consistent field (RSCF) procedure both these problems are solved to self-consistency. Having a set of radial functions $\{P(n\kappa; r), Q(n\kappa; r)\}$, it is possible to find the expansion coefficients $\{c_j\}$ by solving the related matrix eigenvalue problem. At this relativistic configuration interaction (RCI) level, higher order terms can be added to the Dirac-Coulomb Hamiltonian (3). Normally the Breit interaction operator

$$H_{\text{Breit}} = - \sum_{i < j}^N \left[\boldsymbol{\alpha}_i \cdot \boldsymbol{\alpha}_j \frac{\cos(\omega_{ij} r_{ij}/c)}{r_{ij}} + (\boldsymbol{\alpha}_i \cdot \boldsymbol{\nabla}_i)(\boldsymbol{\alpha}_j \cdot \boldsymbol{\nabla}_j) \frac{\cos(\omega_{ij} r_{ij}/c) - 1}{\omega_{ij}^2 r_{ij}/c^2} \right] \quad (4)$$

as well as leading quantum electrodynamic (QED) corrections, self-energy and vacuum polarization, are included [23].

Calculations can be done for single states, but also for portions of a spectrum in the extended optimal level (EOL) scheme, where optimization is on a weighted sum of energies [24]. Using the latter scheme a balanced description of a number of fine-structure states belonging to one or more configurations can be obtained in a single calculation. All calculations were performed with the new release [18] of the GRASP2K code [17].

3. Computation of hyperfine structures and Landé g_J -factors

Once the ASFs have been obtained, measurable properties such as hyperfine structures and Landé g_J -factors can be expressed in terms of reduced matrix elements of spherical tensor operators $\mathbf{T}^{(k)}$ of different rank k ,

$$\langle \gamma P J || \mathbf{T}^{(k)} || \gamma' P' J' \rangle. \quad (5)$$

Inserting the CSF expansions, the matrix element above splits into a sum over reduced matrix elements between CSFs. Using Racah algebra techniques, these matrix elements, in turn, can be obtained as weighted sums over radial integrals where the weights are obtained from the angular integration [25].

3.1. Hyperfine structure

The hyperfine interaction is due to the interaction between the electrons and the non-spherical part of the electromagnetic field produced by the nucleus. The corresponding contribution to the Hamiltonian can be written as a multipole expansion

$$H_{\text{hfs}} = \sum_{k \geq 1} \mathbf{T}^{(k)} \cdot \mathbf{M}^{(k)}, \quad (6)$$

where $\mathbf{T}^{(k)}$ and $\mathbf{M}^{(k)}$ are spherical tensor operators of rank k in the electronic- and nuclear-spaces, respectively [26]. The terms with $k = 1$ and $k = 2$ are, respectively, the magnetic dipole and the electric quadrupole parts of the hyperfine

interaction. Explicit forms of the electronic operators can be found in [19]. Higher order terms are much smaller and can often be neglected. By looking at (6), it comes naturally that this operator does not commute neither with the total angular momentum of the electrons \mathbf{J} nor with the total angular momentum of the nucleus \mathbf{I} , but with the total atomic angular momentum $\mathbf{F}=\mathbf{I}+\mathbf{J}$. Denoting the nuclear wave function by $|\kappa\pi IM_I\rangle$, where π , I and M_I are, respectively, the parity, the total angular momentum and its projection, the coupled states are expressed as

$$|\kappa\gamma\pi PIJFM_F\rangle = \sum_{M_I, M_J} \langle IJM_IM_J|FM_F\rangle |\kappa\pi IM_I\rangle |\gamma PJM_J\rangle . \quad (7)$$

In first-order perturbation theory the fine-structure levels J are split into closely spaced hyperfine levels F in atoms with non-zero nuclear spin I according to

$$\langle\kappa\gamma\pi PIJFM_F|\mathbf{T}^{(1)} \cdot \mathbf{M}^{(1)} + \mathbf{T}^{(2)} \cdot \mathbf{M}^{(2)}|\kappa\gamma\pi PIJFM_F\rangle , \quad (8)$$

which corresponds to the diagonal hyperfine effect. Expressing the magnetic dipole ($k=1$) and the electric quadrupole ($k=2$) contributions in terms of the reduced electronic and nuclear matrix elements, we get

$$\begin{aligned} \langle\kappa\gamma\pi PIJFM_F|\mathbf{T}^{(1)} \cdot \mathbf{M}^{(1)}|\kappa\gamma\pi PIJFM_F\rangle &= (-1)^{I+J+F} \left\{ \begin{array}{ccc} I & J & F \\ J & I & 1 \end{array} \right\} \sqrt{2J+1} \sqrt{2I+1} \\ &\quad \langle\gamma PJ||\mathbf{T}^{(1)}||\gamma PJ\rangle \langle\kappa\pi I||\mathbf{M}^{(1)}||\kappa\pi I\rangle \end{aligned} \quad (9)$$

$$\begin{aligned} \langle\kappa\gamma\pi PIJFM_F|\mathbf{T}^{(2)} \cdot \mathbf{M}^{(2)}|\kappa\gamma\pi PIJFM_F\rangle &= (-1)^{I+J+F} \left\{ \begin{array}{ccc} I & J & F \\ J & I & 2 \end{array} \right\} \sqrt{2J+1} \sqrt{2I+1} \\ &\quad \langle\gamma PJ||\mathbf{T}^{(2)}||\gamma PJ\rangle \langle\kappa\pi I||\mathbf{M}^{(2)}||\kappa\pi I\rangle . \end{aligned} \quad (10)$$

Using the conventional definition of the nuclear magnetic dipole moment μ_I and the nuclear electric quadrupole moment Q , we define hyperfine interaction constants that are not depending on the F quantum numbers

$$A_J = \frac{\mu_I}{I} \frac{1}{\sqrt{J(J+1)}} \langle\gamma PJ||\mathbf{T}^{(1)}||\gamma PJ\rangle \quad (11)$$

$$B_J = 2Q \sqrt{\frac{J(2J-1)}{(J+1)(2J+3)}} \langle\gamma PJ||\mathbf{T}^{(2)}||\gamma PJ\rangle . \quad (12)$$

The hyperfine energies are then given by

$$E_{\text{hfs}}(\gamma JF) = \frac{1}{2} A_J C + B_J \frac{\frac{3}{4}C(C+1) - I(I+1)J(J+1)}{2I(2I-1)J(2J-1)} , \quad (13)$$

where $C = F(F+1) - J(J+1) - I(I+1)$.

The hyperfine interaction constants were evaluated using the hyperfine module of GRASP2K [18]. Angular data needed for the integration were saved on computer disc to reduce computational time for the full isoelectronic sequences. To allow an easy use of the provided results we have set the nuclear parameters to 1, i.e. $I = \mu_I = Q = 1$. The reader may simply multiply the tabulated values of $A_J(I/\mu_I)$ and B_J/Q by the factors μ_I/I and Q , respectively, to get the hyperfine interaction constants for the specific isotope of interest. The nuclear quantities have been tabulated by Stone [27].

3.2. Landé g_J -factor

This work also provides the Landé g_J -factors of the considered levels all along the isoelectronic sequences. The Landé g_J -factor is given by

$$g_J = \frac{2}{\sqrt{J(J+1)}} \langle \gamma P J | \sum_{j=1}^N \left[-i \frac{\sqrt{2}}{2\alpha^2} r_j (\boldsymbol{\alpha}_j \mathbf{C}_j^{(1)})^{(1)} + \frac{g_s - 2}{2} \beta_j \boldsymbol{\Sigma}_j \right] | \gamma P J \rangle , \quad (14)$$

where $i = \sqrt{-1}$ is the imaginary unit, $\boldsymbol{\Sigma}$ the relativistic spin-matrix, and $g_s = 2.00232$ the g -factor of the electron spin corrected for QED effects. The Landé g_J -factor determines the splitting of magnetic sub-levels in an external magnetic field [28]. In addition it gives valuable information about the coupling conditions in the system [12]. In the case of a pure LSJ coupling scheme, the Landé factor is equal to 1 for singlet terms ($S = 0$), equal to 2.00232 for S states ($L = 0$) and equal to 1.5012 for terms with $L = S$. The development of the transformation between the jj and LSJ coupling schemes [29, 30], however, provides more complete information.

The Landé g_J -factors were evaluated using the hyperfine module of GRASP2K [18]. For a complete write-up of the module see [20].

4. Electron correlation effects on the hyperfine structure

The hyperfine structure is sensitive to different electron correlation effects. These effects need to be analyzed in order to assess the accuracy of the computed hyperfine structure constants in this work. In the Dirac-Fock approximation the charge distribution within a closed subshell is spherically symmetric, and the contribution to the magnetic dipole and electric quadrupole interaction constants is zero. The contribution from a closed s subshell is also zero, since the spin-densities from the two electrons are equal and the spin directions opposite. Polarization of closed subshells in the core, due to the Coulomb interaction with open subshells, may have large effects on the hyperfine interaction constants. The Coulomb exchange interaction reduces the repulsion between core and valence electrons with the same spin orientation, pulling the core electron towards the valence subshell. Especially spin polarization is important. If the two s -electrons in the same subshell have different spin-densities a magnetic hyperfine interaction, which in the non-relativistic limit is referred to as the contact interaction, is induced [31, 32]. As inner s -electrons have high densities at the nucleus, a very small imbalance is sufficient to cause a net interaction, which is comparable to that of an open valence subshell. In addition to the spin polarization there is the orbital polarization, which is the distortion of the charge distribution of the core. The orbital polarization leads to contributions to the parts of the magnetic hyperfine interaction that in the non-relativistic limit are referred to as the orbital- and spin-dipolar interactions [31]. In addition there is an important contribution also to the electric quadrupole interaction.

In the MCDHF approach polarization effects are accounted for by including, in the wave function expansion, CSFs obtained by single excitations from the Dirac-Hartree-Fock reference configuration followed by a change in spin- and orbital coupling [31, 32]. The CSFs that describe polarization effects are however energetically unimportant, and a large energy optimized orbital basis is needed to converge the contributions [32]. Although not used in the present work, non-orthogonal orbitals, specifically targeted for describing polarization effects, drastically improve convergence [33]. In addition to being affected by polarization effects, hyperfine structures are known to be sensitive also to higher order-correlation effects.

The importance of correlation effects are enhanced in cases where there are strong cancellations or when the interaction is zero in the Hartree-Fock (HF) or Dirac-Hartree-Fock (DHF) approximation. As an example, relevant for the present study, we may look at $1s^2 2s^2 2p\ ^2P$ in B-like ions. For these states there are large, but canceling, contributions from the spin-polarization of the $1s$ and $2s$ subshells. Using only energy optimized orbitals, the convergence of the magnetic contact interaction is slow and oscillatory [34]. The cancellation also makes the contact interaction sensitive to higher-order correlation effects. Another very difficult case is $1s^2 2s^2 2p^2\ ^3P_1$ in C-like ions. Here the A_J constant is close to zero in the DHF approximation due to an almost perfect cancellation between the large orbital- and spin-dipole interaction constants. The contact interaction is zero. The introduction of polarization and correlation effects induces a contact interaction and changes the degree of cancellation between the orbital- and spin-dipole interaction constants, making calculations extremely challenging [34]. Among the studied states in this work there are several with half-filled $2p$ subshells, yielding B_J constants that are zero at the non-relativistic HF level. Since the full interaction contribution comes from correlation effects, these B_J constants are also very challenging to compute. Comparatively small relativistic effects, coupling different LS terms, may also be of importance [35, 36]. Thus, even at the low- Z limit, a comparison between non-relativistic calculations and relativistic calculations may not be meaningful.

5. Generation of configurations expansions

MCDHF and RCI calculations can be performed for single levels, but also for portions of a spectrum. In this work calculations were carried out by parity and configuration, that is, wave functions for all states belonging to a specific configuration were determined simultaneously in an EOL calculation [24]. The EOL scheme has shown to be surprisingly efficient, and a balanced description of a large number of fine-structure states, belonging to one or more configurations, can be obtained in a single calculation [37, 38]. The expansions for the ASFs were obtained using the active set method [39]. Here CSFs of a specified parity and J -symmetry are generated by excitations from a number of reference configurations to a set of relativistic orbitals. By applying restrictions on the allowed excitations, different electron correlation effects can be targeted. To monitor the convergence of the calculated energies and the physical quantities of interest, the active sets are increased in a systematic way by progressively adding layers of correlation orbitals. The configuration expansions strategies for the different ions, outlined in our previous work on isotope shifts [21] and included in the subsections below for the sake of completeness, were aimed at generating wave functions with high overall quality, yielding accurate values for a number of expectation values such as energies, transition rates, and isotope shifts. Thus no special efforts were made to target electron correlation effects close to the nucleus by using, for example, separately optimized orbitals accounting specifically for polarization effects [32].

5.1. Boron-, carbon-, and nitrogen-like systems

The starting point was a number of MCDHF calculations, where the CSF expansions for the states belonging to a configuration were obtained by single and double (SD) excitations from a multireference (MR) consisting of the set of configurations that can be formed by the same principal quantum numbers as the studied configuration, to an increasing active set of orbitals. The MCDHF calculations were followed by RCI calculations including the Breit interaction and leading QED. The CSF expansions for the RCI calculations were obtained by SD-excitations from a larger MR, including the most important configurations outside the complex, to the largest active set of orbitals. The correlation models used

Table A

Generated CSF expansions for the MCDHF and RCI calculations for the boron-, carbon-, and nitrogen-like ions.

Configuration	MR for MCDHF	MR for RCI	Active set	N_{CSFs} in RCI
boron-like				
$1s^2 2s^2 2p$	$1s^2 \{2s^2 2p, 2p^3\}$	$1s^2 \{2s^2 2p, 2p^3, 2s2p3d, 2p3d^2\}$	$\{9s8p7d6f5g3h1i\}$	200 100
$1s^2 2p^3$	$1s^2 \{2s^2 2p, 2p^3\}$	$1s^2 \{2s^2 2p, 2p^3, 2s2p3d, 2p3d^2\}$	$\{9s8p7d6f5g3h1i\}$	360 100
$1s^2 2s2p^2$	$1s^2 2s2p^2$	$1s^2 \{2s2p^2, 2p^2 3d, 2s^2 3d, 2s3d^2\}$	$\{9s8p7d6f5g3h1i\}$	300 100
carbon-like				
$1s^2 2s^2 2p^2$	$1s^2 \{2s^2 2p^2, 2p^4\}$	$1s^2 \{2s^2 2p^2, 2p^4, 2s2p^2 3d, 2s^2 3d^2\}$	$\{8s7p6d5f4g2h\}$	340 100
$1s^2 2p^4$	$1s^2 \{2s^2 2p^2, 2p^4\}$	$1s^2 \{2s^2 2p^2, 2p^4, 2s2p^2 3d, 2s^2 3d^2\}$	$\{8s7p6d5f4g2h\}$	340 100
$1s^2 2s2p^3$	$1s^2 2s2p^3$	$1s^2 \{2s2p^3, 2p^3 3d, 2s^2 2p3d, 2s2p3d^2\}$	$\{8s7p6d5f4g2h\}$	1 000 100
nitrogen-like				
$1s^2 2s^2 2p^3$	$1s^2 \{2s^2 2p^3, 2p^5\}$	$1s^2 \{2s^2 2p^3, 2p^5, 2s2p^3 3d, 2s^2 2p3d^2\}$	$\{8s7p6d5f4g1h\}$	698 100
$1s^2 2p^5$	$1s^2 \{2s^2 2p^3, 2p^5\}$	$1s^2 \{2s^2 2p^3, 2p^5, 2s2p^3 3d, 2s^2 2p3d^2\}$	$\{8s7p6d5f4g1h\}$	382 100
$1s^2 2s2p^4$	$1s^2 2s2p^4$	$1s^2 \{2s2p^4, 2p^4 3d, 2s^2 2p^2 3d, 2s2p^2 3d^2\}$	$\{8s7p6d5f4g1h\}$	680 100

for the boron-, carbon-, and nitrogen-like ions are summarized in Table A. The reference configuration is shown on the left. Columns two and three display the MR for, respectively, the MCDHF and RCI expansions. The largest active set is shown in column four, where the number of orbitals for each l -angular symmetry is specified. The last column gives the number of CSFs for the RCI calculations. The described computational strategy has previously been used by Rynkun *et al.* [40–42] to compute energies and transition rates, and more details can be found in these papers.

5.2. Beryllium-like systems

The beryllium-like systems are a little different. For each parity, the wave functions for all states belonging to the $1s^2 2s^2$ and $1s^2 2p^2$ even configurations, and to the $1s^2 2s2p$ odd configuration, were determined simultaneously. For the MCDHF calculations, the CSF expansions were obtained by merging CSFs generated by SD-excitations from the reference configurations to an increasing active set with CSFs obtained by single, double, triple, and quadruple (SDTQ) excitations to a subset of the active set of orbitals. The largest active set consisted of orbitals with principal quantum numbers $n \leq 8$ and the subset was formed by orbitals with principal quantum numbers $n \leq 4$. The MCDHF calculations were followed by RCI calculations including the Breit interaction and leading QED. The expansions for the RCI calculations were obtained by merging CSFs generated by SDTQ-excitations from the reference configurations to the largest active set with the restriction that there in each CSF is at least two orbitals with $n \leq 3$ with CSFs generated by SDTQ-excitations from the reference configurations to the active set of orbitals with principal quantum numbers $n \leq 4$. The RCI expansions included about 296 000 relativistic CSFs.

6. Results and discussion

All the results of our calculations are presented in the tables 1, 4, 8, and 10 for beryllium-, boron-, carbon-, and nitrogen-like systems, respectively. In the following subsections, the results of the calculations are presented for the four isoelectronic sequences, and compared with values from the literature when available. The identification of the levels is based on the LS composition obtained by transforming from jj - to LSJ -coupling schemes using the JJ2LSJ tool integrated in the new release of GRASP2K [18]. The two first CSFs with weight $|c_j|^2 \geq 0.1\%$ are also displayed in the level compositions.

6.1. Beryllium-like systems

Table 1 displays total energies, excitation energies, hyperfine magnetic dipole constants $A_J(I/\mu_I)$, electric quadrupole constants B_J/Q , and Landé g_J -factors. The reported isoelectronic sequence covers nuclear charges from $Z = 5$ to $Z = 74$. We investigate, for each nuclear charge, the six states $1s^22p^2\ ^1D_2$, $1s^22p^2\ ^3P_{1,2}$, $1s^22s2p\ ^1P_1^o$, and $1s^22s2p\ ^3P_{1,2}^o$, which are the lowest ones having hyperfine structures. One may note the interesting evolution along the sequence of the LSJ composition of each state. At low Z values, the states are quite pure and present almost no term mixing, but for high Z values the spin-orbit interaction increases and term mixing appears.

Table 2 presents the comparison between values from the present work and the data provided by Litzén *et al.* [43] for B II. This table brings to light the very good agreement that exists between these two theoretical works. The agreement is slightly better for the magnetic dipole constants than for the electric quadrupole constants. This is due to the more oscillating and slowly convergent behavior of the latter with respect to the increasing set of active orbitals [44]. Note that we had to scale the data provided by Litzén *et al.* [43] ($I = 1$, $\mu_I = 1\mu_N$ and $Q = 1$ barn) for allowing the comparison with our “normalized” hyperfine constants.

As quoted by Johnson [45], Be-like systems are the most studied systems beyond the He isoelectronic sequence for the study of hyperfine quenching. Systematic theoretical calculations of hyperfine interaction constants along this sequence have been performed by Marques *et al.* [46], and Cheng *et al.* [47]. Table 3 compares our results with the ones obtained by Marques *et al.* [46] and Cheng *et al.* [47]. The work by Marques *et al.* evaluates energies and wave functions using the MCDHF method, including corrections for the Breit interaction and for the leading QED terms. As it has been pointed out by Cheng *et al.* [47], some effects, as the correlation effects, are not enough considered, due to limited computational resources, in the pioneering calculations by Marques *et al.* [46]. The work by Cheng *et al.* uses the RCI method for evaluating energy levels and hyperfine matrix elements. We use the reported reduced matrix elements ($T(a,b) = \langle a || T^{(1)} || b \rangle$) associated with the magnetic dipole interaction, for computing the A_J constants that are reported in table 3. The latter table shows that there is an almost perfect agreement between our values and the ones provided by Cheng *et al.* [47]. Due the very good agreement that Cheng *et al.* [47] gets with the experiment, we are therefore very confident in the values that we provide for this isoelectronic sequence.

It is often interesting to investigate atomic properties along an isoelectronic sequence to check their expected smoothness in the trend or possibly detect some anomaly in the calculation for a given ion, or to point out some problem in the level assignment. Figures 1, 2 and 3 present, respectively, the evolution of $A(I/\mu_I)$, B/Q and Landé g_J -factor along the beryllium isoelectronic sequence ($5 \leq Z \leq 74$) for a few chosen states. Other figures of isoelectronic evolution for all states are available on demand from the corresponding author.

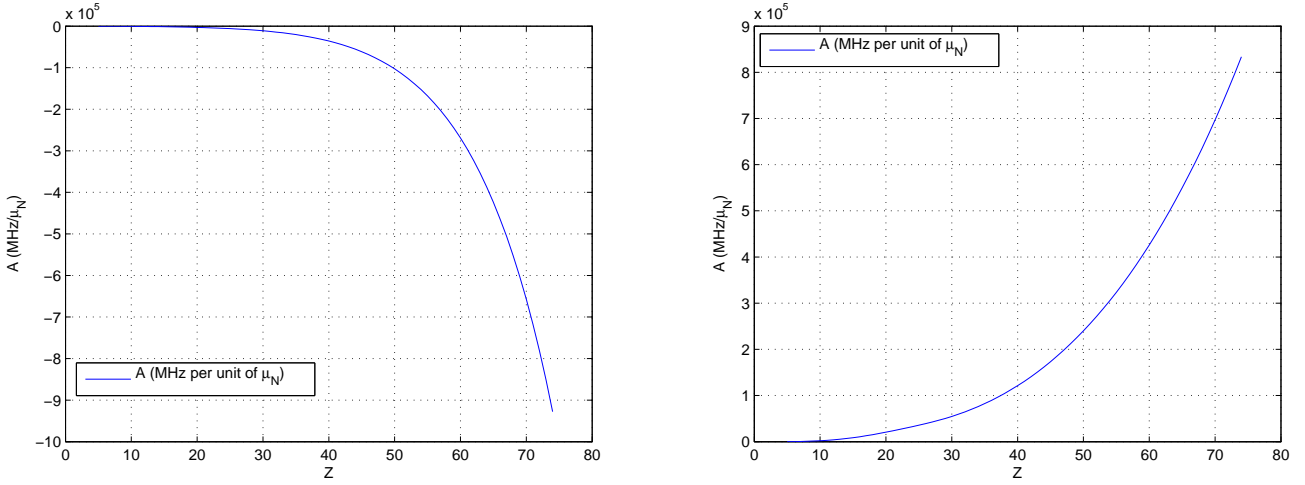


Fig. 1: Evolution along the beryllium isoelectronic sequence ($5 \leq Z \leq 74$) of the hyperfine constants $A(I/\mu_I)$ for : (on left side) the third root characterized by $J = 1$. (on right side) the third root characterized by $J = 2$. They present, respectively, a $1s^22p^2\ 3P_1$ and a $1s^22p^2\ 1D_2$ dominant character all along the sequence.

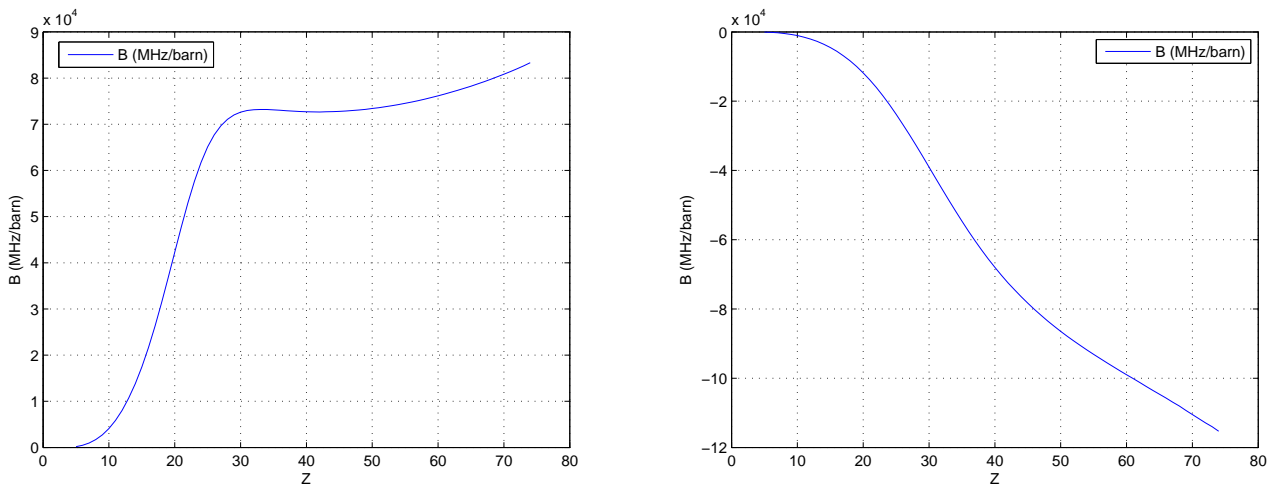


Fig. 2: Evolution along the beryllium isoelectronic sequence ($5 \leq Z \leq 74$) of the hyperfine constants B/Q for : (left side) the third root characterized by $J = 2$. (right side) the first root characterized by $J = 1$. They present, respectively, a $1s^22p^2\ 1D_2$ and a $1s^22s2p\ 3P_1^o$ dominant character all along the sequence.

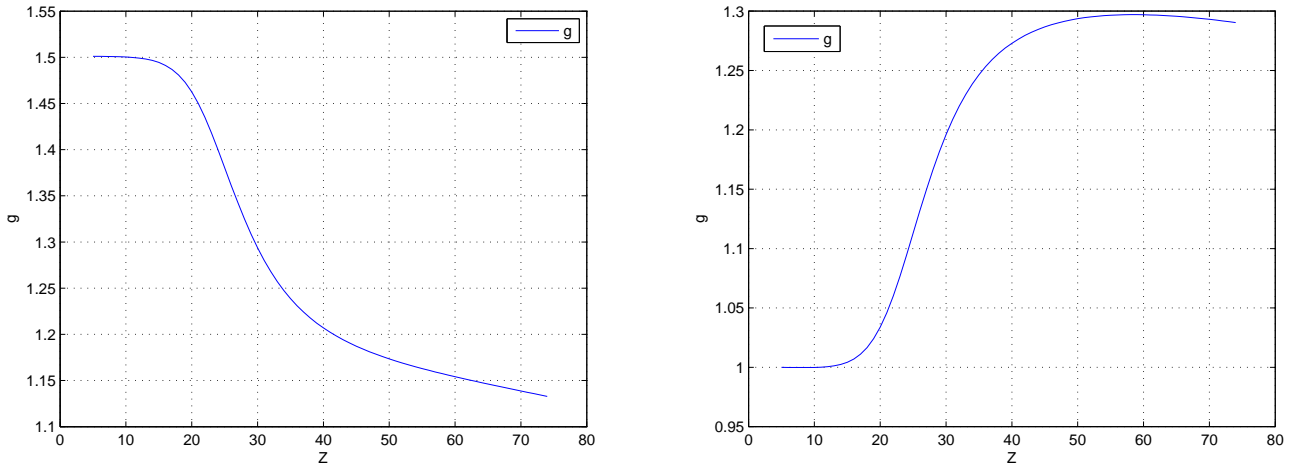


Fig. 3: Evolution along the beryllium isoelectronic sequence ($5 \leq Z \leq 74$) of the Landé g_J -factor for : (left side) the second root characterized by $J = 2$. (right side) the third root characterized by $J = 2$. They present, respectively, a $1s^2 2p^2 3P_2$ and a $1s^2 2p^2 1D_2$ dominant character all along the sequence.

6.2. Boron-like systems

Table 4 displays total energies, transition energies, hyperfine interaction constants, and Landé g_J -factors along the boron isoelectronic sequence. Once again, it is quite interesting to observe the rising of the spin-orbit interaction with increasing nuclear charge. The resulting term mixing becomes so important that for the molybdenum (Mo) ion, the dominant contributor, and then the dominant character, of two different states is the $1s^2 2p^3 2P_{3/2}^o$ CSF. Recently, the O IV ion has been studied by Dutta and Majumber [48] with the relativistic coupled-cluster method, Jönsson *et al.* [49], with the multiconfiguration Dirac-Hartree-Fock method, and Sun *et al.* [50] using Rayleigh-Ritz variation method with configuration interaction. Table 5 compares the results of these calculations with the ones obtained in this work. For the $1s^2 2s^2 2p^2 P_{1/2,3/2}^o$ states, the multiconfiguration works agree very well, but differ slightly with the values obtained by Dutta and Majumber. As for the states $1s^2 2s^2 2p^2 4P_{1/2,3/2,5/2}$, the electric quadrupole constants B_J fit well with both Sun *et al.* [50] and Jönsson *et al.* [49]. On the other hand, the present magnetic dipole A_J values agree with the values of Jönsson *et al.*, but differ by around 2% with the values given by from Sun *et al.*. Dutta and Majumber studied other ions along the B-like isoelectronic sequence up to $Z = 21$. The third and fourth columns of table 6 give the magnetic dipole constant $A_J(I/\mu_I)$ in MHz per units of μ_N , for the calculations of Dutta and Majumber and ours, respectively. Strangely enough, the values of the $^2P_{1/2}$ states agree within $\sim 0.5\%$ while the values of the states $^2P_{3/2}$ agree only within 4% or 5%. To discriminate between the different calculations, and to further validate the present results, we performed large scale multiconfiguration Hartree-Fock (MCHF) calculations for the states in O IV. The MCHF calculations are fully variational and the expansions obtained by SD-excitations from large MR sets to an active set of orbitals with $nl \leq 9h$. The MCHF results were relativistically corrected by scaling the interaction constants with the ratio of DHF and HF values. Results from the independent MCHF calculation are compared with the RCI values in table 7. The two different calculations give values of A_J that are in excellent agreement (to within less than 0.02 % for the magnetic dipole constant). Based on this we can say that the present RCI calculations give very accurate values of the magnetic hyperfine interaction constants A_J and, furthermore, that these values are more accurate than the values from the calculations by

Dutta and Majumber [48] and by Sun *et al.* [50]. Comparing the B_J constants from the MCHF and RCI calculations we see that there are large differences for the $1s^22p^3\ ^2D_{3/2}$ and $1s^22p^3\ ^2P_{3/2}$ states. The B_J constants for these two states are zero at the HF level, making correlation and relativistic effects comparatively more important. For the two states above the difference between the B_J constants from the RCI and MCHF calculations is due to the fact that the MCHF calculations do not include the LS term mixing. The values from the RCI calculations are more accurate and the preferred ones.

6.3. Carbon-like systems

Table 8 presents the total and transition energies, the hyperfine interaction constants, the Landé g_J factors, and the leading components of the many-electron wave function within the LSJ coupling scheme.

The reader should observe the slow drift, along the sequence, from a quite pure LSJ -coupling scheme (for low Z value) to a jj coupling scheme for the highly charged ions. This evolution along the isoelectronic sequence of the $1s^22s2p^3\ ^3S_1^o$ state is illustrated by figure 4. It is quite interesting to note the progressive decreasing of the g_J factor when the nuclear charge increase. This behavior is explained by having a look at the second contributor in the LSJ composition, i.e. $1s^22s2p^3\ ^1P_1^o$, which increases in importance for higher nuclear charges.

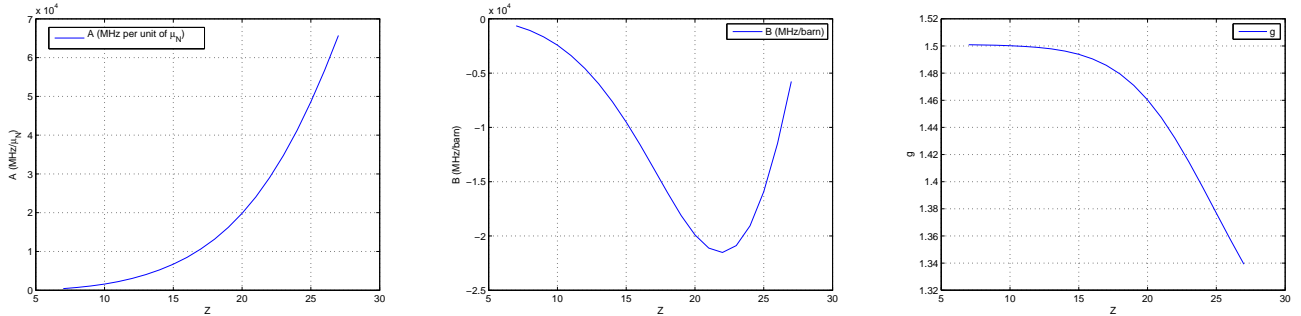


Fig. 4: Evolution along the carbon isoelectronic sequence of the hyperfine constants A (left), B (middle), and the Landé g_J -factor (right) for the fourth root characterized by a $J = 1$ total quantum number. This state presents a $1s^22s2p^3\ ^3S_1^o$ dominant character all along the sequence

Jönsson and Bieroń [51] used the relativistic configuration interaction method to obtain energy levels, transition rates, hyperfine structure parameters and Landé g_J -factors for low-lying states in N II, O III, F IV, Ne V and Ti XVII. Their values are not reported in this work, since they also used the GRASP2K package to build them. The small relative differences compared with the present work, about 0.03% and 0.3% for, respectively, the A_J and B_J constants in Ti XVII, come from differences in CSFs expansions and optimization strategies. To validate the hyperfine interaction constants from current RCI calculations we performed independent MCHF calculations for O III. Again, the MCHF calculations were fully variational, and the expansions were obtained by SD-excitations from large MR sets to an active set of orbitals with $nl \leq 9h$. The MCHF results were relativistically corrected by scaling the interaction constants with the ratio of DHF and HF values. The A_J and B_J constants are compared in table 9. For all A_J constants, except the one for the $1s^22s2p^2\ ^3P_1$ state, there is a very good agreement between the RCI and MCHF calculations. The constants for $1s^22s2p^2\ ^3P_1$ disagree with a factor of 2. This disagreement is due to a combination of severe cancellation effects, as discussed in section 4. In this case the A_J constant from the MCHF calculation, that includes more correlation, is

believed to be the more accurate. As Z increases, electron correlation decrease in importance and the A_J constant for the $1s^22s^22p^2\ ^3P_1$ state from the RCI calculations gradually becomes more accurate. There are also very large differences between the B_J constants based on RCI and MCHF for the states belonging to the $1s^22s2p^3$ configuration. Due to the half filled $2p$ subshell the B_J constants are all zero at the HF level, making them sensitive to both polarization and higher order correlation effects as well as effects from relativistic mixing of states belonging to different LS terms. Based on the fact that there is a good agreement between the two calculations for $1s^22s2p^3\ ^3D_3^o$, which is not affected by the LS mixing, we draw the conclusion that the correlation effects have been reasonably captured in both the RCI and MCHF calculations. The differences for the other states are thus due to neglected relativistic LS mixing in the MCHF calculations. To conclude, B_J constants for states belonging to the $1s^22s2p^3$ configuration are less accurate than the corresponding A_J constants due to the fact that the HF values are zero, making correlation and relativistic effects comparatively more important. The B_J values from the RCI calculations are the more accurate ones.

6.4. Nitrogen-like systems

Table 10 presents the total and transition energies, the hyperfine interaction constants, the Landé g_J -factors, and the leading components of the many-electron wave function within the LSJ coupling scheme. All figures of isoelectronic evolution for all states are available on demand from the corresponding author.

In Table 11 the hyperfine interaction constants from the RCI calculations are compared with constants from large-scale fully variational MCHF calculations in Ne IV. The MCHF results were relativistically corrected by scaling the interaction constants with the ratio of DHF and HF values. There is a very good agreement between the A_J constants for all states except for $1s^22s^22p^3\ ^4S_{3/2}^o$. The A_J constant for the latter state is zero at the HF level and, as discussed in [32], higher order correlation effects are very important. The MCHF calculation includes more electron correlation and the corresponding A_J constant is believed to be more accurate than the constant from the RCI calculation. Turning to the B_J constants we see that there is a perfect consistency for states belonging to the $1s^22s2p^4$ and $1s^22p^5$ configurations. However, for the two $J = 3/2$ states belonging to $1s^22s^22p^3$, with a half filled $2p$ subshell, there is no agreement at all between the relativistic and non-relativistic calculations. Not even the signs are consistent. The fact that the non-relativistic MCHF calculations do not include effects of the LS term mixing makes them virtually meaningless in this case. For the $J = 5/2$ state there is no LS term mixing, and the B_J constants from the RCI and MCHF calculations agree remarkably well, indicating that the correlation effects are indeed accurately described in both cases.

Acknowledgments

Part of this work was supported by the Communauté française of Belgium (Action de Recherche Concertée), the Belgian National Fund for Scientific Research (FRFC/IISN Convention) and by the IUAP Belgian State Science Policy (BriX network P7/12). CN and SV are grateful to the “Fonds pour la formation la Recherche dans l’Industrie et dans l’Agriculture” of Belgium for a PhD grant (Boursier F.R.S.-FNRS). PJ gratefully acknowledges financial support from the Swedish Research Council (VR). PJ and GG acknowledges support from the Visby program of the Swedish Institute.

References

- [1] T. Brage, P. Judge, A. Aboussaïd, M. Godefroid, C. Froese Fischer, P. Jönsson, A. Ynnerman, D. Leckrone, *Astrophys. J* 500 (1998) 507–521.
- [2] T. Brage, P. Judge, C.R. Proffitt, *Phys. Rev. Lett.* 89 (2002) 281101.
- [3] D. Sundholm, J. Olsen, *Phys. Rev. Lett.* 68 (1992) 927–930.
- [4] N. Stone, J. Stone, P. Jönsson, *Hyperfine Interactions* 197 (2010) 29–35.
- [5] R. L. Kurucz, *Phys. Scr.* T47 (1993) 110.
- [6] M. Andersson, N. Ryde, J. Grumer, R. Blackwell-Whitehead, R. Hutton, Y. Zou, P. Jönsson, T. Brage, *Astrophysical Journal Supplement Series* (2014). Submitted.
- [7] P. Beiersdorfer, A. L. Osterheld, J. H. Scofield, J. R. Crespo López-Urrutia, K. Widmann, *Phys. Rev. Lett.* 80 (1998) 3022.
- [8] M. Godefroid, C. Froese Fischer, P. Jönsson, *J. Phys. B : At. Mol. Phys.* 34 (2001) 1079–1104.
- [9] Y. S. Kozhedub, A. V. Volotka, A. N. Artemyev, D. A. Glazov, G. Plunien, V. M. Shabaev, I. I. Tupitsyn, T. Stöhlker, *Phys. Rev. A* 81 (2010) 042513.
- [10] E. Biémont, P. Palmeri, P. Quinet, *J. Phys. B : At. Mol. Phys.* 43 (2010) 074010.
- [11] T. Brage, P. G. Judge, P. Jönsson, D. P. Edwards, *Astrophys. J* 540 (2000) 1114–1118.
- [12] C. Froese Fischer, P. Jönsson, *J. Mol. Struct.: Theochem* 537 (2001) 55–62.
- [13] A. Hibbert, *Comput. Phys. Commun.* 9 (1975) 141 – 172.
- [14] P. Jönsson, C.-G. Wahlström, C. Froese Fischer, *Comput. Phys. Commun.* 74 (1993) 399–414.
- [15] C. Froese Fischer, G. Tachiev, G. Gaigalas, M. Godefroid, *Comput. Phys. Commun.* 176 (2007) 559–579.
- [16] I. Lindgren, A. Rosén, *Case Stud. At. Phys.* 4 (1974) 93–196.
- [17] P. Jönsson, X. He, C. Froese Fischer, I. Grant, *Comput. Phys. Commun.* 177 (2007) 597–622.
- [18] P. Jönsson, G. Gaigalas, J. Bieroń, C. Froese Fischer, I. Grant, *Comput. Phys. Commun.* 184 (2013) 2197–2203.
- [19] P. Jönsson, F. Parpia, C. Froese Fischer, *Comput. Phys. Commun.* 96 (1996) 301–310.
- [20] M. Andersson, P. Jönsson, *Comput. Phys. Commun.* 178 (2008) 156–170.
- [21] C. Nazé, S. Verdebout, P. Rynkun, G. Gaigalas, M. Godefroid, P. Jönsson, *At. Data Nucl. Data Tables* (2013). in press.
- [22] I. P. Grant, *Relativistic Quantum Theory of Atoms and Molecules. Theory and Computation, Atomic, Optical and Plasma Physics*, Springer, New York, USA, 2007.
- [23] B. J. McKenzie, I. P. Grant, P. H. Norrington, *Comput. Phys. Commun.* 21 (1980) 233–246.
- [24] K. G. Dyall, I. P. Grant, C. T. Johnson, F. A. Parpia, E. P. Plummer, *Comput. Phys. Commun.* 55 (1989) 425 – 456.

- [25] G. Gaigalas, S. Fritzsche, I. P. Grant, *Comput. Phys. Commun.* 139 (2001) 263–278.
- [26] J. L. Armstrong, *Theory of the Hyperfine Structure of Free Atoms*, John Wiley & Sons, NY, 1971.
- [27] N. Stone, *At. Data Nucl. Data Tables* 90 (2005) 75–176.
- [28] K. T. Cheng, W. J. Childs, *Phys. Rev. A* 31 (1985) 2775–2784.
- [29] G. Gaigalas, T. Žalandauskas, Z. Rudzikas, *At. Data Nucl. Data Tables* 84 (2003) 99 – 190.
- [30] G. Gaigalas, T. Žalandauskas, S. Fritzsche, *Comput. Phys. Commun.* 157 (2004) 239 – 253.
- [31] C. Froese Fischer, T. Brage, P. Jönsson, *Computational Atomic Structure: An MCHF Approach*, Institute of Physics Publishing, Bristol and Philadelphia, 1997.
- [32] M. Godefroid, G. V. Meulebeke, P. Jönsson, C. Froese Fischer, *Z. Phys.D–Atoms, Molecules and Clusters* 42 (1997) 193–201.
- [33] S. Verdebout, P. Jönsson, G. Gaigalas, M. Godefroid, C. Froese Fischer, *J. Phys. B : At. Mol. Phys.* 43 (2010) 074017.
- [34] P. Jönsson, C. Froese Fischer, *Phys. Rev. A* 48 (1993) 4113–4123.
- [35] T. Carette, M. Godefroid, *Phys. Rev. A* 83 (2011) 062505.
- [36] T. Carette, M. Godefroid, *Phys. Rev. A* (2014). In press.
- [37] P. Jönsson, J. Ekman, S. Gustafsson, H. Hartman, L. B. Karlsson, R. du Rietz, G. Gaigalas, M. Godefroid, C. Froese Fischer, *Astron. Astrophys.* 559 (2013) A100.
- [38] J. Ekman, P. Jönsson, S. Gustafsson, H. Hartman, G. Gaigalas, M. R. Godefroid, C. Froese Fischer, *Astron. Astrophys.* 564 (2014) A24.
- [39] L. Sturesson, P. Jönsson, C. Froese Fischer, *Comput. Phys. Commun.* 177 (2007) 539 – 550.
- [40] P. Rynkun, P. Jönsson, G. Gaigalas, C. Froese Fischer, *At. Data Nucl. Data Tables* 98 (2012) 481–556.
- [41] P. Jönsson, P. Rynkun, G. Gaigalas, *At. Data Nucl. Data Tables* 97 (2011) 648 – 691.
- [42] P. Rynkun, P. Jönsson, G. Gaigalas, C. Froese Fischer, *At. Data Nucl. Data Tables* 100 (2014) 315–402.
- [43] U. Litzén, T. Zethson, P. Jönsson, J. Kasten, R. Kling, F. Launay, *Phys. Rev. A* 57 (1998) 2477–2484.
- [44] S. Verdebout, P. Rynkun, P. Jönsson, G. Gaigalas, C. Froese Fischer, M. Godefroid, *J. Phys. B : At. Mol. Phys.* 46 (2013) 085003.
- [45] W. Johnson, *Canadian Journal of Physics* 99 (2010) 1–9.
- [46] J. P. Marques, F. Parente, P. Indelicato, *Phys. Rev. A* 47 (1993) 929–935.
- [47] K. T. Cheng, M. H. Chen, W. R. Johnson, *Phys. Rev. A* 77 (2008) 052504.
- [48] N. N. Dutta, S. Majumder, *Phys. Rev. A* 85 (2012) 032512.
- [49] P. Jönsson, J. Li, G. Gaigalas, C. Dong, *At. Data Nucl. Data Tables* 96 (2010) 271 – 298.
- [50] Y. Sun, F. Chen, L. Zhuo, B. C. Gou, *Int. J. Quantum Chem.* 112 (2012) 1114–1121.

[51] P. Jönsson, J. Bieroń, *J. Phys. B : At. Mol. Phys.* 43 (2010) 074023.

Explanation of Tables

Table 1. Total energies (in E_h), excitation energies (in cm^{-1}), hyperfine magnetic dipole constants $A_J(I/\mu_I)$ (MHz per unit of μ_N), electric quadrupole constants B_J/Q (MHz/barn) and Landé g_J -factors for levels in the beryllium isoelectronic sequence ($5 \leq Z \leq 74$). For each of the many-electron wave functions, the leading components are given in the LSJ coupling scheme. The number in square brackets is the power of 10.

Level composition in LSJ coupling	Leading components expressed within the LSJ coupling scheme for each calculated level.
Energy	The calculated absolute energies in atomic units (E_h).
ΔE	Calculated energies relatively to the lowest state reported in the table (in cm^{-1}).
$A_J(I/\mu_I)$	Magnetic dipole hyperfine interaction constant (MHz per units of μ_N).
B_J/Q	Electric quadrupole hyperfine interaction constant (MHz/barn).
g_J	Landé g_J -factor.

Table 2. Comparison of calculated hyperfine interaction constants $A_J(I/\mu_I)$ (in MHz per units of μ_N) and B_J/Q (MHz/barn) for the $2s2p$ and $2p^2$ states in B II with Litzén *et al.* [43].

Config.	
$A_J(I/\mu_I)$	Magnetic dipole hyperfine interaction constants (MHz per units of μ_N).
B_J/Q	Electric quadrupole hyperfine interaction constant (MHz/barn).

Table 3. Comparison of the calculated hyperfine interaction constants $A_J(I/\mu_I)$ (MHz per unit of μ_N) of the $1s^22s2p\ ^3P_1$ state for Be-like ions with the results obtained by Marques *et al.* [46] and Cheng *et al.* [47].

$A_J(I/\mu_I)$	Magnetic dipole hyperfine interaction constant (MHz per units of μ_N).
Z	nuclear charge.

Table 4. Total energies (in E_h), excitation energies (in cm^{-1}), hyperfine magnetic dipole constants $A_J(I/\mu_I)$ (MHz per unit of μ_N), electric quadrupole constants B_J/Q (MHz/barn) and Landé g_J -factors for levels in the boron isoelectronic sequence ($8 \leq Z \leq 30$ and $Z = 36, 42$). For each of the many-electron wave functions, the leading components are given in the LSJ coupling scheme. The number in square brackets is the power of 10.

Same as table 1.

Table 5. Comparison of calculated hyperfine interaction constants $A_J(I/\mu_I)$ (MHz per unit of μ_N) and B_J/Q (MHz/barn) with Dutta and Majumber [48] and Jönsson *et al.* [49] for the O IV ion .

$A_J(I/\mu_I)$	Magnetic dipole hyperfine interaction constant (MHz per units of μ_N).
B_J/Q	Electric quadrupole hyperfine interaction constant (MHz/barn).

Table 6. Comparison of calculated hyperfine interaction constants $A_J(I/\mu_I)$ (MHz per unit of μ_N) with Dutta and Majumber [48] for B-like ions from $Z = 9$ to $Z = 21$.

$A_J(I/\mu_I)$ Magnetic dipole hyperfine interaction constant (MHz per units of μ_N).

Table 7. Hyperfine magnetic dipole constants $A_J(I/\mu_I)$ (MHz per unit of μ_N) and electric quadrupole constants B_J/Q (MHz/barn) in O IV. Comparison of values from RCI and MCHF calculations.

Same as table 5.

Table 8. Total energies (in E_h), excitation energies (in cm^{-1}), hyperfine magnetic dipole constants $A_J(I/\mu_I)$ (MHz per unit of μ_N), electric quadrupole constants B_J/Q (MHz/barn) and Landé g_J -factors for levels in the carbon isoelectronic sequence ($7 \leq Z \leq 28$). For each of the many-electron wave functions, the leading components are given in the LSJ coupling scheme. The number in square brackets is the power of 10.

Same as table 1.

Table 9. Hyperfine magnetic dipole constants $A_J(I/\mu_I)$ (MHz per unit of μ_N) and electric quadrupole constants B_J/Q (MHz/barn) in O III. Comparison of values from RCI and MCHF calculations.

Same as table 5.

Table 10. Total energies (in E_h), excitation energies (in cm^{-1}), hyperfine magnetic dipole constants $A_J(I/\mu_I)$ (MHz per unit of μ_N), electric quadrupole constants B_J/Q (MHz/barn) and Landé g_J -factors for levels in the nitrogen isoelectronic sequence ($7 \leq Z \leq 36$ and $Z = 42, 74$). For each of the many-electron wave functions, the leading components are given in the LSJ coupling scheme. The number in square brackets is the power of 10.

Same as table 1.

Table 11. Hyperfine magnetic dipole constants $A_J(I/\mu_I)$ (MHz per unit of μ_N) and electric quadrupole constants B_J/Q (MHz/barn) in Ne IV. Comparison of values from RCI and MCHF calculations.

Same as table 5.

Table 1

Total energies (in E_h), excitation energies (in cm^{-1}), hyperfine magnetic dipole constants $A_J(I/\mu_I)$ (MHz per unit of μ_N), electric quadrupole constants B_J/Q (MHz/barn), and Landé g_J -factors for levels in the beryllium isoelectronic sequence ($5 \leq Z \leq 74$). For each of the many-electron wave functions, the leading components are given in the LSJ coupling scheme. The number in square brackets is the power of 10. See page 17 for Explanation of Tables.

Level composition in LSJ coupling		J	Energy (E_h)	$\Delta E \text{ cm}^{-1}$	$A_J(I/\mu_I)$	B_J/Q	g_J	
B II								
$1s^2 2s2p \ ^3P^o$	(99%)	1	-24.1835957	37277.92	5.132[2]	-5.247[1]	1.501085	
	(99%)	2	-24.1835226	37293.97	4.428[2]	1.049[2]	1.501095	
$1s^2 2s2p \ ^1P^o$	(96%)	+ $1s^2 2p3d \ ^1P^o$	(3%)	1 -24.0185813 1 -23.9028320	73494.38 98898.43	1.015[2] -6.309[1]	9.441[1] 5.183[1]	0.999946 1.501107
$1s^2 2p^2 \ ^3P$	(99%)	1	-23.9027712	98911.77	6.098	-1.038[2]	1.501091	
	(99%)	2	-23.8868692	102401.85	1.001[2]	1.887[2]	0.999954	
C III								
$1s^2 2s2p \ ^3P^o$	(100%)	1	-36.3080969	52345.30	1.114[3]	-1.292[2]	1.501022	
	(100%)	2	-36.3078401	52401.66	9.430[2]	2.581[2]	1.501041	
$1s^2 2s2p \ ^1P^o$	(98%)	+ $1s^2 2p3d \ ^1P^o$	(2%)	1 -36.0796648 1 -35.9203054	102480.34 137455.69	2.641[2] -1.189[2]	2.513[2] 1.273[2]	0.999898 1.501061
$1s^2 2p^2 \ ^3P$	(100%)	1	-35.9200881	137503.37	4.884[1]	-2.549[2]	1.501031	
	(100%)	2	-35.8815892	145952.90	2.539[2]	4.831[2]	0.999915	
N IV								
$1s^2 2s2p \ ^3P^o$	(100%)	1	-50.9406808	67228.87	2.056[3]	-2.554[2]	1.500939	
	(100%)	2	-50.9400241	67373.00	1.717[3]	5.100[2]	1.500971	
$1s^2 2s2p \ ^1P^o$	(98%)	+ $1s^2 2p3d \ ^1P^o$	(1%)	1 -50.6507583	130859.51	5.284[2]	5.108[2]	0.999838
$1s^2 2p^2 \ ^3P$	(100%)	1	-50.4468509	175612.01	-1.918[2]	2.522[2]	1.501002	
	(100%)	2	-50.4462839	175736.44	1.376[2]	-5.053[2]	1.500941	
$1s^2 2p^2 \ ^1D$	(98%)	+ $1s^2 2s3d \ ^1D$	(2%)	2 -50.3859686	188974.12	5.073[2]	9.738[2]	0.999874
O V								
$1s^2 2s2p \ ^3P^o$	(100%)	1	-68.0823306	82034.87	3.417[3]	-4.436[2]	1.500838	
	(100%)	2	-68.0809356	82341.03	2.824[3]	8.853[2]	1.500888	
$1s^2 2s2p \ ^1P^o$	(99%)	+ $1s^2 2p3d \ ^1P^o$	(1%)	1 -67.7318850	158948.79	9.111[2]	8.946[2]	0.999762
$1s^2 2p^2 \ ^3P$	(100%)	1	-67.4827968	213617.33	-2.803[2]	4.383[2]	1.500928	
	(100%)	2	-67.4815738	213885.75	2.898[2]	-8.785[2]	1.500809	
$1s^2 2p^2 \ ^1D$	(99%)	+ $1s^2 2s3d \ ^1D$	(1%)	2 -67.3998597	231819.91	8.838[2]	1.708[3]	0.999846
F VI								
$1s^2 2s2p \ ^3P^o$	(100%)	1	-87.7351344	96827.94	5.280[3]	-7.054[2]	1.500714	
	(100%)	2	-87.7325093	97404.10	4.323[3]	1.407[3]	1.500788	
$1s^2 2s2p \ ^1P^o$	(99%)	+ $1s^2 2p3d \ ^1P^o$	(1%)	1 -87.3242038	187016.78	1.429[3]	1.429[3]	0.999680
$1s^2 2p^2 \ ^3P$	(100%)	1	-87.0297018	251652.50	-3.857[2]	6.975[2]	1.500842	
	(100%)	2	-87.0273805	252161.97	5.210[2]	-1.398[3]	1.500614	
$1s^2 2p^2 \ ^1D$	(99%)	+ $1s^2 2s3d \ ^1D$	(1%)	2 -86.9246298	274713.15	1.406[3]	2.733[3]	0.999852
Ne VII								
$1s^2 2s2p \ ^3P^o$	(100%)	1	-109.9017247	111662.06	7.736[3]	-1.053[3]	1.500565	
	(100%)	2	-109.8971979	112655.56	6.274[3]	2.099[3]	1.500673	
$1s^2 2s2p \ ^1P^o$	(99%)	1	-109.4302639	215135.73	2.094[3]	2.136[3]	0.999591	
$1s^2 2p^2 \ ^3P$	(100%)	1	-109.0898452	289848.99	-5.090[2]	1.042[3]	1.500743	
	(100%)	2	-109.0858269	290730.92	8.489[2]	-2.088[3]	1.500320	
$1s^2 2p^2 \ ^1D$	(99%)	+ $1s^2 2s3d \ ^1D$	(1%)	2 -108.9624161	317816.45	2.095[3]	4.096[3]	0.999928
Na VIII								
$1s^2 2s2p \ ^3P^o$	(100%)	1	-134.5853726	126574.79	1.088[4]	-1.499[3]	1.500387	
	(100%)	2	-134.5780613	128179.42	8.740[3]	2.985[3]	1.500544	
$1s^2 2s2p \ ^1P^o$	(99%)	1	-134.0530508	243405.90	2.907[3]	3.041[3]	0.999501	
$1s^2 2p^2 \ ^3P$	(100%)	1	-133.6661265	328325.99	-6.498[2]	1.482[3]	1.500630	
	(100%)	2	-133.6596392	329749.79	1.294[3]	-2.969[3]	1.499872	
$1s^2 2p^2 \ ^1D$	(99%)	2	-133.5159606	361283.58	2.971[3]	5.842[3]	1.000128	
Mg IX								
$1s^2 2s2p \ ^3P^o$	(100%)	1	-161.7898295	141601.31	1.483[4]	-2.054[3]	1.500172	
	(100%)	2	-161.7786065	144064.48	1.178[4]	4.089[3]	1.500399	
$1s^2 2s2p \ ^1P^o$	(99%)	1	-161.1961034	271909.14	3.865[3]	4.167[3]	0.999416	
$1s^2 2p^2 \ ^3P$	(100%)	1	-160.7620418	367174.64	-8.104[2]	2.032[3]	1.500504	
	(100%)	2	-160.7520449	369368.69	1.877[3]	-4.061[3]	1.499190	
$1s^2 2p^2 \ ^1D$	(99%)	2	-160.5885063	405261.27	4.052[3]	8.016[3]	1.000532	
Al X								
$1s^2 2s2p \ ^3P^o$	(100%)	1	-191.5193017	156772.00	1.969[4]	-2.732[3]	1.499912	
	(100%)	2	-191.5027634	160401.75	1.546[4]	5.435[3]	1.500238	
$1s^2 2s2p \ ^1P^o$	(100%)	1	-190.8634218	300721.00	4.952[3]	5.539[3]	0.999346	
$1s^2 2p^2 \ ^3P$	(100%)	1	-190.3812847	406537.86	-9.923[2]	2.702[3]	1.500364	
	(100%)	2	-190.3666893	409741.17	2.624[3]	-5.380[3]	1.498166	

Table 1 (continued)

Level composition in LSJ coupling		J	Energy (E_h)	ΔE cm $^{-1}$	$A_J(I/\mu_I)$	B_J/Q	g_J		
$1s^2 2p^2 \ ^1D$	(99%)	2	-190.1836779	449907.54	5.352[3]	1.066[4]	1.001249		
Si XI									
$1s^2 2s2p \ ^3P^o$	(100%)	1	-223.7784707	172119.47	2.561[4]	-3.545[3]	1.499594		
	(100%)	2	-223.7548979	177293.10	1.985[4]	7.047[3]	1.500063		
$1s^2 2s2p \ ^1P^o$	(100%)	1	-223.0594554	329925.09	6.142[3]	7.181[3]	0.999301		
$1s^2 2p^2 \ ^3P$	(100%)	1	-222.5282182	446518.16	-1.198[3]	3.506[3]	1.500211		
(99%)	+ $1s^2 2p^2 \ ^1D$	(1%)	2	-222.5076895	451023.70	3.565[3]	-6.933[3]	1.496647	
$1s^2 2p^2 \ ^1D$	(99%)	+ $1s^2 2p^2 \ ^3P$	(1%)	2	-222.3055325	495392.03	6.883[3]	1.380[4]	1.002432
P XII									
$1s^2 2s2p \ ^3P^o$	(100%)	1	-258.5724531	187674.13	3.273[4]	-4.503[3]	1.499203		
	(100%)	2	-258.5397721	194846.78	2.500[4]	8.950[3]	1.499872		
$1s^2 2s2p \ ^1P^o$	(100%)	1	-257.7890617	359608.66	7.391[3]	9.117[3]	0.999299		
$1s^2 2p^2 \ ^3P$	(100%)	1	-257.2075465	487236.50	-1.429[3]	4.454[3]	1.500045		
(99%)	+ $1s^2 2p^2 \ ^1D$	(1%)	2	-257.1795809	493374.23	4.735[3]	-8.715[3]	1.494432	
$1s^2 2p^2 \ ^1D$	(99%)	+ $1s^2 2p^2 \ ^3P$	(1%)	2	-256.9584710	541902.25	8.648[3]	1.745[4]	1.004282
S XIII									
$1s^2 2s2p \ ^3P^o$	(100%)	1	-295.9068587	203465.11	4.122[4]	-5.618[3]	1.498721		
	(100%)	2	-295.8625978	213179.26	3.100[4]	1.117[4]	1.499666		
$1s^2 2s2p \ ^1P^o$	(100%)	1	-295.0575531	389866.14	8.643[3]	1.137[4]	0.999356		
$1s^2 2p^2 \ ^3P$	(100%)	1	-294.4244270	528821.25	-1.688[3]	5.560[3]	1.499866		
(98%)	+ $1s^2 2p^2 \ ^1D$	(2%)	2	-294.3873825	536951.58	6.178[3]	-1.070[4]	1.491264	
$1s^2 2p^2 \ ^1D$	(98%)	+ $1s^2 2p^2 \ ^3P$	(2%)	2	-294.1472760	589648.87	1.065[4]	2.162[4]	1.007054
Cl XIV									
$1s^2 2s2p \ ^3P^o$	(100%)	1	-335.7877256	219520.06	5.128[4]	-6.900[3]	1.498126		
	(100%)	2	-335.7289682	232415.83	3.790[4]	1.373[4]	1.499445		
$1s^2 2s2p \ ^1P^o$	(100%)	1	-334.8706238	420800.64	9.821[3]	1.396[4]	0.999495		
$1s^2 2p^2 \ ^3P$	(100%)	1	-334.1844053	571408.18	-1.979[3]	6.835[3]	1.499674		
(97%)	+ $1s^2 2p^2 \ ^1D$	(2%)	2	-334.1365468	581911.90	7.946[3]	-1.284[4]	1.486837	
$1s^2 2p^2 \ ^1D$	(97%)	+ $1s^2 2p^2 \ ^3P$	(2%)	2	-333.8770301	638869.24	1.287[4]	2.628[4]	1.011057
Ar XV									
$1s^2 2s2p \ ^3P^o$	(100%)	1	-378.2215804	235864.98	6.312[4]	-8.359[3]	1.497391		
	(100%)	2	-378.1449140	252691.31	4.578[4]	1.665[4]	1.499209		
$1s^2 2s2p \ ^1P^o$	(99%)	1	-377.2344001	452526.02	1.083[4]	1.692[4]	0.999742		
$1s^2 2p^2 \ ^3P$	(100%)	1	-376.4934675	615141.91	-2.306[3]	8.292[3]	1.499468		
(96%)	+ $1s^2 2p^2 \ ^1D$	(4%)	2	-376.4330292	628406.60	1.010[4]	-1.503[4]	1.480803	
$1s^2 2p^2 \ ^1D$	(96%)	+ $1s^2 2p^2 \ ^3P$	(4%)	2	-376.1531514	689832.66	1.529[4]	3.136[4]	1.016637
K XVI									
$1s^2 2s2p \ ^3P^o$	(100%)	1	-423.2155219	252524.11	7.697[4]	-1.000[4]	1.496489		
	(100%)	2	-423.1169829	274150.91	5.472[4]	1.996[4]	1.498957		
$1s^2 2s2p \ ^1P^o$	(99%)	1	-422.1555158	485168.54	1.156[4]	2.025[4]	1.000125		
$1s^2 2p^2 \ ^3P$	(100%)	1	-421.3581121	660178.43	-2.673[3]	9.943[3]	1.499249		
(95%)	+ $1s^2 2p^2 \ ^1D$	(5%)	2	-421.2833736	676581.63	1.272[4]	-1.714[4]	1.472816	
$1s^2 2p^2 \ ^1D$	(95%)	+ $1s^2 2p^2 \ ^3P$	(5%)	2	-420.9814490	742846.42	1.789[4]	3.675[4]	1.024140
Ca XVII									
$1s^2 2s2p \ ^3P^o$	(99%)	+ $1s^2 2s2p \ ^1P^o$	(1%)	1	-470.7769912	269517.84	9.309[4]	-1.183[4]	1.495388
	(100%)	2	-470.6520059	296948.94	6.479[4]	2.369[4]	1.498691		
$1s^2 2s2p \ ^1P^o$	(99%)	+ $1s^2 2s2p \ ^3P^o$	(1%)	1	-469.6408769	518866.10	1.187[4]	2.398[4]	1.000675
$1s^2 2p^2 \ ^3P$	(100%)	1	-468.7851319	706680.40	-3.084[3]	1.180[4]	1.499017		
(93%)	+ $1s^2 2p^2 \ ^1D$	(7%)	2	-468.6945040	726570.93	1.587[4]	-1.899[4]	1.462587	
$1s^2 2p^2 \ ^1D$	(93%)	+ $1s^2 2p^2 \ ^3P$	(7%)	2	-468.3678968	798252.93	2.064[4]	4.228[4]	1.038565
Sc XVIII									
$1s^2 2s2p \ ^3P^o$	(99%)	+ $1s^2 2s2p \ ^1P^o$	(1%)	1	-520.9139525	286853.73	1.118[5]	-1.385[4]	1.494055
	(100%)	2	-520.7572760	321240.25	7.605[4]	2.786[4]	1.498408		
$1s^2 2s2p \ ^1P^o$	(99%)	+ $1s^2 2s2p \ ^3P^o$	(1%)	1	-519.6978413	553759.28	1.162[4]	2.813[4]	1.001425
$1s^2 2p^2 \ ^3P$	(100%)	1	-518.7811424	754951.43	-3.546[3]	1.388[4]	1.498771		
(90%)	+ $1s^2 2p^2 \ ^1D$	(10%)	2	-518.6738061	778509.02	1.963[4]	-2.034[4]	1.450016	
$1s^2 2p^2 \ ^1D$	(90%)	+ $1s^2 2p^2 \ ^3P$	(10%)	2	-518.3187558	856433.55	2.349[4]	4.776[4]	1.045884
Ti XIX									
$1s^2 2s2p \ ^3P^o$	(99%)	+ $1s^2 2s2p \ ^1P^o$	(1%)	1	-573.6350094	304563.28	1.333[5]	-1.606[4]	1.492459
	(100%)	2	-573.4406505	347220.13	8.861[4]	3.250[4]	1.498111		
$1s^2 2s2p \ ^1P^o$	(99%)	+ $1s^2 2s2p \ ^3P^o$	(1%)	1	-572.3342888	590038.44	1.064[4]	3.270[4]	1.002407
$1s^2 2p^2 \ ^3P$	(100%)	1	-571.3551240	804940.28	-4.063[3]	1.619[4]	1.498513		
(87%)	+ $1s^2 2p^2 \ ^1D$	(13%)	2	-571.2295207	832507.02	2.409[4]	-2.094[4]	1.435078	
$1s^2 2p^2 \ ^1D$	(87%)	+ $1s^2 2p^2 \ ^3P$	(13%)	2	-570.8408559	917809.08	2.642[4]	5.296[4]	1.060251
V XX									
$1s^2 2s2p \ ^3P^o$	(99%)	+ $1s^2 2s2p \ ^1P^o$	(1%)	1	-628.9491702	322647.41	1.579[5]	-1.845[4]	1.490567
	(100%)	2	-628.7103287	375067.05	1.025[5]	3.763[4]	1.497798		

Table 1 (continued)

Level composition in LSJ coupling			J	Energy (E_h)	ΔE cm $^{-1}$	$A_J(I/\mu_I)$	B_J/Q	g_J
$1s^2 2s2p \ ^1P^o$ (99%)	+ $1s^2 2s2p \ ^3P^o$	(1%)	1	-627.5584405	627877.29	8.754[3]	3.770[4]	1.003653
$1s^2 2p^2 \ ^3P$ (100%)			1	-626.5146940	856953.16	-4.644[3]	1.875[4]	1.498241
(84%)	+ $1s^2 2p^2 \ ^1D$	(16%)	2	-626.3700687	888694.73	2.928[4]	-2.057[4]	1.418131
$1s^2 2p^2 \ ^1D$ (84%)	+ $1s^2 2p^2 \ ^3P$	(16%)	2	-625.9411607	982829.15	2.942[4]	5.767[4]	1.076595
Cr XXI								
$1s^2 2s2p \ ^3P^o$ (98%)	+ $1s^2 2s2p \ ^1P^o$	(2%)	1	-686.8660514	341111.11	1.861[5]	-2.102[4]	1.488352
(100%)			2	-686.5750432	404980.02	1.179[5]	4.328[4]	1.497469
$1s^2 2s2p \ ^1P^o$ (98%)	+ $1s^2 2s2p \ ^3P^o$	(2%)	1	-685.3790225	667476.22	5.777[3]	4.314[4]	1.005190
$1s^2 2p^2 \ ^3P$ (100%)			1	-684.2685405	911198.84	-5.296[3]	2.157[4]	1.497956
(81%)	+ $1s^2 2p^2 \ ^1D$	(19%)	2	-684.1044723	947207.63	3.527[4]	-1.905[4]	1.399728
$1s^2 2p^2 \ ^1D$ (80%)	+ $1s^2 2p^2 \ ^3P$	(19%)	2	-683.6271476	1051968.30	3.250[4]	6.174[4]	1.094367
Mn XXII								
$1s^2 2s2p \ ^3P^o$ (98%)	+ $1s^2 2s2p \ ^1P^o$	(2%)	1	-747.3956397	359953.13	2.180[5]	-2.375[4]	1.485790
(100%)			2	-747.0438219	437168.19	1.348[5]	4.947[4]	1.497126
$1s^2 2s2p \ ^1P^o$ (98%)	+ $1s^2 2s2p \ ^3P^o$	(2%)	1	-745.8050301	709051.56	1.525[3]	4.901[4]	1.007042
$1s^2 2p^2 \ ^3P$ (100%)			1	-744.6256556	967894.33	-6.028[3]	2.465[4]	1.497657
(77%)	+ $1s^2 2p^2 \ ^1D$	(23%)	2	-744.4420306	1008195.37	4.206[4]	-1.626[4]	1.380558
$1s^2 2p^2 \ ^1D$ (77%)	+ $1s^2 2p^2 \ ^3P$	(23%)	2	-743.9065760	1125714.08	3.568[4]	6.509[4]	1.112875
Fe XXIII								
$1s^2 2s2p \ ^3P^o$ (97%)	+ $1s^2 2s2p \ ^1P^o$	(3%)	1	-810.5487741	379152.24	2.542[5]	-2.662[4]	1.482866
(100%)			2	-810.1264665	471838.04	1.534[5]	5.623[4]	1.496765
$1s^2 2s2p \ ^1P^o$ (97%)	+ $1s^2 2s2p \ ^3P^o$	(3%)	1	-808.8460911	752847.93	-4.175[3]	5.532[4]	1.009227
$1s^2 2p^2 \ ^3P$ (100%)			1	-807.5957152	1027273.72	-6.849[3]	2.803[4]	1.497346
(73%)	+ $1s^2 2p^2 \ ^1D$	(27%)	2	-807.3926734	1071836.25	4.967[4]	-1.217[4]	1.361330
$1s^2 2p^2 \ ^1D$ (73%)	+ $1s^2 2p^2 \ ^3P$	(27%)	2	-806.7878908	1204570.68	3.902[4]	6.771[4]	1.131412
Co XXIV								
$1s^2 2s2p \ ^3P^o$ (97%)	+ $1s^2 2s2p \ ^1P^o$	(3%)	1	-876.3362317	398753.77	2.948[5]	-2.961[4]	1.479575
(100%)			2	-875.8326601	509274.95	1.737[5]	6.361[4]	1.496392
$1s^2 2s2p \ ^1P^o$ (97%)	+ $1s^2 2s2p \ ^3P^o$	(3%)	1	-874.5121580	799091.66	-1.153[4]	6.204[4]	1.011742
$1s^2 2p^2 \ ^3P$ (100%)			1	-873.1886099	1089576.88	-7.769[3]	3.170[4]	1.497021
(69%)	+ $1s^2 2p^2 \ ^1D$	(31%)	2	-872.9664813	1138328.46	5.809[4]	-6.834[3]	1.342656
$1s^2 2p^2 \ ^1D$ (69%)	+ $1s^2 2p^2 \ ^3P$	(31%)	2	-872.2797635	1289045.59	4.254[4]	6.968[4]	1.149366
Ni XXV								
$1s^2 2s2p \ ^3P^o$ (96%)	+ $1s^2 2s2p \ ^1P^o$	(4%)	1	-944.7702858	418691.49	3.402[5]	-3.269[4]	1.475916
(100%)			2	-944.1734813	549674.93	1.959[5]	7.160[4]	1.496001
$1s^2 2s2p \ ^1P^o$ (96%)	+ $1s^2 2s2p \ ^3P^o$	(4%)	1	-942.8138643	848076.35	-2.066[4]	6.918[4]	1.014595
$1s^2 2p^2 \ ^3P$ (100%)			1	-941.4151154	1155066.24	-8.800[3]	3.569[4]	1.496684
(66%)	+ $1s^2 2p^2 \ ^1D$	(34%)	2	-941.1743577	1207906.45	6.733[4]	-3.051[2]	1.324991
$1s^2 2p^2 \ ^1D$ (66%)	+ $1s^2 2p^2 \ ^3P$	(34%)	2	-940.3917613	1379666.50	4.631[4]	7.108[4]	1.166280
Cu XXVI								
$1s^2 2s2p \ ^3P^o$ (96%)	+ $1s^2 2s2p \ ^1P^o$	(4%)	1	-1015.8625946	438966.63	3.907[5]	-3.585[4]	1.471903
(100%)			2	-1015.1593420	593312.74	2.199[5]	8.025[4]	1.495596
$1s^2 2s2p \ ^1P^o$ (95%)	+ $1s^2 2s2p \ ^3P^o$	(4%)	1	-1013.7616245	900076.25	-3.172[4]	7.672[4]	1.017769
$1s^2 2p^2 \ ^3P$ (100%)			1	-1012.2857294	1223997.79	-9.954[3]	4.000[4]	1.496333
(63%)	+ $1s^2 2p^2 \ ^1D$	(37%)	2	-1012.0268741	1280809.94	7.741[4]	7.329[3]	1.308616
$1s^2 2p^2 \ ^1D$ (63%)	+ $1s^2 2p^2 \ ^3P$	(37%)	2	-1011.1331720	1476954.89	5.037[4]	7.203[4]	1.181874
Zn XXVII								
$1s^2 2s2p \ ^3P^o$ (95%)	+ $1s^2 2s2p \ ^1P^o$	(5%)	1	-1089.6265867	459566.81	4.466[5]	-3.904[4]	1.467559
(100%)			2	-1088.8023517	640465.48	2.460[5]	8.958[4]	1.495174
$1s^2 2s2p \ ^1P^o$ (95%)	+ $1s^2 2s2p \ ^3P^o$	(5%)	1	-1087.3674188	955396.84	-4.484[4]	8.464[4]	1.021242
$1s^2 2p^2 \ ^3P$ (100%)			1	-1085.8124818	1296666.05	-1.125[4]	4.465[4]	1.495969
(60%)	+ $1s^2 2p^2 \ ^1D$	(40%)	2	-1085.5360945	1357326.06	8.834[4]	1.599[4]	1.293662
$1s^2 2p^2 \ ^1D$ (60%)	+ $1s^2 2p^2 \ ^3P$	(40%)	2	-1084.5148004	1581474.19	5.475[4]	7.264[4]	1.196017
Ga XXVIII								
$1s^2 2s2p \ ^3P^o$ (94%)	+ $1s^2 2s2p \ ^1P^o$	(6%)	1	-1166.0751751	480463.11	5.082[5]	-4.224[4]	1.462916
(100%)			2	-1165.1140428	691407.26	2.743[5]	9.963[4]	1.494737
$1s^2 2s2p \ ^1P^o$ (94%)	+ $1s^2 2s2p \ ^3P^o$	(6%)	1	-1163.6426389	1014343.09	-6.010[4]	9.293[4]	1.024981
$1s^2 2p^2 \ ^3P$ (100%)			1	-1162.0068702	1373352.80	-1.269[4]	4.966[4]	1.495592
(57%)	+ $1s^2 2p^2 \ ^1D$	(43%)	2	-1161.7135217	1437735.36	1.001[5]	2.562[4]	1.280146
$1s^2 2p^2 \ ^1D$ (57%)	+ $1s^2 2p^2 \ ^3P$	(43%)	2	-1160.5468898	1693781.46	5.948[4]	7.299[4]	1.208693
Ge XXIX								
$1s^2 2s2p \ ^3P^o$ (93%)	+ $1s^2 2s2p \ ^1P^o$	(7%)	1	-1245.2226190	501639.94	5.757[5]	-4.542[4]	1.458013
(100%)			2	-1244.1072295	746439.63	3.049[5]	1.104[5]	1.494284
$1s^2 2s2p \ ^1P^o$ (93%)	+ $1s^2 2s2p \ ^3P^o$	(7%)	1	-1242.5999603	1077246.98	-7.759[4]	1.016[5]	1.028948
$1s^2 2p^2 \ ^3P$ (100%)			1	-1240.8816530	1454371.82	-1.430[4]	5.504[4]	1.495201
(55%)	+ $1s^2 2p^2 \ ^1D$	(45%)	2	-1240.5719033	1522354.03	1.129[5]	3.616[4]	1.268008
$1s^2 2p^2 \ ^1D$ (55%)	+ $1s^2 2p^2 \ ^3P$	(45%)	2	-1239.2409046	1814474.45	6.460[4]	7.316[4]	1.219960

Table 1 (continued)

Level composition in LSJ coupling			J	Energy (E_h)	ΔE cm $^{-1}$	$A_J(I/\mu_I)$	B_J/Q	g_J
As XXX								
$1s^2 2s2p \ ^3P^o$	(92%)	+ $1s^2 2s2p \ ^1P^o$	(8%)	1	-1327.0839417	523084.68	6.496[5]	-4.856[4]
	(100%)			2	-1325.7954328	805879.69	3.378[5]	1.220[5]
$1s^2 2s2p \ ^1P^o$	(92%)	+ $1s^2 2s2p \ ^3P^o$	(8%)	1	-1324.2527671	1144455.67	-9.741[4]	1.106[5]
$1s^2 2p^2 \ ^3P$	(100%)			1	-1322.4502850	1540054.76	-1.611[4]	6.081[4]
	(53%)	+ $1s^2 2p^2 \ ^1D$	(47%)	2	-1322.1246724	1611518.46	1.265[5]	4.759[4]
$1s^2 2p^2 \ ^1D$	(53%)	+ $1s^2 2p^2 \ ^3P$	(47%)	2	-1320.6089543	1944180.12	7.012[4]	7.321[4]
Se XXXI								
$1s^2 2s2p \ ^3P^o$	(91%)	+ $1s^2 2s2p \ ^1P^o$	(9%)	1	-1411.6735610	544775.17	7.298[5]	-5.164[4]
	(100%)			2	-1410.1915092	870047.93	3.733[5]	1.343[5]
$1s^2 2s2p \ ^1P^o$	(91%)	+ $1s^2 2s2p \ ^3P^o$	(9%)	1	-1408.6137854	1216318.28	-1.196[5]	1.199[5]
$1s^2 2p^2 \ ^3P$	(100%)			1	-1406.7256373	1630718.88	-1.811[4]	6.697[4]
	(51%)	+ $1s^2 2p^2 \ ^1D$	(49%)	2	-1406.3846743	1705551.59	1.412[5]	5.989[4]
$1s^2 2p^2 \ ^1D$	(51%)	+ $1s^2 2p^2 \ ^3P$	(49%)	2	-1406.6625084	2083523.31	7.606[4]	7.319[4]
Br XXXII								
$1s^2 2s2p \ ^3P^o$	(90%)	+ $1s^2 2s2p \ ^1P^o$	(10%)	1	-1499.0083502	566707.73	8.170[5]	-5.464[4]
	(100%)			2	-1497.3107164	939295.28	4.115[5]	1.475[5]
$1s^2 2s2p \ ^1P^o$	(90%)	+ $1s^2 2s2p \ ^3P^o$	(10%)	1	-1495.6981436	1293214.07	-1.442[5]	1.296[5]
$1s^2 2p^2 \ ^3P$	(100%)			1	-1493.7228578	1726739.18	-2.035[4]	7.355[4]
	(51%)	+ $1s^2 2p^2 \ ^1D$	(49%)	2	-1493.3670306	1804834.23	1.569[5]	7.307[4]
$1s^2 2p^2 \ ^3P$	(51%)	+ $1s^2 2p^2 \ ^1D$	(49%)	2	-1491.4152516	2233200.20	8.243[4]	7.312[4]
Kr XXXIII								
$1s^2 2s2p \ ^3P^o$	(89%)	+ $1s^2 2s2p \ ^1P^o$	(11%)	1	-1589.1026872	588846.93	9.112[5]	-5.754[4]
	(100%)			2	-1587.1657617	1013952.95	4.524[5]	1.616[5]
$1s^2 2s2p \ ^1P^o$	(89%)	+ $1s^2 2s2p \ ^3P^o$	(11%)	1	-1585.5184340	1375499.57	-1.712[5]	1.396[5]
$1s^2 2p^2 \ ^3P$	(100%)			1	-1583.4547236	1828431.64	-2.284[4]	8.056[4]
	(52%)	+ $1s^2 2p^2 \ ^3P$	(48%)	2	-1583.0844924	1909688.00	1.737[5]	8.713[4]
$1s^2 2p^2 \ ^3P$	(52%)	+ $1s^2 2p^2 \ ^1D$	(48%)	2	-1580.8784321	2393862.24	8.925[4]	7.303[4]
Rb XXXIV								
$1s^2 2s2p \ ^3P^o$	(88%)	+ $1s^2 2s2p \ ^1P^o$	(12%)	1	-1681.9775676	611218.45	1.013[6]	-6.032[4]
	(100%)			2	-1679.7759131	1094425.74	4.963[5]	1.766[5]
$1s^2 2s2p \ ^1P^o$	(88%)	+ $1s^2 2s2p \ ^3P^o$	(12%)	1	-1678.0938165	1463603.27	-2.008[5]	1.499[5]
$1s^2 2p^2 \ ^3P$	(100%)			1	-1675.9402893	1936247.85	-2.560[4]	8.802[4]
	(53%)	+ $1s^2 2p^2 \ ^3P$	(47%)	2	-1675.5560892	2020570.02	1.916[5]	1.021[5]
$1s^2 2p^2 \ ^3P$	(53%)	+ $1s^2 2p^2 \ ^1D$	(47%)	2	-1673.0695051	2566312.12	9.654[4]	7.293[4]
Sr XXXV								
$1s^2 2s2p \ ^3P^o$	(87%)	+ $1s^2 2s2p \ ^1P^o$	(13%)	1	-1777.6472138	633804.41	1.122[6]	-6.300[4]
	(100%)			2	-1775.1536103	1181087.11	5.434[5]	1.924[5]
$1s^2 2s2p \ ^1P^o$	(87%)	+ $1s^2 2s2p \ ^3P^o$	(13%)	1	-1773.4366379	1557918.99	-2.329[5]	1.606[5]
$1s^2 2p^2 \ ^3P$	(100%)			1	-1771.1920112	2050557.60	-2.867[4]	9.593[4]
	(55%)	+ $1s^2 2p^2 \ ^3P$	(45%)	2	-1770.7942567	2137854.61	2.107[5]	1.180[5]
$1s^2 2p^2 \ ^3P$	(55%)	+ $1s^2 2p^2 \ ^1D$	(45%)	2	-1767.9992590	2751285.69	1.043[5]	7.285[4]
Y XXXVI								
$1s^2 2s2p \ ^3P^o$	(86%)	+ $1s^2 2s2p \ ^1P^o$	(14%)	1	-1876.1316807	656592.12	1.239[6]	-6.555[4]
	(100%)			2	-1873.3170653	1274328.78	5.937[5]	2.093[5]
$1s^2 2s2p \ ^1P^o$	(86%)	+ $1s^2 2s2p \ ^3P^o$	(14%)	1	-1871.5650243	1658857.31	-2.676[5]	1.717[5]
$1s^2 2p^2 \ ^3P$	(100%)			1	-1869.2280968	2171753.60	-3.207[4]	1.043[5]
	(56%)	+ $1s^2 2p^2 \ ^3P$	(44%)	2	-1868.8171835	2261938.64	2.311[5]	1.348[5]
$1s^2 2p^2 \ ^3P$	(56%)	+ $1s^2 2p^2 \ ^1D$	(44%)	2	-1865.6841576	2949558.32	1.126[5]	7.277[4]
Zr XXXVII								
$1s^2 2s2p \ ^3P^o$	(86%)	+ $1s^2 2s2p \ ^1P^o$	(14%)	1	-1977.4498707	679642.19	1.365[6]	-6.798[4]
	(100%)			2	-1974.2832768	1374629.19	6.475[5]	2.271[5]
$1s^2 2s2p \ ^1P^o$	(85%)	+ $1s^2 2s2p \ ^3P^o$	(14%)	1	-1972.4959047	1766912.01	-3.051[5]	1.831[5]
$1s^2 2p^2 \ ^3P$	(100%)			1	-1970.0656693	2300287.03	-3.578[4]	1.132[5]
	(56%)	+ $1s^2 2p^2 \ ^3P$	(44%)	2	-1969.6419590	2393280.68	2.528[5]	1.526[5]
$1s^2 2p^2 \ ^3P$	(56%)	+ $1s^2 2p^2 \ ^1D$	(44%)	2	-1966.1394872	3161984.37	1.213[5]	7.271[4]
Nb XXXVIII								
$1s^2 2s2p \ ^3P^o$	(85%)	+ $1s^2 2s2p \ ^1P^o$	(15%)	1	-2081.6214772	702865.85	1.499[6]	-7.030[4]
	(100%)			2	-2078.0699704	1482331.47	7.048[5]	2.460[5]
$1s^2 2s2p \ ^1P^o$	(85%)	+ $1s^2 2s2p \ ^3P^o$	(15%)	1	-2076.2469429	1882439.76	-3.453[5]	1.950[5]
$1s^2 2p^2 \ ^3P$	(100%)			1	-2073.7220925	2436580.35	-3.992[4]	1.226[5]
	(57%)	+ $1s^2 2p^2 \ ^3P$	(43%)	2	-2073.2859624	2532299.85	2.759[5]	1.714[5]
$1s^2 2p^2 \ ^3P$	(57%)	+ $1s^2 2p^2 \ ^1D$	(43%)	2	-2069.3807458	3389395.78	1.306[5]	7.268[4]
Mo XXXIX								
$1s^2 2s2p \ ^3P^o$	(84%)	+ $1s^2 2s2p \ ^1P^o$	(16%)	1	-2188.6666512	726222.48	1.642[6]	-7.249[4]
	(100%)			2	-2184.6952614	1597841.76	7.660[5]	2.659[5]
$1s^2 2s2p \ ^1P^o$	(84%)	+ $1s^2 2s2p \ ^3P^o$	(16%)	1	-2182.8362002	2005858.51	-3.884[5]	2.072[5]
								1.071294

Table 1 (continued)

Level composition in LSJ coupling			J	Energy (E_h)	ΔE cm $^{-1}$	$A_J(I/\mu_I)$	B_J/Q	g_J
$1s^2 2p^2 \ ^3P$ (100%)			1	-2180.2153007	2581079.45	-4.455[4]	1.326[5]	1.490576
$1s^2 2p^2 \ ^1D$ (58%)	+ $1s^2 2p^2 \ ^3P$	(42%)	2	-2179.7671108	2679445.76	3.005[5]	1.912[5]	1.198042
$1s^2 2p^2 \ ^3P$ (58%)	+ $1s^2 2p^2 \ ^1D$	(42%)	2	-2175.4238967	3632671.06	1.404[5]	7.266[4]	1.279558
Tc XL								
$1s^2 2s2p \ ^3P^o$ (83%)	+ $1s^2 2s2p \ ^1P^o$	(17%)	1	-2298.6068896	749910.93	1.795[6]	-7.448[4]	1.399495
(100%)			2	-2294.1786841	1721789.67	8.313[5]	2.867[5]	1.488249
$1s^2 2s2p \ ^1P^o$ (83%)	+ $1s^2 2s2p \ ^3P^o$	(17%)	1	-2292.2826541	2137920.14	-4.344[5]	2.200[5]	1.075014
$1s^2 2p^2 \ ^3P$ (100%)			1	-2289.5654704	2734273.03	-4.973[4]	1.430[5]	1.490045
$1s^2 2p^2 \ ^1D$ (59%)	+ $1s^2 2p^2 \ ^3P$	(41%)	2	-2289.1052941	2835270.05	3.267[5]	2.121[5]	1.194147
$1s^2 2p^2 \ ^3P$ (59%)	+ $1s^2 2p^2 \ ^1D$	(41%)	2	-2284.2868572	3892794.69	1.508[5]	7.271[4]	1.282246
Ru XLI								
$1s^2 2s2p \ ^3P^o$ (82%)	+ $1s^2 2s2p \ ^1P^o$	(18%)	1	-2411.4658809	773779.90	1.958[6]	-7.646[4]	1.394632
(100%)			2	-2406.5414634	1854564.58	9.008[5]	3.088[5]	1.487604
$1s^2 2s2p \ ^1P^o$ (82%)	+ $1s^2 2s2p \ ^3P^o$	(18%)	1	-2404.6085288	2278794.68	-4.837[5]	2.332[5]	1.078540
$1s^2 2p^2 \ ^3P$ (100%)			1	-2401.7930578	2896719.12	-5.533[4]	1.541[5]	1.489499
$1s^2 2p^2 \ ^1D$ (59%)	+ $1s^2 2p^2 \ ^3P$	(41%)	2	-2401.3214970	3000214.76	3.545[5]	2.341[5]	1.190532
$1s^2 2p^2 \ ^3P$ (59%)	+ $1s^2 2p^2 \ ^1D$	(41%)	2	-2395.9883070	4170714.63	1.617[5]	7.274[4]	1.284625
Rh XLII								
$1s^2 2s2p \ ^3P^o$ (81%)	+ $1s^2 2s2p \ ^1P^o$	(19%)	1	-2527.2659390	797867.03	2.132[6]	-7.833[4]	1.389922
(100%)			2	-2521.8037885	1996670.46	9.747[5]	3.321[5]	1.486942
$1s^2 2s2p \ ^1P^o$ (81%)	+ $1s^2 2s2p \ ^3P^o$	(19%)	1	-2519.8334645	2429106.58	-5.364[5]	2.469[5]	1.081880
$1s^2 2p^2 \ ^3P$ (100%)			1	-2516.9183633	3068897.32	-6.151[4]	1.657[5]	1.488938
$1s^2 2p^2 \ ^1D$ (60%)	+ $1s^2 2p^2 \ ^3P$	(40%)	2	-2516.4357519	3174818.28	3.839[5]	2.572[5]	1.187185
$1s^2 2p^2 \ ^3P$ (60%)	+ $1s^2 2p^2 \ ^1D$	(40%)	2	-2510.5461381	4467439.07	1.733[5]	7.279[4]	1.286705
Pd XLIII								
$1s^2 2s2p \ ^3P^o$ (81%)	+ $1s^2 2s2p \ ^1P^o$	(19%)	1	-2646.0298076	822191.82	2.317[6]	-8.011[4]	1.385368
(100%)			2	-2639.9860584	2148641.41	1.053[6]	3.566[5]	1.486265
$1s^2 2s2p \ ^1P^o$ (81%)	+ $1s^2 2s2p \ ^3P^o$	(19%)	1	-2637.9778377	2589394.89	-5.925[5]	2.610[5]	1.085029
$1s^2 2p^2 \ ^3P$ (100%)			1	-2634.9618382	3251330.25	-6.831[4]	1.779[5]	1.488366
$1s^2 2p^2 \ ^1D$ (60%)	+ $1s^2 2p^2 \ ^3P$	(40%)	2	-2634.4684973	3359606.06	4.151[5]	2.815[5]	1.184074
$1s^2 2p^2 \ ^3P$ (60%)	+ $1s^2 2p^2 \ ^1D$	(40%)	2	-2627.9784717	4784001.99	1.854[5]	7.287[4]	1.288518
Ag XLIV								
$1s^2 2s2p \ ^3P^o$ (80%)	+ $1s^2 2s2p \ ^1P^o$	(20%)	1	-2767.7843431	846807.96	2.513[6]	-8.181[4]	1.380969
(100%)			2	-2761.1126994	2311064.46	1.137[6]	3.824[5]	1.485570
$1s^2 2s2p \ ^1P^o$ (80%)	+ $1s^2 2s2p \ ^3P^o$	(20%)	1	-2759.0660532	2760251.36	-6.524[5]	2.758[5]	1.087987
$1s^2 2p^2 \ ^3P$ (100%)			1	-2755.9478374	3444620.61	-7.579[4]	1.908[5]	1.487780
$1s^2 2p^2 \ ^1D$ (61%)	+ $1s^2 2p^2 \ ^3P$	(39%)	2	-2755.4440972	3555178.79	4.482[5]	3.071[5]	1.181170
$1s^2 2p^2 \ ^3P$ (61%)	+ $1s^2 2p^2 \ ^1D$	(39%)	2	-2748.3072609	5121533.26	1.981[5]	7.297[4]	1.290093
Cd XLV								
$1s^2 2s2p \ ^3P^o$ (79%)	+ $1s^2 2s2p \ ^1P^o$	(21%)	1	-2892.5504608	871568.06	2.722[6]	-8.342[4]	1.376724
(100%)			2	-2885.2021074	2484345.17	1.225[6]	4.094[5]	1.484859
$1s^2 2s2p \ ^1P^o$ (79%)	+ $1s^2 2s2p \ ^3P^o$	(21%)	1	-2883.1164958	2942084.00	-7.159[5]	2.910[5]	1.090757
$1s^2 2p^2 \ ^3P$ (100%)			1	-2879.8945814	3649212.45	-8.399[4]	2.043[5]	1.487183
$1s^2 2p^2 \ ^1D$ (61%)	+ $1s^2 2p^2 \ ^3P$	(39%)	2	-2879.3807467	3761986.13	4.832[5]	3.339[5]	1.178447
$1s^2 2p^2 \ ^3P$ (61%)	+ $1s^2 2p^2 \ ^1D$	(39%)	2	-2871.5482007	5481031.21	2.114[5]	7.310[4]	1.291455
In XLVI								
$1s^2 2s2p \ ^3P^o$ (79%)	+ $1s^2 2s2p \ ^1P^o$	(21%)	1	-3020.3612329	896424.65	2.944[6]	-8.497[4]	1.372630
(100%)			2	-3012.2847314	2669011.78	1.320[6]	4.378[5]	1.484131
$1s^2 2s2p \ ^1P^o$ (79%)	+ $1s^2 2s2p \ ^3P^o$	(21%)	1	-3010.1595969	3135424.88	-7.838[5]	3.069[5]	1.093341
$1s^2 2p^2 \ ^3P$ (100%)			1	-3006.8315492	3865846.90	-9.298[4]	2.184[5]	1.486573
$1s^2 2p^2 \ ^1D$ (61%)	+ $1s^2 2p^2 \ ^3P$	(39%)	2	-3006.3079314	3980767.72	5.203[5]	3.620[5]	1.175884
$1s^2 2p^2 \ ^3P$ (61%)	+ $1s^2 2p^2 \ ^1D$	(39%)	2	-2997.7281650	5863808.74	2.254[5]	7.324[4]	1.292626
Sn XLVII								
$1s^2 2s2p \ ^3P^o$ (78%)	+ $1s^2 2s2p \ ^1P^o$	(22%)	1	-3151.2382346	921716.41	3.180[6]	-8.645[4]	1.368681
(100%)			2	-3142.3794349	2865998.16	1.420[6]	4.675[5]	1.483387
$1s^2 2s2p \ ^1P^o$ (78%)	+ $1s^2 2s2p \ ^3P^o$	(22%)	1	-3140.2142157	3341208.82	-8.559[5]	3.234[5]	1.095744
$1s^2 2p^2 \ ^3P$ (100%)			1	-3136.7792895	4095087.95	-1.028[5]	2.332[5]	1.485949
$1s^2 2p^2 \ ^1D$ (62%)	+ $1s^2 2p^2 \ ^3P$	(38%)	2	-3136.2462322	4212080.51	5.596[5]	3.914[5]	1.173462
$1s^2 2p^2 \ ^3P$ (62%)	+ $1s^2 2p^2 \ ^1D$	(38%)	2	-3126.8650121	6271020.26	2.400[5]	7.341[4]	1.293624
Sb XLVIII								
$1s^2 2s2p \ ^3P^o$ (77%)	+ $1s^2 2s2p \ ^1P^o$	(23%)	1	-3285.2152208	947414.45	3.430[6]	-8.788[4]	1.364872
(100%)			2	-3275.5171461	3075895.75	1.526[6]	4.987[5]	1.482626
$1s^2 2s2p \ ^1P^o$ (77%)	+ $1s^2 2s2p \ ^3P^o$	(23%)	1	-3273.3112669	3560030.26	-9.329[5]	3.405[5]	1.097972
$1s^2 2p^2 \ ^3P$ (100%)			1	-3269.7680489	4337676.71	-1.137[5]	2.488[5]	1.485312
$1s^2 2p^2 \ ^1D$ (62%)	+ $1s^2 2p^2 \ ^3P$	(38%)	2	-3269.2258529	4456674.97	6.011[5]	4.222[5]	1.171165
$1s^2 2p^2 \ ^3P$ (62%)	+ $1s^2 2p^2 \ ^1D$	(38%)	2	-3258.9861185	6704036.85	2.553[5]	7.359[4]	1.294466
Te XLIX								

Table 1 (continued)

Level composition in LSJ coupling			J	Energy (E_h)	ΔE cm $^{-1}$	$A_J(I/\mu_I)$	B_J/Q	g_J	
$1s^2 2s2p \ ^3P^o$	(77%)	+ $1s^2 2s2p \ ^1P^o$	(23%)	1	-3422.3124065	973301.78	3.696[6]	-8.925[4]	1.361196
	(100%)			2	-3411.7151609	3299128.30	1.638[6]	5.313[5]	1.481847
$1s^2 2s2p \ ^1P^o$	(77%)	+ $1s^2 2s2p \ ^3P^o$	(23%)	1	-3409.4680457	3792313.06	-1.014[6]	3.584[5]	1.100030
$1s^2 2p^2 \ ^3P$	(100%)			1	-3405.8151666	4594027.33	-1.255[5]	2.650[5]	1.484663
$1s^2 2p^2 \ ^1D$	(62%)	+ $1s^2 2p^2 \ ^3P$	(38%)	2	-3405.2641440	4714962.81	6.450[5]	4.544[5]	1.168977
$1s^2 2p^2 \ ^3P$	(62%)	+ $1s^2 2p^2 \ ^1D$	(38%)	2	-3394.1059260	7163908.52	2.713[5]	7.380[4]	1.295167
I L									
$1s^2 2s2p \ ^3P^o$	(76%)	+ $1s^2 2s2p \ ^1P^o$	(24%)	1	-3562.5768763	999714.08	3.979[6]	-9.057[4]	1.357646
	(100%)			2	-3551.0175003	3536703.80	1.758[6]	5.653[5]	1.481052
$1s^2 2s2p \ ^1P^o$	(76%)	+ $1s^2 2s2p \ ^3P^o$	(24%)	1	-3548.7285584	4039068.45	-1.102[6]	3.769[5]	1.101927
$1s^2 2p^2 \ ^3P$	(100%)			1	-3544.9639896	4865295.80	-1.385[5]	2.820[5]	1.484001
$1s^2 2p^2 \ ^1D$	(63%)	+ $1s^2 2p^2 \ ^3P$	(37%)	2	-3544.4044722	4988095.65	6.914[5]	4.881[5]	1.166885
$1s^2 2p^2 \ ^3P$	(63%)	+ $1s^2 2p^2 \ ^1D$	(37%)	2	-3532.2647111	7652465.17	2.880[5]	7.403[4]	1.295739
Xe LI									
$1s^2 2s2p \ ^3P^o$	(76%)	+ $1s^2 2s2p \ ^1P^o$	(24%)	1	-3706.0230076	1026270.64	4.278[6]	-9.186[4]	1.354214
	(100%)			2	-3693.4354015	3788930.77	1.884[6]	6.009[5]	1.480239
$1s^2 2s2p \ ^1P^o$	(76%)	+ $1s^2 2s2p \ ^3P^o$	(24%)	1	-3691.1040478	4300603.74	-1.194[6]	3.961[5]	1.103668
$1s^2 2p^2 \ ^3P$	(100%)			1	-3687.2260650	5151722.56	-1.526[5]	2.998[5]	1.483327
$1s^2 2p^2 \ ^1D$	(63%)	+ $1s^2 2p^2 \ ^3P$	(37%)	2	-3686.6584466	5276300.40	7.404[5]	5.234[5]	1.164876
$1s^2 2p^2 \ ^3P$	(63%)	+ $1s^2 2p^2 \ ^1D$	(37%)	2	-3673.4709535	8170620.50	3.054[5]	7.428[4]	1.296197
Cs LII									
$1s^2 2s2p \ ^3P^o$	(75%)	+ $1s^2 2s2p \ ^1P^o$	(25%)	1	-3852.6947621	1053364.54	4.596[6]	-9.311[4]	1.350894
	(100%)			2	-3839.0095266	4056926.47	2.018[6]	6.381[5]	1.479410
$1s^2 2s2p \ ^1P^o$	(75%)	+ $1s^2 2s2p \ ^3P^o$	(25%)	1	-3836.6351619	4578039.27	-1.293[6]	4.162[5]	1.105262
$1s^2 2p^2 \ ^3P$	(100%)			1	-3832.6422291	5454386.70	-1.681[5]	3.184[5]	1.482640
$1s^2 2p^2 \ ^1D$	(63%)	+ $1s^2 2p^2 \ ^3P$	(37%)	2	-3832.0667530	5580689.10	7.922[5]	5.602[5]	1.162946
$1s^2 2p^2 \ ^3P$	(63%)	+ $1s^2 2p^2 \ ^1D$	(37%)	2	-3817.7620132	8720216.51	3.236[5]	7.454[4]	1.296544
Ba LIII									
$1s^2 2s2p \ ^3P^o$	(75%)	+ $1s^2 2s2p \ ^1P^o$	(25%)	1	-4002.6173924	1080708.77	4.932[6]	-9.433[4]	1.347678
	(100%)			2	-3987.7617271	4341150.35	2.160[6]	6.769[5]	1.478563
$1s^2 2s2p \ ^1P^o$	(75%)	+ $1s^2 2s2p \ ^3P^o$	(25%)	1	-3985.3437569	4871833.45	-1.398[6]	4.370[5]	1.106715
$1s^2 2p^2 \ ^3P$	(100%)			1	-3981.2340453	5773810.87	-1.850[5]	3.377[5]	1.481941
$1s^2 2p^2 \ ^1D$	(63%)	+ $1s^2 2p^2 \ ^3P$	(37%)	2	-3980.6510421	5901765.27	8.469[5]	5.986[5]	1.161081
$1s^2 2p^2 \ ^3P$	(63%)	+ $1s^2 2p^2 \ ^1D$	(37%)	2	-3965.1561527	9302500.32	3.425[5]	7.483[4]	1.296793
La LIV									
$1s^2 2s2p \ ^3P^o$	(75%)	+ $1s^2 2s2p \ ^1P^o$	(25%)	1	-4155.8355024	1108546.61	5.290[6]	-9.552[4]	1.344558
	(100%)			2	-4139.7330450	4642627.42	2.310[6]	7.174[5]	1.477698
$1s^2 2s2p \ ^1P^o$	(75%)	+ $1s^2 2s2p \ ^3P^o$	(25%)	1	-4137.2708611	5183014.31	-1.509[6]	4.586[5]	1.108034
$1s^2 2p^2 \ ^3P$	(100%)			1	-4133.0423288	6111069.85	-2.034[5]	3.579[5]	1.481229
$1s^2 2p^2 \ ^1D$	(64%)	+ $1s^2 2p^2 \ ^3P$	(36%)	2	-4132.4521230	6240605.05	9.047[5]	6.386[5]	1.159275
$1s^2 2p^2 \ ^3P$	(64%)	+ $1s^2 2p^2 \ ^1D$	(36%)	2	-4115.6905651	9919341.68	3.622[5]	7.513[4]	1.296951
Ce LV									
$1s^2 2s2p \ ^3P^o$	(74%)	+ $1s^2 2s2p \ ^1P^o$	(26%)	1	-4312.3810897	1136804.99	5.670[6]	-9.669[4]	1.341528
	(100%)			2	-4294.9517953	4962092.83	2.469[6]	7.596[5]	1.476817
$1s^2 2s2p \ ^1P^o$	(74%)	+ $1s^2 2s2p \ ^3P^o$	(26%)	1	-4292.4447880	5512317.32	-1.628[6]	4.810[5]	1.109226
$1s^2 2p^2 \ ^3P$	(100%)			1	-4288.0954639	6466883.60	-2.235[5]	3.790[5]	1.480505
$1s^2 2p^2 \ ^1D$	(64%)	+ $1s^2 2p^2 \ ^3P$	(36%)	2	-4287.4983882	6597926.57	9.657[5]	6.803[5]	1.157521
$1s^2 2p^2 \ ^3P$	(64%)	+ $1s^2 2p^2 \ ^1D$	(36%)	2	-4269.3899596	10572267.13	3.826[5]	7.546[4]	1.297025
Pr LVI									
$1s^2 2s2p \ ^3P^o$	(74%)	+ $1s^2 2s2p \ ^1P^o$	(26%)	1	-4472.2919159	1165519.73	6.072[6]	-9.785[4]	1.338580
	(100%)			2	-4453.4519051	5300424.02	2.638[6]	8.036[5]	1.475917
$1s^2 2s2p \ ^1P^o$	(74%)	+ $1s^2 2s2p \ ^3P^o$	(26%)	1	-4450.8994591	5860621.17	-1.755[6]	5.044[5]	1.110297
$1s^2 2p^2 \ ^3P$	(100%)			1	-4446.4273451	6842136.70	-2.453[5]	4.009[5]	1.479769
$1s^2 2p^2 \ ^1D$	(64%)	+ $1s^2 2p^2 \ ^3P$	(36%)	2	-4445.8237272	6974615.51	1.030[6]	7.238[5]	1.155812
$1s^2 2p^2 \ ^3P$	(64%)	+ $1s^2 2p^2 \ ^1D$	(36%)	2	-4426.2843754	11263007.42	4.039[5]	7.580[4]	1.297022
Nd LVII									
$1s^2 2s2p \ ^3P^o$	(73%)	+ $1s^2 2s2p \ ^1P^o$	(27%)	1	-4635.6071229	1194658.52	6.500[6]	-9.899[4]	1.335708
	(100%)			2	-4615.2685288	5658463.82	2.817[6]	8.494[5]	1.475000
$1s^2 2s2p \ ^1P^o$	(73%)	+ $1s^2 2s2p \ ^3P^o$	(27%)	1	-4612.6700270	6228769.03	-1.890[6]	5.286[5]	1.111255
$1s^2 2p^2 \ ^3P$	(100%)			1	-4608.0729143	7237718.61	-2.692[5]	4.237[5]	1.479020
$1s^2 2p^2 \ ^1D$	(64%)	+ $1s^2 2p^2 \ ^3P$	(36%)	2	-4607.4631004	7371557.31	1.098[6]	7.690[5]	1.154142
$1s^2 2p^2 \ ^3P$	(64%)	+ $1s^2 2p^2 \ ^1D$	(36%)	2	-4586.4047634	11993327.91	4.260[5]	7.616[4]	1.296946
Pm LVIII									
$1s^2 2s2p \ ^3P^o$	(73%)	+ $1s^2 2s2p \ ^1P^o$	(27%)	1	-4802.3632779	1224199.61	6.952[6]	-1.001[5]	1.332906
	(100%)			2	-4780.4340948	6037098.85	3.006[6]	8.971[5]	1.474065
$1s^2 2s2p \ ^1P^o$	(73%)	+ $1s^2 2s2p \ ^3P^o$	(27%)	1	-4777.7889110	6617649.56	-2.033[6]	5.538[5]	1.112104
$1s^2 2p^2 \ ^3P$	(100%)			1	-4773.0648213	7654467.39	-2.951[5]	4.475[5]	1.478259

Table 1 (continued)

Level composition in LSJ coupling			J	Energy (E_h)	ΔE cm $^{-1}$	$A_J(I/\mu_I)$	B_J/Q	g_J
$1s^2 2p^2$ 1D (64%)	$+ 1s^2 2p^2$ 3P (36%)		2	-4772.4491582	7789589.80	1.170[6]	8.161[5]	1.152507
$1s^2 2p^2$ 3P (64%)	$+ 1s^2 2p^2$ 1D (36%)		2	-4749.7796168	12764978.91	4.490[5]	7.654[4]	1.296802
Sm LXIX								
$1s^2 2s2p$ $^3P^o$ (73%)	$+ 1s^2 2s2p$ $^1P^o$ (27%)		1	-4972.5969979	1254189.38	7.431[6]	-1.012[5]	1.330167
(100%)			2	-4948.9809177	6437319.73	3.205[6]	9.467[5]	1.473112
$1s^2 2s2p$ $^1P^o$ (73%)	$+ 1s^2 2s2p$ $^3P^o$ (27%)		1	-4946.2884289	7028252.69	-2.185[6]	5.799[5]	1.112852
$1s^2 2p^2$ 3P (100%)			1	-4941.4361115	8093213.25	-3.233[5]	4.722[5]	1.477486
$1s^2 2p^2$ 1D (64%)	$+ 1s^2 2p^2$ 3P (36%)		2	-4940.8149481	8229542.85	1.246[6]	8.652[5]	1.150901
$1s^2 2p^2$ 3P (64%)	$+ 1s^2 2p^2$ 1D (36%)		2	-4916.4376413	13579743.12	4.728[5]	7.694[4]	1.296596
Eu LX								
$1s^2 2s2p$ $^3P^o$ (73%)	$+ 1s^2 2s2p$ $^1P^o$ (27%)		1	-5146.3754059	1284677.47	7.941[6]	-1.024[5]	1.327486
(100%)			2	-5120.9715835	6860171.87	3.417[6]	9.983[5]	1.472140
$1s^2 2s2p$ $^1P^o$ (73%)	$+ 1s^2 2s2p$ $^3P^o$ (27%)		1	-5118.2311370	7461630.33	-2.348[6]	6.070[5]	1.113503
$1s^2 2p^2$ 3P (100%)			1	-5113.2465256	8555626.05	-3.539[5]	4.979[5]	1.476700
$1s^2 2p^2$ 1D (64%)	$+ 1s^2 2p^2$ 3P (36%)		2	-5112.6202179	8693084.71	1.326[6]	9.161[5]	1.149322
$1s^2 2p^2$ 3P (64%)	$+ 1s^2 2p^2$ 1D (36%)		2	-5086.4340677	14440280.19	4.975[5]	7.736[4]	1.296331
Gd LXI								
$1s^2 2s2p$ $^3P^o$ (72%)	$+ 1s^2 2s2p$ $^1P^o$ (28%)		1	-5323.7143725	1315561.02	8.480[6]	-1.035[5]	1.324856
(100%)			2	-5296.4173535	7306564.04	3.641[6]	1.052[6]	1.471151
$1s^2 2s2p$ $^1P^o$ (72%)	$+ 1s^2 2s2p$ $^3P^o$ (28%)		1	-5293.6283166	7918686.85	-2.521[6]	6.352[5]	1.114063
$1s^2 2p^2$ 3P (100%)			1	-5288.5103691	9041946.48	-3.873[5]	5.246[5]	1.475903
$1s^2 2p^2$ 1D (65%)	$+ 1s^2 2p^2$ 3P (35%)		2	-5287.8792769	9180455.19	1.410[6]	9.691[5]	1.147764
$1s^2 2p^2$ 3P (65%)	$+ 1s^2 2p^2$ 1D (35%)		2	-5259.7785302	15347856.04	5.232[5]	7.779[4]	1.296011
Tb LXII								
$1s^2 2s2p$ $^3P^o$ (72%)	$+ 1s^2 2s2p$ $^1P^o$ (28%)		1	-5504.6875783	1347121.96	9.053[6]	-1.046[5]	1.322274
(100%)			2	-5475.3869855	7777858.57	3.879[6]	1.108[6]	1.470143
$1s^2 2s2p$ $^1P^o$ (72%)	$+ 1s^2 2s2p$ $^3P^o$ (28%)		1	-5472.5469929	8400791.77	-2.705[6]	6.644[5]	1.114536
$1s^2 2p^2$ 3P (100%)			1	-5467.2941503	9554030.53	-4.235[5]	5.524[5]	1.475093
$1s^2 2p^2$ 1D (65%)	$+ 1s^2 2p^2$ 3P (35%)		2	-5466.6586417	9693508.56	1.499[6]	1.024[6]	1.146225
$1s^2 2p^2$ 3P (65%)	$+ 1s^2 2p^2$ 1D (35%)		2	-5436.5326055	16305409.05	5.497[5]	7.825[4]	1.295638
Dy LXIII								
$1s^2 2s2p$ $^3P^o$ (72%)	$+ 1s^2 2s2p$ $^1P^o$ (28%)		1	-5689.3195308	1379283.50	9.660[6]	-1.057[5]	1.319733
(100%)			2	-5657.8999813	8275077.34	4.130[6]	1.166[6]	1.469117
$1s^2 2s2p$ $^1P^o$ (72%)	$+ 1s^2 2s2p$ $^3P^o$ (28%)		1	-5655.0117746	8908965.41	-2.901[6]	6.947[5]	1.114927
$1s^2 2p^2$ 3P (100%)			1	-5649.6198401	10092358.23	-4.631[5]	5.812[5]	1.474273
$1s^2 2p^2$ 1D (65%)	$+ 1s^2 2p^2$ 3P (35%)		2	-5648.9802749	10232726.57	1.594[6]	1.081[6]	1.144700
$1s^2 2p^2$ 3P (65%)	$+ 1s^2 2p^2$ 1D (35%)		2	-5616.7131988	17314530.98	5.771[5]	7.874[4]	1.295216
Ho LXIV								
$1s^2 2s2p$ $^3P^o$ (72%)	$+ 1s^2 2s2p$ $^1P^o$ (28%)		1	-5877.6840997	1411935.58	1.031[7]	-1.069[5]	1.317230
(100%)			2	-5844.0248762	8799281.03	4.397[6]	1.226[6]	1.468072
$1s^2 2s2p$ $^1P^o$ (72%)	$+ 1s^2 2s2p$ $^3P^o$ (28%)		1	-5841.0860806	9444272.09	-3.111[6]	7.261[5]	1.115240
$1s^2 2p^2$ 3P (100%)			1	-5835.5525155	10658749.21	-5.059[5]	6.111[5]	1.473439
$1s^2 2p^2$ 1D (65%)	$+ 1s^2 2p^2$ 3P (35%)		2	-5834.9092812	10799922.83	1.693[6]	1.141[6]	1.143189
$1s^2 2p^2$ 3P (65%)	$+ 1s^2 2p^2$ 1D (35%)		2	-5800.3801030	18378201.26	6.055[5]	7.923[4]	1.294747
Er LXV								
$1s^2 2s2p$ $^3P^o$ (71%)	$+ 1s^2 2s2p$ $^1P^o$ (29%)		1	-6069.8223964	1445154.51	1.099[7]	-1.080[5]	1.314759
(100%)			2	-6033.7973151	9351745.71	4.679[6]	1.288[6]	1.467009
$1s^2 2s2p$ $^1P^o$ (71%)	$+ 1s^2 2s2p$ $^3P^o$ (29%)		1	-6030.8072447	10007990.30	-3.334[6]	7.586[5]	1.115481
$1s^2 2p^2$ 3P (100%)			1	-6025.1293652	11254140.76	-5.525[5]	6.422[5]	1.472594
$1s^2 2p^2$ 1D (65%)	$+ 1s^2 2p^2$ 3P (35%)		2	-6024.4828476	11396034.96	1.798[6]	1.202[6]	1.141689
$1s^2 2p^2$ 3P (65%)	$+ 1s^2 2p^2$ 1D (35%)		2	-5987.5649813	19498569.83	6.349[5]	7.975[4]	1.294234
Tm LXVI								
$1s^2 2s2p$ $^3P^o$ (71%)	$+ 1s^2 2s2p$ $^1P^o$ (29%)		1	-6265.7796292	1478827.36	1.172[7]	-1.093[5]	1.312323
(100%)			2	-6227.2568412	9933601.80	4.977[6]	1.353[6]	1.465933
$1s^2 2s2p$ $^1P^o$ (71%)	$+ 1s^2 2s2p$ $^3P^o$ (29%)		1	-6224.2149486	10601220.06	-3.570[6]	7.922[5]	1.115642
$1s^2 2p^2$ 3P (100%)			1	-6218.3903996	11879560.75	-6.027[5]	6.745[5]	1.471736
$1s^2 2p^2$ 1D (65%)	$+ 1s^2 2p^2$ 3P (35%)		2	-6217.7409995	12022087.61	1.909[6]	1.266[6]	1.140197
$1s^2 2p^2$ 3P (65%)	$+ 1s^2 2p^2$ 1D (35%)		2	-6178.3021567	20677912.83	6.655[5]	8.028[4]	1.293680
Yb LXVII								
$1s^2 2s2p$ $^3P^o$ (71%)	$+ 1s^2 2s2p$ $^1P^o$ (29%)		1	-6465.6162027	1513093.68	1.249[7]	-1.105[5]	1.309907
(100%)			2	-6424.4578167	10546315.00	5.293[6]	1.420[6]	1.464832
$1s^2 2s2p$ $^1P^o$ (71%)	$+ 1s^2 2s2p$ $^3P^o$ (29%)		1	-6421.3632414	11225495.76	-3.822[6]	8.272[5]	1.115748
$1s^2 2p^2$ 3P (100%)			1	-6415.3900712	12536455.04	-6.574[5]	7.079[5]	1.470867
$1s^2 2p^2$ 1D (65%)	$+ 1s^2 2p^2$ 3P (35%)		2	-6414.7381775	12679529.16	2.027[6]	1.333[6]	1.138710
$1s^2 2p^2$ 3P (65%)	$+ 1s^2 2p^2$ 1D (35%)		2	-6372.6399828	21919014.67	6.970[5]	8.084[4]	1.293086
Lu LXVIII								
$1s^2 2s2p$ $^3P^o$ (71%)	$+ 1s^2 2s2p$ $^1P^o$ (29%)		1	-6669.4030550	1548020.92	1.331[7]	-1.117[5]	1.307511

Table 1 (continued)

Level composition in LSJ coupling			J	Energy (E_h)	$\Delta E \text{ cm}^{-1}$	$A_J(I/\mu_I)$	B_J/Q	g_J
(100%)			2	-6625.4649364	11191323.03	5.629[6]	1.489[6]	1.463710
$1s^2 2s2p \ ^1P^o$	(71%)	+ $1s^2 2s2p \ ^3P^o$	(29%)	1	-6622.3169560	11882224.85	-4.092[6]	8.634[5]
$1s^2 2p^2 \ ^3P$	(100%)			1	-6616.1916040	13226584.18	-7.169[5]	7.426[5]
$1s^2 2p^2 \ ^1D$	(65%)	+ $1s^2 2p^2 \ ^3P$	(35%)	2	-6615.5376180	13370117.51	2.151[6]	1.401[6]
$1s^2 2p^2 \ ^3P$	(65%)	+ $1s^2 2p^2 \ ^1D$	(35%)	2	-6570.6354568	23225002.50	7.295[5]	8.142[4]
Hf LXIX								
$1s^2 2s2p \ ^3P^o$	(71%)	+ $1s^2 2s2p \ ^1P^o$	(29%)	1	-6877.1773115	1583257.44	1.418[7]	-1.129[5]
(100%)				2	-6830.3089193	11869680.23	5.983[6]	1.562[6]
$1s^2 2s2p \ ^1P^o$	(71%)	+ $1s^2 2s2p \ ^3P^o$	(29%)	1	-6827.1067834	12572467.81	-4.379[6]	9.010[5]
$1s^2 2p^2 \ ^3P$	(100%)			1	-6820.8271405	13950690.07	-7.814[5]	7.785[5]
$1s^2 2p^2 \ ^1D$	(65%)	+ $1s^2 2p^2 \ ^3P$	(35%)	2	-6820.1714727	14094592.52	2.283[6]	1.473[6]
$1s^2 2p^2 \ ^3P$	(65%)	+ $1s^2 2p^2 \ ^1D$	(35%)	2	-6772.3142638	24598035.50	7.631[5]	8.203[4]
Ta LXX								
$1s^2 2s2p \ ^3P^o$	(70%)	+ $1s^2 2s2p \ ^1P^o$	(30%)	1	-7089.0410978	1618591.81	1.510[7]	-1.140[5]
(100%)				2	-7039.0845004	12582797.28	6.362[6]	1.636[6]
$1s^2 2s2p \ ^1P^o$	(70%)	+ $1s^2 2s2p \ ^3P^o$	(30%)	1	-7035.8274523	13297636.70	-4.687[6]	9.399[5]
$1s^2 2p^2 \ ^3P$	(100%)			1	-7029.3861295	14711343.59	-8.515[5]	8.158[5]
$1s^2 2p^2 \ ^1D$	(65%)	+ $1s^2 2p^2 \ ^3P$	(35%)	2	-7028.7291971	14855523.59	2.422[6]	1.546[6]
$1s^2 2p^2 \ ^3P$	(65%)	+ $1s^2 2p^2 \ ^1D$	(35%)	2	-6977.7589077	26042208.75	7.977[5]	8.266[4]
W LXXI								
$1s^2 2s2p \ ^3P^o$	(70%)	+ $1s^2 2s2p \ ^1P^o$	(30%)	1	-7317.3151885	271570.75	1.608[7]	-1.153[5]
(100%)				2	-7264.1537164	11939164.91	6.761[6]	1.714[6]
$1s^2 2s2p \ ^1P^o$	(70%)	+ $1s^2 2s2p \ ^3P^o$	(30%)	1	-7260.8409814	12666226.18	-5.014[6]	9.803[5]
$1s^2 2p^2 \ ^3P$	(100%)			1	-7241.8978000	16823773.81	-9.276[5]	8.543[5]
$1s^2 2p^2 \ ^1D$	(65%)	+ $1s^2 2p^2 \ ^3P$	(35%)	2	-7241.2400286	16968137.93	2.569[6]	1.623[6]
$1s^2 2p^2 \ ^3P$	(65%)	+ $1s^2 2p^2 \ ^1D$	(35%)	2	-7186.9916243	28874286.14	8.335[5]	8.332[4]

Table 2

Be-like boron: comparison of hyperfine interaction constants $A_J(I/\mu_I)$ (MHz per units of μ_N) and B_J/Q (MHz/barn) with Litzén *et al.* [43] for the $2s2p$ and $2p^2$ states.

Designation	$A_1(I/\mu_I)$		$A_2(I/\mu_I)$		B_1/Q		B_2/Q	
	Litzén <i>et al.</i>	This work						
$2s2p\ ^3P^o$	512.60	513.2	443.00	442.8	-51.32	-52.47	102.7	104.9
$2s2p\ ^1P^o$	101.20	101.5			94.23	94.41		
$2p^2\ ^3P$	-62.819	-63.09	6.081	6.098	51.13	51.83	-102.3	-103.8
$2p^2\ ^1D$			99.859	100.1			189.0	188.7

Table 3

Comparison of calculated hyperfine interaction constants $A_J(I/\mu_I)$ (MHz per unit of μ_N) of the $1s^22s2p\ ^3P_1^o$ state for Be-like ions with the results obtained by Marques *et al.* [46] and Cheng *et al.* [47].

$A_J(I/\mu_I)$								
Z	Marques <i>et al.</i> [46]	Cheng <i>et al.</i> [47]	This work	Z	Marques <i>et al.</i> [46]	Cheng <i>et al.</i> [47]	This work	
5	4.669[2]		5.132[2]	40	1.347[6]	1.3599[6]	1.365[6]	
6	1.040[3]	1.1151[3]	1.114[3]	41	1.479[6]	1.4935[6]	1.499[6]	
7	1.948[3]	2.0558[3]	2.056[3]	42	1.621[6]	1.6362[6]	1.642[6]	
8	3.269[3]	3.4158[3]	3.417[3]	43	1.773[6]	1.7884[6]	1.795[6]	
9	5.082[3]	5.2782[3]	5.280[3]	44	1.934[6]	1.9504[6]	1.958[6]	
10	7.481[3]	7.7328[3]	7.736[3]	45	2.106[6]	2.1230[6]	2.132[6]	
11	1.056[4]	1.0877[4]	1.088[4]	46	2.290[6]	2.3065[6]	2.132[6]	
12	1.443[4]	1.4819[4]	1.483[4]	47	2.485[6]	2.5019[6]	2.513[6]	
13	1.919[4]	1.9679[4]	1.969[4]	48	2.691[6]	2.7092[6]	2.722[6]	
14	2.499[4]	2.5590[4]	2.561[4]	49	2.911[6]	2.9296[6]	2.944[6]	
15	3.200[4]	3.2704[4]	3.273[4]	50	3.145[6]	3.1635[6]	3.180[6]	
16	4.034[4]	4.1191[4]	4.122[4]	51	3.393[6]	3.4118[6]	3.430[6]	
17	5.022[4]	5.1237[4]	5.128[4]	52	3.657[6]	3.6750[6]	3.696[6]	
18	/	6.3055[4]	6.312[4]	53	3.936[6]	3.9551[6]	3.979[6]	
19	7.546[4]	7.6885[4]	7.697[4]	54	4.233[6]	4.2514[6]	4.278[6]	
20	9.127[4]	9.2972[4]	9.309[4]	55	4.548[6]	4.5664[6]	4.596[6]	
21	1.096[5]	1.1106[5]	1.118[5]	56	4.882[6]	4.8994[6]	4.932[6]	
22	1.308[5]	1.3251[5]	1.333[5]	57	5.236[6]	5.2534[6]	5.290[6]	
23	1.550[5]	1.5764[5]	1.579[5]	58	/	5.6286[6]	5.670[6]	
24	1.827[5]	1.8572[5]	1.861[5]	59	6.013[6]	6.0268[6]	6.072[6]	
25	2.142[5]	2.1759[5]	2.180[5]	60	6.437[6]	6.4480[6]	6.500[6]	
26	2.497[5]	2.5360[5]	2.542[5]	61	/	6.8953[6]	6.952[6]	
27	2.897[5]	2.9406[5]	2.948[5]	62	7.360[6]	7.3677[6]	7.431[6]	
28	3.344[5]	3.3932[5]	3.402[5]	63	7.865[6]	7.8705[6]	7.941[6]	
29	3.841[5]	3.8966[5]	3.907[5]	64	8.399[6]	8.4010[6]	8.480[6]	
30	4.392[5]	4.4540[5]	4.466[5]	65	8.968[6]	8.9658[6]	9.052[6]	
31	5.000[5]	5.0681[5]	5.082[5]	66	9.574[6]	9.5631[6]	9.660[6]	
32	5.666[5]	5.7418[5]	5.757[5]	67	1.021[7]	1.0197[7]	1.030[7]	
33	6.395[5]	6.4779[5]	6.496[5]	68	1.090[7]	1.0870[7]	1.099[7]	
34	7.188[5]	7.2780[5]	7.298[5]	69	1.161[7]	1.1584[7]	1.172[7]	
35	1.717[6]	8.1464[5]	8.170[5]	70	1.238[7]	1.2340[7]	1.249[7]	
36	8.980[5]	9.0843[5]	9.112[5]	71	1.319[7]	1.3144[7]	1.331[7]	
37	9.983[5]	1.0096[6]	1.013[6]	72	1.424[7]	1.3995[7]	1.418[7]	
38	1.106[6]	1.1183[6]	1.122[6]	73	1.497[7]	1.4900[7]	1.510[7]	
39	1.222[6]	1.2350[6]	1.239[6]	74	1.594[7]	1.5861[7]	1.606[7]	

Table 4

Total energies (in E_h), excitation energies (in cm^{-1}), hyperfine magnetic dipole constants $A_J(I/\mu_I)$ (MHz per unit of μ_N), electric quadrupole constants B_J/Q (MHz/barn), and Landé g_J -factors for levels in the boron isoelectronic sequence ($8 \leq Z \leq 30$ and $Z = 36, 42$). For each of the many-electron wave functions, the leading components are given in the LSJ coupling scheme. The number in square brackets is the power of 10. See page 17 for Explanation of Tables.

Level composition in LSJ coupling			J	Energy (E_h)	$\Delta E \text{ cm}^{-1}$	$A_J(I/\mu_I)$	B_J/Q	g_J
O IV								
$1s^2 2s^2 2p \ ^2P^o$	(95%)	$+ 1s^2 2p^3 \ ^2P^o$	(4%)	1/2	-71.3006468	0.00	2.174[3]	0.0
	(95%)	$+ 1s^2 2p^3 \ ^2P^o$	(4%)	3/2	-71.2988722	389.49	4.262[2]	7.426[2]
$1s^2 2s2p^2 \ ^4P$	(100%)			1/2	-70.9755351	71353.76	4.474[3]	0.0
	(100%)			3/2	-70.9749349	71485.49	2.083[3]	6.101[2]
	(100%)			5/2	-70.9740914	71670.63	2.115[3]	-7.643[2]
$1s^2 2s2p^2 \ ^2D$	(98%)	$+ 1s^2 2s^2 3d \ ^2D$	(1%)	5/2	-70.7218546	127030.20	2.432[3]	1.490[3]
	(98%)	$+ 1s^2 2s^2 3d \ ^2D$	(1%)	3/2	-70.7217904	127044.30	-8.796[2]	1.043[3]
$1s^2 2s2p^2 \ ^2S$	(99%)			1/2	-70.5504716	164644.42	9.060[3]	0.0
$1s^2 2s2p^2 \ ^2P$	(98%)	$+ 1s^2 2p^2 3d \ ^2P$	(1%)	1/2	-70.4776245	180632.51	1.438[3]	0.0
	(98%)	$+ 1s^2 2p^2 3d \ ^2P$	(1%)	3/2	-70.4765123	180876.62	-5.146[2]	-7.657[2]
$1s^2 2p^3 \ ^4S^o$	(99%)			3/2	-70.2459347	231482.54	-4.667[2]	-2.580[-3]
$1s^2 2p^3 \ ^2D^o$	(97%)	$+ 1s^2 2s2p3d \ ^2D^o$	(2%)	5/2	-70.1376733	255243.17	6.484[2]	-4.392[1]
	(97%)	$+ 1s^2 2s2p3d \ ^2D^o$	(2%)	3/2	-70.1375436	255271.63	5.486[2]	-1.526[1]
$1s^2 2p^3 \ ^2P^o$	(94%)	$+ 1s^2 2s^2 2p \ ^2P^o$	(4%)	1/2	-69.9825047	289298.75	2.232[3]	0.0
	(94%)	$+ 1s^2 2s^2 2p \ ^2P^o$	(4%)	3/2	-69.9824759	289305.06	2.583[2]	4.459[1]
F V								
$1s^2 2s^2 2p \ ^2P^o$	(96%)	$+ 1s^2 2p^3 \ ^2P^o$	(4%)	1/2	-92.3744980	0.00	3.531[3]	0.0
	(96%)	$+ 1s^2 2p^3 \ ^2P^o$	(4%)	3/2	-92.3710819	749.75	6.902[2]	1.213[3]
$1s^2 2s2p^2 \ ^4P$	(100%)			1/2	-91.9840119	85701.79	6.904[3]	0.0
	(100%)			3/2	-91.9828551	85955.69	3.225[3]	9.920[2]
	(100%)			5/2	-91.9811967	86319.66	3.302[3]	-1.243[3]
$1s^2 2s2p^2 \ ^2D$	(99%)			5/2	-91.6775124	152970.67	3.808[3]	1.200162
	(99%)			3/2	-91.6774085	152993.48	-1.275[3]	1.708[3]
$1s^2 2s2p^2 \ ^2S$	(99%)			1/2	-91.4731655	197819.62	1.399[4]	0.0
$1s^2 2s2p^2 \ ^2P$	(98%)	$+ 1s^2 2p^2 3d \ ^2P$	(1%)	1/2	-91.3947240	215035.55	2.237[3]	0.0
	(98%)	$+ 1s^2 2p^2 3d \ ^2P$	(1%)	3/2	-91.3925896	215503.99	-7.307[2]	-1.253[3]
$1s^2 2p^3 \ ^4S^o$	(100%)			3/2	-91.1152847	276365.39	-6.524[2]	-4.997[-3]
$1s^2 2p^3 \ ^2D^o$	(98%)	$+ 1s^2 2s2p3d \ ^2D^o$	(1%)	5/2	-90.9742390	307321.32	1.077[3]	-5.397[1]
	(98%)	$+ 1s^2 2s2p3d \ ^2D^o$	(1%)	3/2	-90.9740253	307368.24	8.851[2]	3.769
$1s^2 2p^3 \ ^2P^o$	(95%)	$+ 1s^2 2s^2 2p \ ^2P^o$	(3%)	1/2	-90.7904091	347667.33	3.609[3]	0.0
	(95%)	$+ 1s^2 2s^2 2p \ ^2P^o$	(3%)	3/2	-90.7903223	347686.38	4.514[2]	4.313[1]
Ne VI								
$1s^2 2s^2 2p \ ^2P^o$	(96%)	$+ 1s^2 2p^3 \ ^2P^o$	(3%)	1/2	-116.2144066	0.00	5.348[3]	0.0
	(96%)	$+ 1s^2 2p^3 \ ^2P^o$	(3%)	3/2	-116.2084301	1311.69	1.043[3]	1.844[3]
$1s^2 2s2p^2 \ ^4P$	(100%)			1/2	-115.7578445	100203.78	1.009[4]	0.0
	(100%)			3/2	-115.7558093	100650.45	4.724[3]	1.505[3]
	(100%)			5/2	-115.7528583	101298.12	4.868[3]	-1.887[3]
$1s^2 2s2p^2 \ ^2D$	(99%)			5/2	-115.3983960	179093.62	5.618[3]	3.717[3]
	(99%)			3/2	-115.3982489	179125.89	-1.767[3]	2.602[3]
$1s^2 2s2p^2 \ ^2S$	(99%)			1/2	-115.1614234	231103.08	2.040[4]	0.0
$1s^2 2s2p^2 \ ^2P$	(99%)			1/2	-115.0778033	249455.56	3.290[3]	0.0
	(99%)			3/2	-115.0740873	250271.13	-1.000[3]	-1.906[3]
$1s^2 2p^3 \ ^4S^o$	(100%)			3/2	-114.7492420	321566.45	-8.678[2]	-1.168[-2]
$1s^2 2p^3 \ ^2D^o$	(99%)	$+ 1s^2 2s2p3d \ ^2D^o$	(1%)	5/2	-114.5757414	359645.42	1.660[3]	-6.560[1]
	(99%)	$+ 1s^2 2s2p3d \ ^2D^o$	(1%)	3/2	-114.5754351	359712.64	1.330[3]	5.077[1]
$1s^2 2p^3 \ ^2P^o$	(95%)	$+ 1s^2 2s^2 2p \ ^2P^o$	(3%)	1/2	-114.3633952	406250.02	5.447[3]	0.0
	(95%)	$+ 1s^2 2s^2 2p \ ^2P^o$	(3%)	3/2	-114.3631900	406295.06	7.242[2]	1.837[1]
Na VII								
$1s^2 2s^2 2p \ ^2P^o$	(96%)	$+ 1s^2 2p^3 \ ^2P^o$	(3%)	1/2	-142.8237703	0.00	7.692[3]	0.0
	(96%)	$+ 1s^2 2p^3 \ ^2P^o$	(3%)	3/2	-142.8140130	2141.49	1.498[3]	2.659[3]
$1s^2 2s2p^2 \ ^4P$	(100%)			1/2	-142.3001524	114920.84	1.415[4]	0.0
	(100%)			3/2	-142.2968073	115655.00	6.633[3]	2.168[3]
	(100%)			5/2	-142.2919322	116724.97	6.866[3]	-2.721[3]
$1s^2 2s2p^2 \ ^2D$	(99%)			5/2	-141.8873335	205524.11	7.923[3]	5.371[3]
	(99%)			3/2	-141.8871517	205564.02	-2.365[3]	3.759[3]
$1s^2 2s2p^2 \ ^2S$	(99%)			1/2	-141.6179937	264637.36	2.847[4]	0.0
$1s^2 2s2p^2 \ ^2P$	(99%)			1/2	-141.5295801	284041.90	4.655[3]	0.0
	(99%)			3/2	-141.5235794	285358.92	-1.333[3]	-2.750[3]
$1s^2 2p^3 \ ^4S^o$	(100%)			3/2	-141.1503494	367273.41	-1.113[3]	-1.918[-2]
$1s^2 2p^3 \ ^2D^o$	(99%)	$+ 1s^2 2s2p3d \ ^2D^o$	(1%)	5/2	-140.9445975	412430.74	2.423[3]	-7.864[1]
	(99%)	$+ 1s^2 2s2p3d \ ^2D^o$	(1%)	3/2	-140.9442158	412514.53	1.899[3]	1.473[2]
$1s^2 2p^3 \ ^2P^o$	(96%)	$+ 1s^2 2s^2 2p \ ^2P^o$	(3%)	1/2	-140.7038601	465266.50	7.815[3]	0.0

Table 4 (continued)

Level composition in LSJ coupling			J	Energy (E_h)	ΔE cm $^{-1}$	$A_J(I/\mu_I)$	B_J/Q	g_J	
	(96%)	+ 1s 2 2s 2 2p 2 P o	(3%)	3/2	-140.7034241	465362.18	1.089[3]	-5.064[1]	1.333259
Mg VIII									
1s 2 2s 2 2p 2 P o	(96%)	+ 1s 2 2p 3 2P o	(3%)	1/2	-172.2522077	0.00	1.064[4]	0.0	0.665084
	(96%)	+ 1s 2 2p 3 2P o	(3%)	3/2	-172.2359746	3562.75	2.069[3]	3.684[3]	1.333448
1s 2 2s2p 2 4P	(100%)			1/2	-171.6599151	129993.19	1.920[4]	0.0	2.669280
	(100%)			3/2	-171.6543128	131222.75	9.008[3]	3.003[3]	1.734263
1s 2 2s2p 2 2D	(100%)			5/2	-171.6453553	133188.70	9.351[3]	-3.771[3]	1.600509
	(99%)			3/2	-171.1917122	232751.84	-3.070[3]	5.218[3]	0.799182
	(99%)			5/2	-171.1915763	232781.68	1.078[4]	7.455[3]	1.199916
1s 2 2s2p 2 2S	(99%)	+ 1s 2 2s2p 2 2P	(1%)	1/2	-170.8912185	298702.60	3.827[4]	0.0	1.989283
1s 2 2s2p 2 2P	(98%)	+ 1s 2 2s2p 2 2S	(1%)	1/2	-170.7983140	319092.76	6.473[3]	0.0	0.677885
	(99%)			3/2	-170.7880871	321337.31	-1.748[3]	-3.814[3]	1.333250
1s 2 2p 3 4S o	(100%)			3/2	-170.3653716	414112.65	-1.389[3]	-1.728[-1]	2.001215
1s 2 2p 3 2D o	(99%)			3/2	-170.1273282	466357.13	2.606[3]	3.541[2]	0.800110
	(99%)			5/2	-170.1267928	466474.64	3.390[3]	-9.278[1]	1.199786
1s 2 2p 3 2P o	(96%)	+ 1s 2 2s 2 2p 2 P o	(3%)	1/2	-169.8589223	525265.42	1.079[4]	0.0	0.665096
	(96%)	+ 1s 2 2s 2 2p 2 P o	(3%)	3/2	-169.8577120	525531.04	1.560[3]	-2.258[2]	1.332721
Al IX									
1s 2 2s 2 2p 2 P o	(97%)	+ 1s 2 2p 3 2P o	(3%)	1/2	-204.3677652	0.00	1.424[4]	0.0	0.664903
	(96%)	+ 1s 2 2p 3 2P o	(3%)	3/2	-204.3454432	4899.11	2.766[3]	4.935[3]	1.333303
1s 2 2s2p 2 4P	(100%)			1/2	-203.7060540	145228.82	2.535[4]	0.0	2.668943
	(100%)			3/2	-203.6982488	146941.86	1.190[4]	4.021[3]	1.734083
	(100%)			5/2	-203.6869237	149427.43	1.238[4]	-5.051[3]	1.600270
1s 2 2s2p 2 2D	(99%)			5/2	-203.1838311	259843.49	1.426[4]	9.998[3]	1.199842
	(99%)			3/2	-203.1837081	259870.49	-3.909[3]	6.999[3]	0.799179
1s 2 2s2p 2 2S	(98%)	+ 1s 2 2s2p 2 2P	(2%)	1/2	-202.8507077	332955.62	5.002[4]	0.0	1.979994
1s 2 2s2p 2 2P	(98%)	+ 1s 2 2s2p 2 2S	(2%)	1/2	-202.7534770	354295.29	8.830[3]	0.0	0.687019
	(99%)			3/2	-202.7403253	357181.75	-2.242[3]	-5.109[3]	1.332996
1s 2 2p 3 4S o	(100%)			3/2	-202.2674885	460957.44	-1.696[3]	1.460[-1]	2.000880
1s 2 2p 3 2D o	(99%)			5/2	-201.9975386	520204.58	4.582[3]	-1.087[2]	1.199635
	(99%)			3/2	-201.9972745	520262.54	3.466[3]	6.263[2]	0.800581
1s 2 2p 3 2P o	(96%)	+ 1s 2 2s 2 2p 2 P o	(3%)	1/2	-201.7002951	585442.00	1.442[4]	0.0	0.664917
	(96%)	+ 1s 2 2s 2 2p 2 P o	(3%)	3/2	-201.6986870	585794.92	2.148[3]	-4.575[2]	1.332162
Si X									
1s 2 2s 2 2p 2 P o	(97%)	+ 1s 2 2p 3 2P o	(3%)	1/2	-239.3122890	0.00	1.859[4]	0.0	0.664704
	(97%)	+ 1s 2 2p 3 2P o	(3%)	3/2	-239.2803928	7000.41	3.604[3]	6.444[3]	1.333143
1s 2 2s2p 2 4P	(100%)			1/2	-238.5789330	160953.04	3.276[4]	0.0	2.668478
	(100%)			3/2	-238.5676404	163431.48	1.536[4]	5.250[3]	1.733861
	(100%)			5/2	-238.5513952	166996.89	1.602[4]	-6.596[3]	1.599954
1s 2 2s2p 2 2D	(99%)			3/2	-238.0000781	287997.00	-4.867[3]	9.147[3]	0.799271
	(100%)			5/2	-238.0000140	288011.06	1.841[4]	1.307[4]	1.199814
1s 2 2s2p 2 2S	(97%)	+ 1s 2 2s2p 2 2P	(3%)	1/2	-237.6358161	367943.26	6.338[4]	0.0	1.960914
1s 2 2s2p 2 2P	(96%)	+ 1s 2 2s2p 2 2S	(3%)	1/2	-237.5340012	390289.05	1.220[4]	0.0	0.706023
	(99%)			3/2	-237.5158806	394266.05	-2.855[3]	-6.669[3]	1.332645
1s 2 2p 3 4S o	(100%)			3/2	-236.9916034	509331.61	-2.032[3]	6.944[-1]	2.000375
1s 2 2p 3 2D o	(99%)			3/2	-236.6896928	575593.32	4.489[3]	1.110[3]	0.801596
	(99%)			5/2	-236.6895686	575620.57	6.027[3]	-1.257[2]	1.199469
1s 2 2p 3 2P o	(96%)	+ 1s 2 2s 2 2p 2 P o	(3%)	1/2	-236.3641953	647031.75	1.879[4]	0.0	0.664720
	(96%)	+ 1s 2 2s 2 2p 2 P o	(3%)	3/2	-236.3613352	647659.49	2.870[3]	-8.960[2]	1.331186
P XI									
1s 2 2s 2 2p 2 P o	(97%)	+ 1s 2 2p 3 2P o	(3%)	1/2	-277.0459879	0.00	2.375[4]	0.0	0.664487
	(97%)	+ 1s 2 2p 3 2P o	(3%)	3/2	-277.0017287	9713.78	4.596[3]	8.232[3]	1.332970
1s 2 2s2p 2 4P	(100%)			1/2	-276.2387474	177168.82	4.158[4]	0.0	2.667881
	(100%)			3/2	-276.2228542	180656.97	1.947[4]	6.707[3]	1.733599
	(100%)			5/2	-276.2002741	185612.72	2.032[4]	-8.423[3]	1.599551
1s 2 2s2p 2 2D	(99%)			3/2	-275.6018165	316958.98	-5.954[3]	1.169[4]	0.799470
	(100%)			5/2	-275.6013532	317060.67	2.329[4]	1.670[4]	1.199842
1s 2 2s2p 2 2S	(94%)	+ 1s 2 2s2p 2 2P	(5%)	1/2	-275.2071965	403568.06	7.802[4]	0.0	1.929712
1s 2 2s2p 2 2P	(94%)	+ 1s 2 2s2p 2 2S	(5%)	1/2	-275.0998940	427118.23	1.718[4]	0.0	0.737233
	(99%)			3/2	-275.0759675	432369.50	-3.608[3]	-8.515[3]	1.332186
1s 2 2p 3 4S o	(100%)			3/2	-274.4989753	559004.63	-2.397[3]	2.313	1.999689
1s 2 2p 3 2D o	(99%)	+ 1s 2 2p 3 2P o	(1%)	3/2	-274.1656950	632151.21	5.686[3]	1.847[3]	0.803181
	(100%)			5/2	-274.1647534	632357.86	7.749[3]	-1.441[2]	1.199289
1s 2 2p 3 2P o	(97%)	+ 1s 2 2s 2 2p 2 P o	(3%)	1/2	-273.8113344	709924.36	2.399[4]	0.0	0.664504
	(96%)	+ 1s 2 2s 2 2p 2 P o	(3%)	3/2	-273.8064552	710995.22	3.739[3]	-1.583[3]	1.329779
S XII									
1s 2 2s 2 2p 2 P o	(97%)	+ 1s 2 2p 3 2P o	(3%)	1/2	-317.5751423	0.00	2.979[4]	0.0	0.664252
	(97%)	+ 1s 2 2p 3 2P o	(3%)	3/2	-317.5152326	13148.65	5.755[3]	1.032[4]	1.332783

Table 4 (continued)

Level composition in LSJ coupling		J	Energy (E_h)	ΔE cm $^{-1}$	$A_J(I/\mu_I)$	B_J/Q	g_J		
$1s^2 2s 2p^2 \ ^4P$	(100%)	1/2	-316.6915340	193929.59	5.196[4]	0.0	2.667110		
	(100%)	3/2	-316.6696738	198727.35	2.428[4]	8.411[3]	1.733288		
	(100%)	5/2	-316.6391188	205433.41	2.536[4]	-1.055[4]	1.599034		
$1s^2 2s 2p^2 \ ^2D$	(99%)	3/2	-315.9945601	346897.68	-7.168[3]	1.466[4]	0.799817		
	(99%)	5/2	-315.9933667	347159.60	2.898[4]	2.095[4]	1.199954		
$1s^2 2s 2p^2 \ ^2S$	(91%)	+ $1s^2 2s 2p^2 \ ^2P$	(9%)	1/2	-315.5708559	439890.00	9.317[4]	0.0	1.882391
$1s^2 2s 2p^2 \ ^2P$	(91%)	+ $1s^2 2s 2p^2 \ ^2S$	(9%)	1/2	-315.4562330	465046.82	2.474[4]	0.0	0.784689
	(99%)			3/2	-315.4259004	471704.06	-4.531[3]	-1.067[4]	1.331583
$1s^2 2p^3 \ ^4S^o$	(100%)			3/2	-314.7948852	610195.88	-2.789[3]	6.467	1.998752
$1s^2 2p^3 \ ^2D^o$	(98%)	+ $1s^2 2p^3 \ ^2P^o$	(1%)	3/2	-314.4306812	690129.43	7.066[3]	2.925[3]	0.805536
	(100%)			5/2	-314.4282598	690660.85	9.773[3]	-1.637[2]	1.199093
$1s^2 2p^3 \ ^2P^o$	(97%)	+ $1s^2 2s 2p^2 \ ^2P^o$	(3%)	1/2	-314.0468851	774362.92	3.007[4]	0.0	0.664271
	(95%)	+ $1s^2 2s 2p^2 \ ^2P^o$	(3%)	3/2	-314.0388639	776123.36	4.770[3]	-2.607[3]	1.327810
Cl XIII									
$1s^2 2s 2p^2 \ ^2P^o$	(97%)	+ $1s^2 2p^3 \ ^2P^o$	(3%)	1/2	-360.9065594	0.00	3.680[4]	0.0	0.663999
	(97%)	+ $1s^2 2p^3 \ ^2P^o$	(3%)	3/2	-360.8271700	17423.96	7.093[3]	1.274[4]	1.332581
$1s^2 2s 2p^2 \ ^4P$	(100%)			1/2	-359.9437693	211308.00	6.411[4]	0.0	2.666115
	(100%)			3/2	-359.9142791	217780.37	2.986[4]	1.038[4]	1.732920
	(100%)			5/2	-359.8738809	226646.73	3.119[4]	-1.300[4]	1.598365
$1s^2 2s 2p^2 \ ^2D$	(99%)			3/2	-359.1844110	377967.87	-8.507[3]	1.808[4]	0.800362
	(99%)			5/2	-359.1819888	378499.48	3.552[4]	2.585[4]	1.200187
$1s^2 2s 2p^2 \ ^2S$	(86%)	+ $1s^2 2s 2p^2 \ ^2P$	(14%)	1/2	-358.7335389	476922.88	1.078[5]	0.0	1.817061
$1s^2 2s 2p^2 \ ^2P$	(86%)	+ $1s^2 2s 2p^2 \ ^2S$	(14%)	1/2	-358.6084552	504375.57	3.611[4]	0.0	0.850329
	(99%)			3/2	-358.5714874	512489.06	-5.664[3]	-1.314[4]	1.330797
$1s^2 2p^3 \ ^4S^o$	(99%)			3/2	-357.8851067	663132.21	-3.201[3]	1.615[1]	1.997472
$1s^2 2p^3 \ ^2D^o$	(98%)	+ $1s^2 2p^3 \ ^2P^o$	(2%)	3/2	-357.4905771	749721.44	8.632[3]	4.440[3]	0.808887
	(100%)			5/2	-357.4857091	750789.84	1.212[4]	-1.848[2]	1.198882
$1s^2 2p^3 \ ^2P^o$	(97%)	+ $1s^2 2s 2p^2 \ ^2P^o$	(3%)	1/2	-357.0764770	840605.91	3.712[4]	0.0	0.664019
	(95%)	+ $1s^2 2s 2p^2 \ ^2P^o$	(3%)	3/2	-357.0637225	843405.20	5.982[3]	-4.068[3]	1.325148
Ar XIV									
$1s^2 2s 2p^2 \ ^2P^o$	(97%)	+ $1s^2 2p^3 \ ^2P^o$	(3%)	1/2	-407.0475470	0.00	4.485[4]	0.0	0.663728
	(97%)	+ $1s^2 2p^3 \ ^2P^o$	(3%)	3/2	-406.9442626	22668.29	8.624[3]	1.552[4]	1.332365
$1s^2 2s 2p^2 \ ^4P$	(100%)			1/2	-406.0025474	229350.90	7.825[4]	0.0	2.664833
	(100%)			3/2	-405.9634163	237939.18	3.628[4]	1.264[4]	1.732482
	(99%)			5/2	-405.9110806	249425.54	3.790[4]	-1.579[4]	1.597497
$1s^2 2s 2p^2 \ ^2D$	(99%)			3/2	-405.1780276	410312.08	-9.959[3]	2.198[4]	0.801163
	(99%)			5/2	-405.1736526	411272.28	4.297[4]	3.144[4]	1.200587
$1s^2 2s 2p^2 \ ^2S$	(80%)	+ $1s^2 2s 2p^2 \ ^2P$	(20%)	1/2	-404.7025142	514675.20	1.209[5]	0.0	1.735882
$1s^2 2s 2p^2 \ ^2P$	(80%)	+ $1s^2 2s 2p^2 \ ^2S$	(20%)	1/2	-404.5623658	545434.20	5.249[4]	0.0	0.932054
	(99%)			3/2	-404.5189891	554954.29	-7.053[3]	-1.595[4]	1.329782
$1s^2 2p^3 \ ^4S^o$	(99%)	+ $1s^2 2p^3 \ ^2P^o$	(1%)	3/2	-403.7758865	718046.46	-3.626[3]	3.714[1]	1.995718
$1s^2 2p^3 \ ^2D^o$	(97%)	+ $1s^2 2p^3 \ ^2P^o$	(3%)	3/2	-403.3518045	811121.70	1.038[4]	6.493[3]	0.813476
	(100%)			5/2	-403.3431453	813022.17	1.483[4]	-2.071[2]	1.198656
$1s^2 2p^3 \ ^2P^o$	(97%)	+ $1s^2 2s 2p^2 \ ^2P^o$	(3%)	1/2	-402.9061634	908928.62	4.521[4]	0.0	0.663749
	(94%)	+ $1s^2 2s 2p^2 \ ^2P^o$	(3%)	3/2	-402.8864896	913246.51	7.392[3]	-6.071[3]	1.321678
K XV									
$1s^2 2s 2p^2 \ ^2P^o$	(97%)	+ $1s^2 2p^3 \ ^2P^o$	(3%)	1/2	-456.0060635	0.00	5.403[4]	0.0	0.663438
	(97%)	+ $1s^2 2p^3 \ ^2P^o$	(3%)	3/2	-455.8738383	29020.08	1.036[4]	1.867[4]	1.332135
$1s^2 2s 2p^2 \ ^4P$	(99%)	+ $1s^2 2s 2p^2 \ ^2S$	(1%)	1/2	-454.8753662	248159.37	9.463[4]	0.0	2.663196
	(100%)			3/2	-454.8241776	259393.97	4.361[4]	1.520[4]	1.731966
	(99%)	+ $1s^2 2s 2p^2 \ ^2D$	(1%)	5/2	-454.7575967	274006.78	4.557[4]	-1.890[4]	1.596373
$1s^2 2s 2p^2 \ ^2D$	(99%)	+ $1s^2 2s 2p^2 \ ^2P$	(1%)	3/2	-453.9824720	444126.99	-1.152[4]	2.637[4]	0.802282
	(99%)	+ $1s^2 2s 2p^2 \ ^4P$	(1%)	5/2	-453.9751220	445740.13	5.141[4]	3.774[4]	1.201212
$1s^2 2s 2p^2 \ ^2S$	(73%)	+ $1s^2 2s 2p^2 \ ^2P$	(27%)	1/2	-453.4856112	553175.33	1.319[5]	0.0	1.645950
$1s^2 2s 2p^2 \ ^2P$	(73%)	+ $1s^2 2s 2p^2 \ ^2S$	(27%)	1/2	-453.3242397	588592.27	7.461[4]	0.0	1.022842
	(99%)	+ $1s^2 2s 2p^2 \ ^2D$	(1%)	3/2	-453.2750713	599383.49	-8.757[3]	-1.910[4]	1.328485
$1s^2 2p^3 \ ^4S^o$	(99%)	+ $1s^2 2p^3 \ ^2P^o$	(1%)	3/2	-452.4740941	775177.65	-4.050[3]	8.005[1]	1.993314
$1s^2 2p^3 \ ^2D^o$	(96%)	+ $1s^2 2p^3 \ ^2P^o$	(4%)	3/2	-452.0214071	874530.96	1.231[4]	9.175[3]	0.819550
	(100%)			5/2	-452.0071691	877655.84	1.792[4]	-2.309[2]	1.198415
$1s^2 2p^3 \ ^2P^o$	(97%)	+ $1s^2 2s 2p^2 \ ^2P^o$	(3%)	1/2	-451.5425548	979626.90	5.443[4]	0.0	0.663461
	(93%)	+ $1s^2 2p^3 \ ^2D^o$	(4%)	3/2	-451.5130476	986102.98	9.019[3]	-8.720[3]	1.317331
Ca XVI									
$1s^2 2s 2p^2 \ ^2P^o$	(97%)	+ $1s^2 2p^3 \ ^2P^o$	(3%)	1/2	-507.7904445	0.00	6.442[4]	0.0	0.663130
	(97%)	+ $1s^2 2p^3 \ ^2P^o$	(3%)	3/2	-507.6235562	36627.74	1.232[4]	2.223[4]	1.331891
$1s^2 2s 2p^2 \ ^4P$	(99%)	+ $1s^2 2s 2p^2 \ ^2S$	(1%)	1/2	-506.5703856	267771.98	1.136[5]	0.0	2.661116
	(100%)			3/2	-506.5042497	282287.11	5.194[4]	1.809[4]	1.731357
	(99%)	+ $1s^2 2s 2p^2 \ ^2D$	(1%)	5/2	-506.4209198	300575.92	5.427[4]	-2.234[4]	1.594923
$1s^2 2s 2p^2 \ ^2D$	(99%)	+ $1s^2 2s 2p^2 \ ^2P$	(1%)	3/2	-505.6053714	479568.11	-1.315[4]	3.126[4]	0.803785

Table 4 (continued)

Level composition in LSJ coupling			J	Energy (E_h)	ΔE cm $^{-1}$	$A_J(I/\mu_I)$	B_J/Q	g_J	
(99%)	+ $1s^2 2s 2p^2$ 4P	(1%)	5/2	-505.5936399	482142.88	6.087[4]	4.478[4]	1.202133	
1s 2 2s2p 2 2S	(66%)	+ $1s^2 2s 2p^2$ 2P	(33%)	1/2	-505.0908667	592488.82	1.408[5]	0.0	
1s 2 2s2p 2 2P	(66%)	+ $1s^2 2s 2p^2$ 2S	(33%)	1/2	-504.9008544	634191.70	1.026[5]	0.0	
(99%)	+ $1s^2 2s 2p^2$ 2D	(1%)	3/2	-504.8468040	646054.39	-1.084[4]	-2.260[4]	1.326852	
1s 2 2p 3 ${}^4S^o$	(99%)	+ $1s^2 2p^3$ ${}^2P^o$	(1%)	3/2	-503.9869914	834761.44	-4.450[3]	1.636[2]	1.990015
1s 2 2p 3 ${}^2D^o$	(95%)	+ $1s^2 2p^3$ ${}^2P^o$	(5%)	3/2	-503.5067784	940156.02	1.440[4]	1.256[4]	0.827346
(100%)				5/2	-503.4846869	945004.54	2.141[4]	-2.560[2]	1.198159
1s 2 2p 3 ${}^2P^o$	(97%)	+ $1s^2 2s^2 2p$ ${}^2P^o$	(3%)	1/2	-502.9925668	1053012.40	6.487[4]	0.0	0.663155
(91%)	+ $1s^2 2p^3$ ${}^2D^o$	(5%)	3/2	-502.9494534	1062474.70	1.088[4]	-1.210[4]	1.312116	
Sc XVII									
1s 2 2s 2 2p ${}^2P^o$	(97%)	+ $1s^2 2p^3$ ${}^2P^o$	(3%)	1/2	-562.4095890	0.00	7.610[4]	0.0	0.662804
(97%)	+ $1s^2 2p^3$ ${}^2P^o$	(3%)	3/2	-562.2015928	45649.90	1.451[4]	2.622[4]	1.331634	
1s 2 2s2p 2 4P	(99%)	+ $1s^2 2s 2p^2$ 2S	(1%)	1/2	-561.0962801	288237.98	1.354[5]	0.0	2.658498
(100%)				3/2	-561.0117596	306788.09	6.134[4]	2.133[4]	1.730644
1s 2 2s2p 2 2D	(99%)	+ $1s^2 2s 2p^2$ 2D	(1%)	5/2	-560.9090114	329338.71	6.409[4]	-2.609[4]	1.593059
(98%)	+ $1s^2 2s 2p^2$ 2P	(1%)	3/2	-560.0548273	516810.44	-1.484[4]	3.667[4]	0.805741	
(98%)	+ $1s^2 2s 2p^2$ 4P	(1%)	5/2	-560.0368198	520762.63	7.141[4]	5.255[4]	1.203436	
1s 2 2s2p 2 2S	(59%)	+ $1s^2 2s 2p^2$ 2P	(40%)	1/2	-559.5266805	632725.28	1.478[5]	0.0	1.471978
1s 2 2s2p 2 2P	(60%)	+ $1s^2 2s 2p^2$ 2S	(40%)	1/2	-559.2995572	682573.06	1.363[5]	0.0	1.199806
(98%)	+ $1s^2 2s 2p^2$ 2D	(1%)	3/2	-559.2416628	695279.41	-1.337[4]	-2.644[4]	1.324829	
1s 2 2p 3 ${}^4S^o$	(98%)	+ $1s^2 2p^3$ ${}^2P^o$	(2%)	3/2	-558.3224197	897029.95	-4.793[3]	3.196[2]	1.985485
1s 2 2p 3 ${}^2D^o$	(93%)	+ $1s^2 2p^3$ ${}^2P^o$	(6%)	3/2	-557.8157893	1008222.48	1.661[4]	1.667[4]	0.837098
(100%)				5/2	-557.7830751	1015402.41	2.535[4]	-2.826[2]	1.197888
1s 2 2p 3 ${}^2P^o$	(97%)	+ $1s^2 2s^2 2p$ ${}^2P^o$	(3%)	1/2	-557.2635849	1129417.32	7.661[4]	0.0	0.662830
(89%)	+ $1s^2 2p^3$ ${}^2D^o$	(7%)	3/2	-557.2021163	1142908.12	1.301[4]	-1.629[4]	1.306134	
Ti XVIII									
1s 2 2s 2 2p ${}^2P^o$	(97%)	+ $1s^2 2p^3$ ${}^2P^o$	(2%)	1/2	-619.8731071	0.00	8.917[4]	0.0	0.662459
(97%)	+ $1s^2 2p^3$ ${}^2P^o$	(3%)	3/2	-619.6167877	56255.61	1.694[4]	3.066[4]	1.331362	
1s 2 2s2p 2 4P	(99%)	+ $1s^2 2s 2p^2$ 2S	(1%)	1/2	-618.4624677	309599.55	1.605[5]	0.0	2.655234
(100%)				3/2	-618.3554939	333077.59	7.189[4]	2.494[4]	1.729813
1s 2 2s2p 2 2D	(98%)	+ $1s^2 2s 2p^2$ 2D	(2%)	5/2	-618.2305351	360502.88	7.514[4]	-3.009[4]	1.590684
(98%)	+ $1s^2 2s 2p^2$ 2P	(2%)	3/2	-617.3396221	556035.66	-1.655[4]	4.258[4]	0.808212	
(98%)	+ $1s^2 2s 2p^2$ 4P	(2%)	5/2	-617.3128361	561914.52	8.309[4]	6.104[4]	1.205221	
1s 2 2s2p 2 2S	(53%)	+ $1s^2 2s 2p^2$ 2P	(45%)	1/2	-616.8019708	674036.48	1.533[5]	0.0	1.398474
1s 2 2s2p 2 2P	(54%)	+ $1s^2 2s 2p^2$ 2S	(45%)	1/2	-616.5283991	734078.54	1.755[5]	0.0	1.275648
(98%)	+ $1s^2 2s 2p^2$ 2D	(2%)	3/2	-616.4677003	747400.38	-1.643[4]	-3.060[4]	1.322364	
1s 2 2p 3 ${}^4S^o$	(97%)	+ $1s^2 2p^3$ ${}^2P^o$	(2%)	3/2	-615.4889618	962208.64	-5.031[3]	5.996[2]	1.979268
1s 2 2p 3 ${}^2D^o$	(91%)	+ $1s^2 2p^3$ ${}^2P^o$	(7%)	3/2	-614.9568704	1078989.21	1.892[4]	2.150[4]	0.849061
(100%)				5/2	-614.9103139	1089207.17	2.974[4]	-3.106[2]	1.197602
1s 2 2p 3 ${}^2P^o$	(97%)	+ $1s^2 2s^2 2p$ ${}^2P^o$	(2%)	1/2	-614.3635964	1209197.80	8.973[4]	0.0	0.662487
(87%)	+ $1s^2 2p^3$ ${}^2D^o$	(8%)	3/2	-614.2779524	1227994.47	1.541[4]	-2.131[4]	1.299584	
V XIX									
1s 2 2s 2 2p ${}^2P^o$	(98%)	+ $1s^2 2p^3$ ${}^2P^o$	(2%)	1/2	-680.1909594	0.00	1.037[5]	0.0	0.662096
(97%)	+ $1s^2 2p^3$ ${}^2P^o$	(3%)	3/2	-679.8782828	68624.58	1.964[4]	3.559[4]	1.331076	
1s 2 2s2p 2 4P	(98%)	+ $1s^2 2s 2p^2$ 2S	(2%)	1/2	-678.6787731	331886.52	1.893[5]	0.0	2.651207
(100%)				3/2	-678.5445554	361343.91	8.368[4]	2.893[4]	1.728854
1s 2 2s2p 2 2D	(97%)	+ $1s^2 2s 2p^2$ 2D	(3%)	5/2	-678.3945250	394271.77	8.753[4]	-3.427[4]	1.587684
(97%)	+ $1s^2 2s 2p^2$ 2P	(2%)	3/2	-677.4688776	597427.88	-1.825[4]	4.897[4]	0.811253	
(97%)	+ $1s^2 2s 2p^2$ 4P	(3%)	5/2	-677.4300658	605946.08	9.594[4]	7.020[4]	1.207598	
1s 2 2s2p 2 2P	(50%)	+ $1s^2 2s 2p^2$ 2S	(48%)	1/2	-676.9258748	716603.22	1.574[5]	0.0	1.336053
1s 2 2s2p 2 2S	(50%)	+ $1s^2 2s 2p^2$ 2P	(49%)	1/2	-676.5957379	789059.90	2.200[5]	0.0	1.341123
1s 2 2s2p 2 2P	(97%)	+ $1s^2 2s 2p^2$ 2D	(2%)	3/2	-676.5331992	802785.55	-2.012[4]	-3.505[4]	1.319416
1s 2 2p 3 ${}^4S^o$	(96%)	+ $1s^2 2p^3$ ${}^2P^o$	(3%)	3/2	-675.4956469	1030501.95	-5.095[3]	1.085[3]	1.970765
1s 2 2p 3 ${}^2D^o$	(89%)	+ $1s^2 2p^3$ ${}^2P^o$	(9%)	3/2	-674.9386193	1152755.38	2.125[4]	2.696[4]	0.863560
(100%)				5/2	-674.8746557	1166793.77	3.463[4]	-3.401[2]	1.197301
1s 2 2p 3 ${}^2P^o$	(97%)	+ $1s^2 2s^2 2p$ ${}^2P^o$	(2%)	1/2	-674.3008596	1292727.45	1.043[5]	0.0	0.662125
(85%)	+ $1s^2 2p^3$ ${}^2D^o$	(10%)	3/2	-674.1840811	1318357.36	1.810[4]	-2.716[4]	1.292744	
Cr XX									
1s 2 2s 2 2p ${}^2P^o$	(98%)	+ $1s^2 2p^3$ ${}^2P^o$	(2%)	1/2	-743.3738851	0.00	1.198[5]	0.0	0.661714
(97%)	+ $1s^2 2p^3$ ${}^2P^o$	(3%)	3/2	-742.9959491	82947.37	2.260[4]	4.103[4]	1.330776	
1s 2 2s2p 2 4P	(98%)	+ $1s^2 2s 2p^2$ 2S	(2%)	1/2	-741.7558453	355118.67	2.225[5]	0.0	2.646291
(99%)				3/2	-741.5887725	391786.92	9.679[4]	3.333[4]	1.727756
1s 2 2s2p 2 2D	(97%)	+ $1s^2 2s 2p^2$ 2D	(3%)	5/2	-741.4108084	430845.53	1.014[5]	-3.853[4]	1.583940
(97%)	+ $1s^2 2s 2p^2$ 2P	(3%)	3/2	-740.4524637	641177.87	-1.990[4]	5.581[4]	0.814903	
(97%)	+ $1s^2 2s 2p^2$ 4P	(3%)	5/2	-740.3974832	653244.70	1.100[5]	7.995[4]	1.210689	
1s 2 2s2p 2 2P	(54%)	+ $1s^2 2s 2p^2$ 2S	(44%)	1/2	-739.9081917	760631.76	1.599[5]	0.0	1.284015
1s 2 2s2p 2 2S	(54%)	+ $1s^2 2s 2p^2$ 2P	(45%)	1/2	-739.5106045	847892.07	2.699[5]	0.0	1.397054
1s 2 2s2p 2 2P	(97%)	+ $1s^2 2s 2p^2$ 2D	(3%)	3/2	-739.4470775	861834.64	-2.452[4]	-3.975[4]	1.315953

Table 4 (continued)

Level composition in LSJ coupling			J	Energy (E_h)	ΔE cm $^{-1}$	$A_J(I/\mu_I)$	B_J/Q	g_J	
$1s^2 2p^3 \ ^4S^o$	(95%)	$+ 1s^2 2p^3 \ ^2P^o$	(4%)	3/2	-738.3523797	1102093.02	-4.893[3]	1.896[3]	1.959222
$1s^2 2p^3 \ ^2D^o$	(87%)	$+ 1s^2 2p^3 \ ^2P^o$	(10%)	3/2	-737.7701285	1229882.37	2.352[4]	3.292[4]	0.881030
	(100%)			5/2	-737.6850170	1248562.20	4.005[4]	-3.710[2]	1.196984
$1s^2 2p^3 \ ^2P^o$	(98%)	$+ 1s^2 2s^2 2p \ ^2P^o$	(2%)	1/2	-737.0842948	1380405.47	1.205[5]	0.0	0.661745
	(83%)	$+ 1s^2 2p^3 \ ^2D^o$	(12%)	3/2	-736.9282423	1414655.04	2.110[4]	-3.384[4]	1.285929
Mn XXI									
$1s^2 2s^2 2p \ ^2P^o$	(98%)	$+ 1s^2 2p^3 \ ^2P^o$	(2%)	1/2	-809.4329406	0.00	1.376[5]	0.0	0.661314
	(97%)	$+ 1s^2 2p^3 \ ^2P^o$	(3%)	3/2	-808.9799245	99425.53	2.586[4]	4.700[4]	1.330463
$1s^2 2s2p^2 \ ^4P$	(97%)	$+ 1s^2 2s2p^2 \ ^2S$	(3%)	1/2	-807.7047191	379300.75	2.606[5]	0.0	2.640360
	(99%)			3/2	-807.4982558	424614.20	1.113[5]	3.816[4]	1.726511
	(96%)	$+ 1s^2 2s2p^2 \ ^2D$	(4%)	5/2	-807.2895729	470414.82	1.168[5]	-4.273[4]	1.579332
$1s^2 2s2p^2 \ ^2D$	(96%)	$+ 1s^2 2s2p^2 \ ^2P$	(4%)	3/2	-806.3005556	687479.01	-2.145[4]	6.308[4]	0.819182
	(95%)	$+ 1s^2 2s2p^2 \ ^4P$	(4%)	5/2	-806.2242050	704236.03	1.254[5]	9.016[4]	1.214612
$1s^2 2s2p^2 \ ^2P$	(58%)	$+ 1s^2 2s2p^2 \ ^2S$	(40%)	1/2	-805.7589570	806346.16	1.606[5]	0.0	1.241054
$1s^2 2s2p^2 \ ^2S$	(57%)	$+ 1s^2 2s2p^2 \ ^2P$	(42%)	1/2	-805.2822369	910974.14	3.255[5]	0.0	1.444874
$1s^2 2s2p^2 \ ^2P$	(96%)	$+ 1s^2 2s2p^2 \ ^2D$	(4%)	3/2	-805.2184465	924974.49	-2.974[4]	-4.466[4]	1.311967
$1s^2 2p^3 \ ^4S^o$	(93%)	$+ 1s^2 2p^3 \ ^2P^o$	(6%)	3/2	-804.0695476	1177128.65	-4.303[3]	3.203[3]	1.943766
$1s^2 2p^3 \ ^2D^o$	(85%)	$+ 1s^2 2p^3 \ ^2P^o$	(11%)	3/2	-803.4604995	1310799.26	2.562[4]	3.916[4]	0.902038
	(100%)			5/2	-803.3505498	1334930.43	4.602[4]	-4.035[2]	1.196653
$1s^2 2p^3 \ ^2P^o$	(98%)	$+ 1s^2 2s^2 2p \ ^2P^o$	(2%)	1/2	-802.7230554	1472649.53	1.384[5]	0.0	0.661345
	(81%)	$+ 1s^2 2p^3 \ ^2D^o$	(14%)	3/2	-802.5183876	1517568.92	2.441[4]	-4.129[4]	1.279447
Fe XXII									
$1s^2 2s^2 2p \ ^2P^o$	(98%)	$+ 1s^2 2p^3 \ ^2P^o$	(2%)	1/2	-878.3799779	0.00	1.572[5]	0.0	0.660895
	(97%)	$+ 1s^2 2p^3 \ ^2P^o$	(2%)	3/2	-877.8410891	118272.41	2.941[4]	5.355[4]	1.330135
$1s^2 2s2p^2 \ ^4P$	(96%)	$+ 1s^2 2s2p^2 \ ^2S$	(3%)	1/2	-876.5372804	404425.33	3.042[5]	0.0	2.633288
	(99%)			3/2	-876.2838589	460044.93	1.274[5]	4.344[4]	1.725113
	(94%)	$+ 1s^2 2s2p^2 \ ^2D$	(6%)	5/2	-876.0418348	513163.08	1.339[5]	-4.668[4]	1.573749
$1s^2 2s2p^2 \ ^2D$	(95%)	$+ 1s^2 2s2p^2 \ ^2P$	(5%)	3/2	-875.0240899	736532.25	-2.287[4]	7.071[4]	0.824085
	(94%)	$+ 1s^2 2s2p^2 \ ^4P$	(6%)	5/2	-874.9199417	759390.13	1.420[5]	1.007[5]	1.219479
$1s^2 2s2p^2 \ ^2P$	(61%)	$+ 1s^2 2s2p^2 \ ^2S$	(37%)	1/2	-874.4889079	853991.13	1.590[5]	0.0	1.205803
$1s^2 2s2p^2 \ ^2S$	(60%)	$+ 1s^2 2s2p^2 \ ^2P$	(39%)	1/2	-873.9205270	978736.31	3.871[5]	0.0	1.486077
$1s^2 2s2p^2 \ ^2P$	(95%)	$+ 1s^2 2s2p^2 \ ^2D$	(5%)	3/2	-873.8570703	992663.45	-3.588[4]	-4.971[4]	1.307464
$1s^2 2p^3 \ ^4S^o$	(90%)	$+ 1s^2 2p^3 \ ^2P^o$	(7%)	3/2	-872.6584922	1255720.92	-3.183[3]	5.230[3]	1.923511
$1s^2 2p^3 \ ^2D^o$	(82%)	$+ 1s^2 2p^3 \ ^2P^o$	(12%)	3/2	-872.0192490	1396018.59	2.743[4]	4.542[4]	0.927209
	(100%)			5/2	-871.8810855	1426341.98	5.257[4]	-4.375[2]	1.196306
$1s^2 2p^3 \ ^2P^o$	(98%)	$+ 1s^2 2s^2 2p \ ^2P^o$	(2%)	1/2	-871.2269712	1569903.46	1.581[5]	0.0	0.660928
	(78%)	$+ 1s^2 2p^3 \ ^2D^o$	(16%)	3/2	-870.9631363	1627808.53	2.806[4]	-4.948[4]	1.273559
Co XXIII									
$1s^2 2s^2 2p \ ^2P^o$	(98%)	$+ 1s^2 2p^3 \ ^2P^o$	(2%)	1/2	-950.2273260	0.00	1.787[5]	0.0	0.660457
	(97%)	$+ 1s^2 2p^3 \ ^2P^o$	(2%)	3/2	-949.5907515	139711.97	3.328[4]	6.068[4]	1.329794
$1s^2 2s2p^2 \ ^4P$	(95%)	$+ 1s^2 2s2p^2 \ ^2S$	(4%)	1/2	-948.2659512	430472.01	3.541[5]	0.0	2.624959
	(99%)	$+ 1s^2 2s2p^2 \ ^2D$	(1%)	3/2	-947.9568619	498309.26	1.450[5]	4.918[4]	1.723558
	(93%)	$+ 1s^2 2s2p^2 \ ^2D$	(7%)	5/2	-947.6791249	559265.50	1.528[5]	-5.015[4]	1.567109
$1s^2 2s2p^2 \ ^2D$	(94%)	$+ 1s^2 2s2p^2 \ ^2P$	(6%)	3/2	-946.6344466	788545.86	-2.412[4]	7.867[4]	0.829585
	(93%)	$+ 1s^2 2s2p^2 \ ^4P$	(7%)	5/2	-946.4946805	819220.99	1.600[5]	1.113[5]	1.225372
$1s^2 2s2p^2 \ ^2P$	(63%)	$+ 1s^2 2s2p^2 \ ^2S$	(34%)	1/2	-946.1091716	903830.40	1.545[5]	0.0	1.177061
$1s^2 2s2p^2 \ ^2S$	(62%)	$+ 1s^2 2s2p^2 \ ^2P$	(36%)	1/2	-945.4357087	1051638.41	4.551[5]	0.0	1.521979
$1s^2 2s2p^2 \ ^2P$	(94%)	$+ 1s^2 2s2p^2 \ ^2D$	(5%)	3/2	-945.3730572	1065388.84	-4.302[4]	-5.485[4]	1.302479
$1s^2 2p^3 \ ^4S^o$	(87%)	$+ 1s^2 2p^3 \ ^2P^o$	(9%)	3/2	-944.1312038	1337944.14	-1.378[3]	8.240[3]	1.897763
$1s^2 2p^3 \ ^2D^o$	(80%)	$+ 1s^2 2p^3 \ ^2P^o$	(12%)	3/2	-943.4560011	1486134.01	2.880[4]	5.140[4]	0.957049
	(100%)			5/2	-943.2868302	1523262.73	5.975[4]	-4.730[2]	1.195944
$1s^2 2p^3 \ ^2P^o$	(98%)	$+ 1s^2 2s^2 2p \ ^2P^o$	(2%)	1/2	-942.6062449	1672633.92	1.796[5]	0.0	0.660491
	(76%)	$+ 1s^2 2p^3 \ ^2D^o$	(17%)	3/2	-942.2714746	1746107.52	3.204[4]	-5.838[4]	1.268452
Ni XXIV									
$1s^2 2s^2 2p \ ^2P^o$	(98%)	$+ 1s^2 2p^3 \ ^2P^o$	(2%)	1/2	-1024.9879299	0.00	2.021[5]	0.0	0.660000
	(98%)	$+ 1s^2 2p^3 \ ^2P^o$	(2%)	3/2	-1024.2407753	163981.48	3.748[4]	6.844[4]	1.329439
$1s^2 2s2p^2 \ ^4P$	(94%)	$+ 1s^2 2s2p^2 \ ^2S$	(5%)	1/2	-1022.9038416	457404.50	4.109[5]	0.0	2.615273
	(99%)	$+ 1s^2 2s2p^2 \ ^2D$	(1%)	3/2	-1022.5291245	539645.38	1.643[5]	5.542[4]	1.721847
	(91%)	$+ 1s^2 2s2p^2 \ ^2D$	(9%)	5/2	-1022.2136354	608887.25	1.738[5]	-5.289[4]	1.559368
$1s^2 2s2p^2 \ ^2D$	(93%)	$+ 1s^2 2s2p^2 \ ^2P$	(7%)	3/2	-1021.1435944	843734.08	-2.516[4]	8.689[4]	0.835627
	(91%)	$+ 1s^2 2s2p^2 \ ^4P$	(9%)	5/2	-1020.9588414	884282.68	1.794[5]	1.219[5]	1.232333
$1s^2 2s2p^2 \ ^2P$	(65%)	$+ 1s^2 2s2p^2 \ ^2S$	(31%)	1/2	-1020.6314140	956144.69	1.466[5]	0.0	1.153852
$1s^2 2s2p^2 \ ^2S$	(64%)	$+ 1s^2 2s2p^2 \ ^2P$	(34%)	1/2	-1019.8385060	1130167.86	5.299[5]	0.0	1.553655
$1s^2 2s2p^2 \ ^2P$	(93%)	$+ 1s^2 2s2p^2 \ ^2D$	(7%)	3/2	-1019.7770139	1143663.83	-5.126[4]	-6.000[4]	1.297066
$1s^2 2p^3 \ ^4S^o$	(84%)	$+ 1s^2 2p^3 \ ^2P^o$	(12%)	3/2	-1018.5004205	1423843.69	1.249[3]	1.251[4]	1.866297
$1s^2 2p^3 \ ^2D^o$	(77%)	$+ 1s^2 2p^3 \ ^2P^o$	(12%)	3/2	-1017.7806689	1581810.90	2.961[4]	5.680[4]	0.991675
	(100%)			5/2	-1017.5785041	1626180.94	6.757[4]	-5.103[2]	1.195567
$1s^2 2p^3 \ ^2P^o$	(98%)	$+ 1s^2 2s^2 2p \ ^2P^o$	(2%)	1/2	-1016.8715900	1781330.64	2.032[5]	0.0	0.660035

Table 4 (continued)

Level composition in LSJ coupling			J	Energy (E_h)	ΔE cm $^{-1}$	$A_J(I/\mu_I)$	B_J/Q	g_J	
	(74%)	+ 1s 2 2p 3 2D o	(19%)	3/2	-1016.4528911	1873224.43	3.635[4]	-6.795[4]	1.264235
Cu XXV									
1s 2 2s 2 2p 2 P o	(98%)	+ 1s 2 2p 3 2P o	(2%)	1/2	-1102.6753597	0.00	2.277[5]	0.0	0.659524
	(98%)	+ 1s 2 2p 3 2P o	(2%)	3/2	-1101.8036001	191329.12	4.201[4]	7.685[4]	1.329069
1s 2 2s 2 p 2 4P	(93%)	+ 1s 2 2s 2 p 2 2S	(6%)	1/2	-1100.4640697	485322.05	4.755[5]	0.0	2.604156
	(99%)	+ 1s 2 2s 2 p 2 2D	(1%)	3/2	-1100.0124047	584451.06	1.854[5]	6.217[4]	1.719981
	(89%)	+ 1s 2 2s 2 p 2 2D	(11%)	5/2	-1099.6575311	662336.80	1.968[5]	-5.464[4]	1.550542
1s 2 2s 2 p 2 2D	(91%)	+ 1s 2 2s 2 p 2 2P	(8%)	3/2	-1098.5634572	902458.26	-2.598[4]	9.533[4]	0.842136
	(89%)	+ 1s 2 2s 2 p 2 4P	(11%)	5/2	-1098.3226560	955308.01	2.002[5]	1.321[5]	1.240351
1s 2 2s 2 p 2 2P	(67%)	+ 1s 2 2s 2 p 2 2S	(28%)	1/2	-1098.0672635	1011360.20	1.347[5]	0.0	1.135427
1s 2 2s 2 p 2 2S	(65%)	+ 1s 2 2s 2 p 2 2P	(32%)	1/2	-1097.1395872	1214961.60	6.118[5]	0.0	1.581932
1s 2 2s 2 p 2 2P	(91%)	+ 1s 2 2s 2 p 2 2D	(8%)	3/2	-1097.0794684	1228156.15	-6.071[4]	-6.510[4]	1.291296
1s 2 2p 3 4S o	(80%)	+ 1s 2 2p 3 2P o	(14%)	3/2	-1095.7795390	1513457.66	4.793[3]	1.826[4]	1.829611
1s 2 2p 3 2D o	(74%)	+ 1s 2 2p 3 4S o	(14%)	3/2	-1095.0035438	1683768.93	2.978[4]	6.137[4]	1.030553
	(100%)			5/2	-1094.7673375	1735610.22	7.609[4]	-5.491[2]	1.195174
1s 2 2p 3 2P o	(98%)	+ 1s 2 2s 2 2p 2 P o	(2%)	1/2	-1094.0342271	1896509.35	2.289[5]	0.0	0.659560
	(72%)	+ 1s 2 2p 3 2D o	(20%)	3/2	-1093.5173665	2009947.13	4.102[4]	-7.817[4]	1.260944
Zn XXVI									
1s 2 2s 2 2p 2 P o	(98%)	+ 1s 2 2p 3 2P o	(2%)	1/2	-1183.3038006	0.00	2.555[5]	0.0	0.659028
	(98%)	+ 1s 2 2p 3 2P o	(2%)	3/2	-1182.2922212	222016.01	4.691[4]	8.594[4]	1.328686
1s 2 2s 2 p 2 4P	(92%)	+ 1s 2 2s 2 p 2 2S	(7%)	1/2	-1180.9630398	513737.60	5.487[5]	0.0	2.591569
	(98%)	+ 1s 2 2s 2 p 2 2D	(1%)	3/2	-1180.4216656	632555.49	2.084[5]	6.945[4]	1.717966
	(86%)	+ 1s 2 2s 2 p 2 2D	(14%)	5/2	-1180.0262029	719349.52	2.222[5]	-5.513[4]	1.540711
1s 2 2s 2 p 2 2D	(90%)	+ 1s 2 2s 2 p 2 2P	(9%)	3/2	-1178.9089573	964556.58	-2.656[4]	1.039[5]	0.849014
	(86%)	+ 1s 2 2s 2 p 2 4P	(14%)	5/2	-1178.5992787	1032523.18	2.225[5]	1.417[5]	1.249338
1s 2 2s 2 p 2 2P	(68%)	+ 1s 2 2s 2 p 2 2S	(26%)	1/2	-1178.4311219	1069429.33	1.183[5]	0.0	1.121120
1s 2 2s 2 p 2 2S	(67%)	+ 1s 2 2s 2 p 2 2P	(30%)	1/2	-1177.3522434	1306215.77	7.013[5]	0.0	1.607505
1s 2 2s 2 p 2 2P	(90%)	+ 1s 2 2s 2 p 2 2D	(9%)	3/2	-1177.2937125	1319061.82	-7.139[4]	-7.010[4]	1.285264
1s 2 2p 3 4S o	(75%)	+ 1s 2 2p 3 2P o	(17%)	3/2	-1175.9824848	1606843.04	9.276[3]	2.563[4]	1.788991
1s 2 2p 3 2D o	(71%)	+ 1s 2 2p 3 4S o	(18%)	3/2	-1175.1354141	1792753.56	2.930[4]	6.496[4]	1.072419
	(100%)			5/2	-1174.8650617	1852089.06	8.532[4]	-5.896[2]	1.194766
1s 2 2p 3 2P o	(98%)	+ 1s 2 2s 2 2p 2 P o	(2%)	1/2	-1174.1058750	2018711.26	2.568[5]	0.0	0.659066
	(70%)	+ 1s 2 2p 3 2D o	(22%)	3/2	-1173.4753563	2157094.11	4.604[4]	-8.905[4]	1.258555
Kr XXXII									
1s 2 2s 2 2p 2 P o	(99%)	+ 1s 2 2p 3 2P o	(1%)	1/2	-1729.7089384	0.00	4.774[5]	0.0	0.655658
	(98%)	+ 1s 2 2p 3 2P o	(2%)	3/2	-1727.4649266	492503.65	8.446[4]	1.564[5]	1.326086
1s 2 2s 2 p 2 4P	(82%)	+ 1s 2 2s 2 p 2 2S	(14%)	1/2	-1726.5292987	697850.23	1.203[6]	0.0	2.488361
	(97%)	+ 1s 2 2s 2 p 2 2D	(2%)	3/2	-1725.0899728	1013745.73	3.910[5]	1.255[5]	1.703336
	(70%)	+ 1s 2 2s 2 p 2 2D	(30%)	5/2	-1724.4497885	1154249.94	4.284[5]	-2.276[4]	1.471485
1s 2 2s 2 p 2 2D	(82%)	+ 1s 2 2s 2 p 2 2P	(17%)	3/2	-1723.1949425	1429656.80	-2.496[4]	1.577[5]	0.892324
1s 2 2s 2 p 2 2P	(73%)	+ 1s 2 2s 2 p 2 2S	(15%)	1/2	-1722.8572958	1503761.68	-9.518[4]	0.0	1.099237
1s 2 2s 2 p 2 2D	(70%)	+ 1s 2 2s 2 p 2 4P	(30%)	5/2	-1722.0964382	1670750.63	3.934[5]	1.798[5]	1.312840
1s 2 2s 2 p 2 2S	(71%)	+ 1s 2 2s 2 p 2 2P	(23%)	1/2	-1720.4630774	2029231.87	1.421[6]	0.0	1.723636
1s 2 2s 2 p 2 2P	(82%)	+ 1s 2 2s 2 p 2 2D	(16%)	3/2	-1720.4134861	2040115.90	-1.659[5]	-9.569[4]	1.248652
1s 2 2p 3 4S o	(50%)	+ 1s 2 2p 3 2P o	(31%)	3/2	-1719.4276001	2256492.87	5.096[4]	9.979[4]	1.559590
1s 2 2p 3 2D o	(56%)	+ 1s 2 2p 3 4S o	(40%)	3/2	-1717.7054514	2634460.80	1.820[4]	7.091[4]	1.294262
	(100%)			5/2	-1717.2590824	2732427.47	1.581[5]	-8.645[2]	1.191996
1s 2 2p 3 2P o	(99%)	+ 1s 2 2s 2 2p 2 P o	(1%)	1/2	-1716.3449392	2933058.72	4.794[5]	0.0	0.655696
	(62%)	+ 1s 2 2p 3 2D o	(26%)	3/2	-1714.6315403	3309106.29	8.401[4]	-1.688[5]	1.258373
Mo XXXVIII									
1s 2 2s 2 2p 2 P o	(99%)			1/2	-2386.3262016	0.00	8.183[5]	0.0	0.651563
1s 2 2s 2 p 2 4P	(72%)	+ 1s 2 2s 2 p 2 2S	(21%)	1/2	-2382.2474243	895188.11	2.301[6]	0.0	2.364178
1s 2 2s 2 2p 2 P o	(98%)	+ 1s 2 2p 3 2P o	(2%)	3/2	-2381.9341181	963950.87	1.386[5]	2.591[5]	1.322967
1s 2 2s 2 p 2 4P	(95%)	+ 1s 2 2s 2 p 2 2D	(3%)	3/2	-2379.0096012	1605808.12	6.681[5]	2.066[5]	1.686557
	(56%)	+ 1s 2 2s 2 p 2 2D	(44%)	5/2	-2378.1592469	1792439.32	7.468[5]	6.953[4]	1.413274
1s 2 2s 2 p 2 2D	(75%)	+ 1s 2 2s 2 p 2 2P	(24%)	3/2	-2376.7393964	2104060.47	-1.735[4]	2.164[5]	0.927769
1s 2 2s 2 p 2 2P	(73%)	+ 1s 2 2s 2 p 2 4P	(19%)	1/2	-2376.5434452	2147066.80	-5.243[5]	0.0	1.136154
1s 2 2s 2 p 2 2D	(56%)	+ 1s 2 2s 2 p 2 4P	(44%)	5/2	-2373.9164184	2723632.51	6.494[5]	1.899[5]	1.364165
1s 2 2p 3 2P o	(39%)	+ 1s 2 2p 3 4S o	(37%)	3/2	-2372.1361097	3114365.08	1.080[5]	2.097[5]	1.441796
1s 2 2s 2 p 2 2S	(71%)	+ 1s 2 2s 2 p 2 2P	(19%)	1/2	-2371.9167572	3162507.40	2.527[6]	0.0	1.800111
1s 2 2s 2 p 2 2P	(74%)	+ 1s 2 2s 2 p 2 2D	(22%)	3/2	-2371.8721146	3172305.31	-3.226[5]	-1.130[5]	1.220481
1s 2 2p 3 4S o	(49%)	+ 1s 2 2p 3 2D o	(49%)	3/2	-2368.5184105	3908358.26	3.197[3]	7.013[4]	1.392660
1s 2 2p 3 2D o	(100%)			5/2	-2367.9521258	4032643.39	2.675[5]	-1.218[3]	1.188665
1s 2 2p 3 2P o	(99%)	+ 1s 2 2s 2 2p 2 P o	(1%)	1/2	-2366.8820306	4267502.12	8.217[5]	0.0	0.651602
	(58%)	+ 1s 2 2p 3 2D o	(28%)	3/2	-2363.1587213	5084674.05	1.373[5]	-2.777[5]	1.268509

Table 5

Comparison of calculated hyperfine interaction constants $A_J(I/\mu_I)$ (MHz per unit of μ_N) and B_J/Q (MHz/barn) with Dutta and Majumber [48], Jönsson *et al.* [49], and Sun *et al.* [50] for the O IV ion. RCI are results from this work.

Level	$A_J(I/\mu_I)$			B_J/Q		
	Ref. [48]	Ref. [49]	RCI	Ref. [49]	Ref. [49]	RCI
$1s^2 2s^2 2p \ ^2P_{1/2}^o$	2192	2174	2174	0.0	0.0	
	453	427.7	426.2	745	742.6	
$1s^2 2s^2 2p \ ^4P_{5/2}$	Ref. [50]	Ref. [49]	RCI	Ref. [50]	Ref. [49]	RCI
	2157.6	2116	2115	-760	-764.27	
$1s^2 2s^2 2p \ ^4P_{3/2}$	2135.9	2083	2083	609	610.1	611.40
	4592.4	4475	4474	0.0	0.0	0.0

Table 6

Comparison of calculated hyperfine interaction constants $A_J(I/\mu_I)$ (MHz per unit of μ_N) and B_J/Q (MHz/barn) with Dutta and Majumber [48] for B-like ions from $Z = 9$ to $Z = 21$. The number in square brackets is the power of 10.

Z	Level	$A_J(I/\mu_I)$	
		Dutta and Majumber [48]	This work
9	$2p \ ^2P_{1/2}^o$	3.5569[3]	3.531[3]
	$^2P_{3/2}^o$	7.30[2]	6.902[2]
10	$2p \ ^2P_{1/2}^o$	5.383[3]	5.348[3]
	$^2P_{3/2}^o$	1.10[3]	1.043[3]
11	$2p \ ^2P_{1/2}^o$	7.7381[3]	7.692[3]
	$^2P_{3/2}^o$	1.576[3]	1.498[3]
12	$2p \ ^2P_{1/2}^o$	1.0696[4]	1.064[4]
	$^2P_{3/2}^o$	2.17[3]	2.069[3]
13	$2p \ ^2P_{1/2}^o$	1.4321[4]	1.424[4]
	$^2P_{3/2}^o$	2.903[3]	2.766[3]
14	$2p \ ^2P_{1/2}^o$	1.8689[4]	1.859[4]
	$^2P_{3/2}^o$	3.779[3]	3.604[3]
15	$2p \ ^2P_{1/2}^o$	2.3873[4]	2.375[4]
	$^2P_{3/2}^o$	4.8149[3]	4.596[3]
16	$2p \ ^2P_{1/2}^o$	2.9948[4]	2.979[4]
	$^2P_{3/2}^o$	6.025[3]	5.755[3]
17	$2p \ ^2P_{1/2}^o$	3.6988[4]	3.680[4]
	$^2P_{3/2}^o$	7.419[3]	7.093[3]
18	$2p \ ^2P_{1/2}^o$	4.5078[4]	4.485[4]
	$^2P_{3/2}^o$	9.015[3]	8.624[3]
19	$2p \ ^2P_{1/2}^o$	5.4292[4]	5.403[4]
	$^2P_{3/2}^o$	1.0823[4]	1.036[4]
20	$2p \ ^2P_{1/2}^o$	6.4722[4]	6.442[4]
	$^2P_{3/2}^o$	1.2855[4]	1.232[4]
21	$2p \ ^2P_{1/2}^o$	7.64496[4]	7.610[4]
	$^2P_{3/2}^o$	1.5127[4]	1.451[4]

Table 7

Hyperfine magnetic dipole constants $A_J(I/\mu_I)$ (MHz per unit of μ_N) and electric quadrupole constants B_J/Q (MHz/barn) in O IV. Comparison of values from RCI and MCHF calculations.

Level	RCI (this work)		MCHF (this work)	
	$A_J(I/\mu_I)$	B_J/Q	$A_J(I/\mu_I)$	B_J/Q
$2s^2 2p \ ^2P_{1/2}^o$	2174		2175	
	426.2	742.6	427.9	743.5
$2s^2 2p \ ^4P_{1/2}$	4474		4473	
	2083	610.1	2081	610.7
	2115	-764.3	2115	-765.0
$2s^2 2p \ ^2D_{3/2}$	-879.6	1043	-879.4	1042
	2432	1490	2431	1489
$2s^2 2p \ ^2P_{1/2}$	1438		1437	
	-514.6	-765.7	-513.1	-765.6
$2s^2 2p \ ^2S_{1/2}$	9060		9051	
$2p^3 \ ^4S_{3/2}^o$	-466.7	-0.0002	-466.5	0
$2p^3 \ ^2D_{3/2}^o$	548.6	-15.3	547.7	-4.5
	648.4	-43.9	648.30	-44.4
$2p^3 \ ^2P_{1/2}^o$	2232		2230.8	
	258.3	44.6	258.9	35.0

Table 8

Total energies (in E_h), excitation energies (in cm^{-1}), hyperfine magnetic dipole constants $A_J(I/\mu_I)$ (MHz per unit of μ_N), electric quadrupole constants B_J/Q (MHz/barn), and Landé g_J -factors for levels in the carbon isoelectronic sequence ($7 \leq Z \leq 28$). For each of the many-electron wave functions, the leading components are given in the LSJ coupling scheme. The number in square brackets is the power of 10. See page 18 for Explanation of Tables.

Level composition in LSJ coupling	J	Energy (E_h)	$\Delta E \text{ cm}^{-1}$	$A_J(I/\mu_I)$	B_J/Q	g_J
N II						
$1s^2 2s^2 2p^2 \ 3P$	(96%)	$+ 1s^2 2p^4 \ 3P$	(2%)	1	-54.0761997	50.41
	(96%)	$+ 1s^2 2p^4 \ 3P$	(2%)	2	-54.0758321	131.07
$1s^2 2s^2 2p^2 \ 1D$	(96%)	$+ 1s^2 2p^4 \ 1D$	(2%)	2	-54.0059995	15457.56
$1s^2 2s^2 p^3 \ 5S^o$	(99%)			2	-53.8639833	46626.52
$1s^2 2s^2 p^3 \ 3D^o$	(96%)	$+ 1s^2 2s^2 2p3d \ 3D^o$	(2%)	3	-53.6555256	92377.69
	(96%)	$+ 1s^2 2s^2 2p3d \ 3D^o$	(2%)	2	-53.6554696	92389.98
	(96%)	$+ 1s^2 2s^2 2p3d \ 3D^o$	(2%)	1	-53.6554634	92391.35
$1s^2 2s^2 p^3 \ 3P^o$	(95%)	$+ 1s^2 2s^2 2p3d \ 3P^o$	(1%)	1	-53.5766488	109689.14
	(95%)	$+ 1s^2 2s^2 2p3d \ 3P^o$	(1%)	2	-53.5766480	109689.33
$1s^2 2s^2 p^3 \ 1D^o$	(91%)	$+ 1s^2 2s^2 2p3d \ 1D^o$	(5%)	2	-53.4167653	144779.52
$1s^2 2s^2 p^3 \ 3S^o$	(95%)	$+ 1s^2 2p^3 3d \ 3S^o$	(3%)	1	-53.3675350	155584.33
O III						
$1s^2 2s^2 2p^2 \ 3P$	(97%)	$+ 1s^2 2p^4 \ 3P$	(2%)	1	-73.3174130	113.63
	(97%)	$+ 1s^2 2p^4 \ 3P$	(2%)	2	-73.3165408	305.05
$1s^2 2s^2 2p^2 \ 1D$	(96%)	$+ 1s^2 2p^4 \ 1D$	(2%)	2	-73.2249452	20407.96
$1s^2 2s^2 p^3 \ 5S^o$	(99%)			2	-73.0439650	60128.52
$1s^2 2s^2 p^3 \ 3D^o$	(97%)	$+ 1s^2 2s^2 2p3d \ 3D^o$	(1%)	3	-72.7706503	120114.15
	(97%)	$+ 1s^2 2s^2 2p3d \ 3D^o$	(1%)	2	-72.7705276	120141.09
	(97%)	$+ 1s^2 2s^2 2p3d \ 3D^o$	(1%)	1	-72.7705022	120146.66
$1s^2 2s^2 p^3 \ 3P^o$	(97%)	$+ 1s^2 2s^2 2p3d \ 3P^o$	(1%)	2	-72.6680198	142638.96
	(97%)	$+ 1s^2 2s^2 2p3d \ 3P^o$	(1%)	1	-72.6680112	142640.83
$1s^2 2s^2 p^3 \ 1D^o$	(95%)	$+ 1s^2 2s^2 2p3d \ 1D^o$	(2%)	2	-72.4640740	187399.88
$1s^2 2s^2 p^3 \ 3S^o$	(97%)	$+ 1s^2 2p^3 3d \ 3S^o$	(2%)	1	-72.4188002	197336.33
$1s^2 2s^2 p^3 \ 1P^o$	(96%)	$+ 1s^2 2p^3 3d \ 1P^o$	(1%)	1	-72.3555087	211227.21
$1s^2 2p^4 \ 3P$	(93%)	$+ 1s^2 2s^2 p^2 3d \ 3P$	(3%)	2	-72.0228535	284236.57
	(93%)	$+ 1s^2 2s^2 p^2 3d \ 3P$	(3%)	1	-72.0218178	284463.89
$1s^2 2p^4 \ 1D$	(92%)	$+ 1s^2 2s^2 p^2 3d \ 1D$	(4%)	2	-71.9565836	298781.15
F IV						
$1s^2 2s^2 2p^2 \ 3P$	(97%)	$+ 1s^2 2p^4 \ 3P$	(2%)	1	-95.5756085	227.03
	(97%)	$+ 1s^2 2p^4 \ 3P$	(2%)	2	-95.5738482	613.37
$1s^2 2s^2 2p^2 \ 1D$	(97%)	$+ 1s^2 2p^4 \ 1D$	(2%)	2	-95.4610400	25371.91
$1s^2 2s^2 p^3 \ 5S^o$	(99%)			2	-95.2395685	73979.29
$1s^2 2s^2 p^3 \ 3D^o$	(98%)	$+ 1s^2 2s^2 2p3d \ 3D^o$	(1%)	3	-94.9026825	147917.21
	(98%)	$+ 1s^2 2s^2 2p3d \ 3D^o$	(1%)	2	-94.9024699	147963.87
	(98%)	$+ 1s^2 2s^2 2p3d \ 3D^o$	(1%)	1	-94.9024123	147976.52
$1s^2 2s^2 p^3 \ 3P^o$	(98%)			2	-94.7772384	175449.01
	(98%)			1	-94.7772199	175453.07
$1s^2 2s^2 p^3 \ 1D^o$	(97%)	$+ 1s^2 2p^3 3d \ 1D^o$	(1%)	2	-94.5322829	229210.53
$1s^2 2s^2 p^3 \ 3S^o$	(98%)	$+ 1s^2 2p^3 3d \ 3S^o$	(1%)	1	-94.4899033	238511.78
$1s^2 2s^2 p^3 \ 1P^o$	(97%)	$+ 1s^2 2p^3 3d \ 1P^o$	(1%)	1	-94.4014914	257915.96
$1s^2 2p^4 \ 3P$	(95%)	$+ 1s^2 2s^2 p^2 3d \ 3P$	(2%)	2	-93.9882702	348607.53
	(95%)	$+ 1s^2 2s^2 p^2 3d \ 3P$	(1%)	1	-93.9862556	349049.68
$1s^2 2p^4 \ 1D$	(94%)	$+ 1s^2 2s^2 p^2 3d \ 1D$	(3%)	2	-93.9009178	367779.14
Ne V						
$1s^2 2s^2 2p^2 \ 3P$	(97%)	$+ 1s^2 2p^4 \ 3P$	(1%)	1	-120.8519610	411.41
	(97%)	$+ 1s^2 2p^4 \ 3P$	(1%)	2	-120.8487841	1108.65
$1s^2 2s^2 2p^2 \ 1D$	(97%)	$+ 1s^2 2p^4 \ 1D$	(1%)	2	-120.7151946	30428.15
$1s^2 2s^2 p^3 \ 5S^o$	(100%)			2	-120.4520734	88176.60
$1s^2 2s^2 p^3 \ 3D^o$	(99%)			3	-120.0523460	175906.61
	(99%)			2	-120.0520265	175976.73
	(99%)			1	-120.0519193	176000.26
$1s^2 2s^2 p^3 \ 3P^o$	(99%)			2	-119.9045366	208347.03
	(99%)			1	-119.9045144	208351.89
$1s^2 2s^2 p^3 \ 1D^o$	(98%)	$+ 1s^2 2p^3 3d \ 1D^o$	(1%)	2	-119.6197268	270855.55
$1s^2 2s^2 p^3 \ 3S^o$	(98%)	$+ 1s^2 2p^3 3d \ 3S^o$	(1%)	1	-119.5799645	279582.37
$1s^2 2s^2 p^3 \ 1P^o$	(98%)	$+ 1s^2 2p^3 3d \ 1P^o$	(1%)	1	-119.4673898	304289.64
$1s^2 2p^4 \ 3P$	(96%)	$+ 1s^2 2s^2 p^2 3P$	(1%)	2	-118.9724357	412919.52
	(96%)	$+ 1s^2 2s^2 p^2 3P$	(1%)	1	-118.9688252	413711.94
$1s^2 2p^4 \ 1D$	(96%)	$+ 1s^2 2s^2 p^2 3d \ 1D$	(2%)	2	-118.8629831	436941.59
Na VI						
$1s^2 2s^2 2p^2 \ 3P$	(98%)	$+ 1s^2 2p^4 \ 3P$	(1%)	1	-149.1491632	694.64
	(98%)	$+ 1s^2 2p^4 \ 3P$	(1%)	2	-149.1438748	1855.29

Table 8 (continued)

Level composition in LSJ coupling			J	Energy (E_h)	$\Delta E \text{ cm}^{-1}$	$A_J(I/\mu_I)$	B_J/Q	g_J
$1s^2 2s^2 2p^2 {}^1D$ (98%)	$+ 1s^2 2p^4 {}^1D$	(1%)	2	-148.9899158	35645.39	2.512[3]	4.778[3]	0.999926
$1s^2 2s2p^3 {}^5S^o$ (100%)			2	-148.6839554	102795.94	6.285[3]	-9.598[-2]	2.001652
$1s^2 2s2p^3 {}^3D^o$ (99%)			3	-148.2218363	204219.37	6.362[3]	-5.598[1]	1.333576
			2	-148.2214102	204312.88	3.650[3]	2.194[2]	1.166905
			1	-148.2212300	204352.43	-4.588[3]	1.041[2]	0.499121
$1s^2 2s2p^3 {}^3P^o$ (99%)			2	-148.0518783	241520.82	7.500[3]	-1.887[2]	1.500297
			1	-148.0518733	241521.92	9.077[3]	-1.542[2]	1.500093
$1s^2 2s2p^3 {}^1D^o$ (98%)	$+ 1s^2 2s^2 2p3d {}^1D^o$	(1%)	2	-147.7278257	312642.15	2.510[3]	-1.003[2]	0.999635
$1s^2 2s2p^3 {}^3S^o$ (98%)	$+ 1s^2 2p^3 3d {}^3S^o$	(1%)	1	-147.6906078	320810.53	-7.300[3]	-2.511[-1]	2.000449
$1s^2 2s2p^3 {}^1P^o$ (98%)			1	-147.5540602	350779.26	2.496[3]	8.279[1]	1.000745
$1s^2 2p^4 {}^3P$ (97%)	$+ 1s^2 2s^2 2p^2 {}^3P$	(1%)	2	-146.9767101	477492.96	9.415[2]	2.234[3]	1.500201
			1	-146.9706997	478812.10	-5.604[2]	-1.115[3]	1.500708
$1s^2 2p^4 {}^1D$ (96%)	$+ 1s^2 2s^2 2p^2 {}^1D$	(1%)	2	-146.8446022	506487.29	2.503[3]	-4.582[3]	0.999980
Mg VII								
$1s^2 2s^2 2p^2 {}^3P$ (98%)	$+ 1s^2 2p^4 {}^3P$	(1%)	1	-180.4708952	1112.14	-6.590[1]	1.692[3]	1.500576
	$+ 1s^2 2p^4 {}^3P$	(1%)	2	-180.4626198	2928.38	2.230[3]	-3.390[3]	1.499736
$1s^2 2s^2 2p^2 {}^1D$ (98%)	$+ 1s^2 2p^4 {}^1D$	(1%)	2	-180.2887088	41097.43	3.497[3]	6.693[3]	1.000154
$1s^2 2s2p^3 {}^5S^o$ (100%)			2	-179.9387744	117899.16	8.593[3]	-1.957[-1]	2.001454
$1s^2 2s2p^3 {}^3D^o$ (99%)			3	-179.4145625	232950.36	8.753[3]	-6.015[1]	1.333440
			2	-179.4140639	233059.80	5.041[3]	4.517[2]	1.167064
			1	-179.4137787	233122.38	-6.180[3]	2.201[2]	0.499541
$1s^2 2s2p^3 {}^3P^o$ (99%)			1	-179.2224979	275103.67	1.247[4]	-2.767[2]	1.499521
			2	-179.2224402	275116.33	1.026[4]	-4.141[2]	1.499851
$1s^2 2s2p^3 {}^1D^o$ (99%)			2	-178.8596168	354746.86	3.520[3]	-1.394[2]	0.999595
$1s^2 2s2p^3 {}^3S^o$ (99%)	$+ 1s^2 2p^3 3d {}^3S^o$	(1%)	1	-178.8248988	362366.58	-9.855[3]	-5.541[-1]	1.999301
$1s^2 2s2p^3 {}^1P^o$ (99%)			1	-178.6642646	397621.71	3.472[3]	1.102[2]	1.001545
$1s^2 2p^4 {}^3P$ (97%)	$+ 1s^2 2s^2 2p^2 {}^3P$	(1%)	2	-178.0038944	542556.21	1.376[3]	3.155[3]	1.499728
			1	-177.9944361	544632.08	-7.173[2]	-1.576[3]	1.500591
$1s^2 2p^4 {}^1D$ (97%)	$+ 1s^2 2s^2 2p^2 {}^1D$	(1%)	2	-177.8485246	576655.93	3.523[3]	-6.443[3]	1.000197
Al VIII								
$1s^2 2s^2 2p^2 {}^3P$ (98%)	$+ 1s^2 2p^4 {}^3P$	(1%)	1	-214.8215927	1708.66	-9.499[1]	2.287[3]	1.500444
	$+ 1s^2 2p^4 {}^3P$	(1%)	2	-214.8092653	4414.19	3.035[3]	-4.573[3]	1.498996
$1s^2 2s^2 2p^2 {}^1D$ (98%)	$+ 1s^2 2p^4 {}^1D$	(1%)	2	-214.6158188	46870.79	4.697[3]	9.050[3]	1.000604
$1s^2 2s2p^3 {}^5S^o$ (100%)			2	-214.2205307	133626.50	1.141[4]	-3.686[-1]	2.001211
$1s^2 2s2p^3 {}^3D^o$ (99%)			3	-213.6344142	262264.20	1.168[4]	-6.431[1]	1.333288
			2	-213.6339348	262369.42	6.754[3]	8.439[2]	1.167392
			1	-213.6335011	262464.60	-8.102[3]	4.167[2]	0.500283
$1s^2 2s2p^3 {}^3P^o$ (99%)			1	-213.4202377	309270.52	1.661[4]	-4.804[2]	1.498656
			2	-213.4200302	309316.05	1.362[4]	-7.987[2]	1.499178
$1s^2 2s2p^3 {}^1D^o$ (99%)			2	-213.0187642	397383.75	4.771[3]	-1.833[2]	0.999597
$1s^2 2s2p^3 {}^3S^o$ (99%)			1	-212.9866294	404436.54	-1.292[4]	-1.105	1.997547
$1s^2 2s2p^3 {}^1P^o$ (99%)			1	-212.8016794	445028.35	4.652[3]	1.412[2]	1.002865
$1s^2 2p^4 {}^3P$ (97%)	$+ 1s^2 2s^2 2p^2 {}^3P$	(1%)	2	-212.0576804	608317.26	1.921[3]	4.289[3]	1.499047
			1	-212.0434414	611442.35	-8.953[2]	-2.148[3]	1.500461
$1s^2 2p^4 {}^1D$ (97%)	$+ 1s^2 2s^2 2p^2 {}^1D$	(1%)	2	-211.8782649	647694.41	4.793[3]	-8.739[3]	1.000592
Si IX								
$1s^2 2s^2 2p^2 {}^3P$ (98%)	$+ 1s^2 2p^4 {}^3P$	(1%)	1	-252.2063456	2540.25	-1.328[2]	3.008[3]	1.500298
	$+ 1s^2 2p^4 {}^3P$	(1%)	2	-252.1887113	6410.52	4.029[3]	-5.987[3]	1.497885
$1s^2 2s^2 2p^2 {}^1D$ (98%)	$+ 1s^2 2p^4 {}^1D$	(1%)	2	-251.9761136	53070.34	6.127[3]	1.189[4]	1.001395
$1s^2 2s2p^3 {}^5S^o$ (100%)			2	-251.5339219	150120.18	1.480[4]	-6.312[-1]	2.000912
$1s^2 2s2p^3 {}^3D^o$ (99%)			3	-250.8859967	292323.33	1.520[4]	-6.852[1]	1.333120
			2	-250.8857182	292384.45	8.832[3]	1.471[3]	1.167973
			1	-250.8850767	292525.24	-1.038[4]	7.323[2]	0.501502
$1s^2 2s2p^3 {}^3P^o$ (99%)			1	-250.6496224	344201.49	2.157[4]	-8.037[2]	1.497369
			2	-250.6491157	344312.68	1.762[4]	-1.417[3]	1.498181
$1s^2 2s2p^3 {}^1D^o$ (99%)			2	-250.2097125	440750.55	6.293[3]	-2.321[2]	0.999667
$1s^2 2s2p^3 {}^3S^o$ (99%)	$+ 1s^2 2s2p^3 {}^1P^o$	(1%)	1	-250.1803542	447193.95	-1.653[4]	-2.008	1.994947
$1s^2 2s2p^3 {}^1P^o$ (99%)	$+ 1s^2 2s2p^3 {}^3S^o$	(1%)	1	-249.9706514	493218.39	6.036[3]	1.758[2]	1.004919
$1s^2 2p^4 {}^3P$ (97%)	$+ 1s^2 2s^2 2p^2 {}^3P$	(1%)	2	-249.1424537	674986.77	2.585[3]	5.653[3]	1.498089
			1	-249.1217695	679526.43	-1.097[3]	-2.842[3]	1.500318
$1s^2 2p^4 {}^1D$ (97%)	$+ 1s^2 2s^2 2p^2 {}^1D$	(1%)	2	-248.9379625	719867.40	6.345[3]	-1.151[4]	1.001235
P X								
$1s^2 2s^2 2p^2 {}^3P$ (98%)	$+ 1s^2 2p^4 {}^3P$	(1%)	1	-292.6308367	3676.45	-1.813[2]	3.865[3]	1.500139
	$+ 1s^2 2p^4 {}^3P$	(1%)	2	-292.6064592	9026.70	5.244[3]	-7.636[3]	1.496244
$1s^2 2s^2 2p^2 {}^1D$ (98%)	$+ 1s^2 2p^4 {}^1D$	(1%)	2	-292.3750067	59824.65	7.797[3]	1.523[4]	1.002687
$1s^2 2s2p^3 {}^5S^o$ (100%)			2	-291.8842161	167540.74	1.880[4]	-9.569[-1]	2.000539
$1s^2 2s2p^3 {}^3D^o$ (99%)	$+ 1s^2 2s2p^3 {}^3P^o$	(1%)	2	-291.1747264	323255.71	1.133[4]	2.428[3]	1.168910
			3	-291.1744907	323307.44	1.937[4]	-7.280[1]	1.332937

Table 8 (continued)

Level composition in LSJ coupling		J	Energy (E_h)	$\Delta E \text{ cm}^{-1}$	$A_J(I/\mu_I)$	B_J/Q	g_J		
$1s^2 2s2p^3 \ 3P^o$	(99%)	1	-291.1737983	323459.40	-1.305[4]	1.217[3]	0.503395		
$1s^2 2s2p^3 \ 3P^o$	(99%)	1	-290.9157546	380093.46	2.742[4]	-1.297[3]	1.495500		
$1s^2 2s2p^3 \ 3D^o$	(99%)	+ $1s^2 2s2p^3 \ 3D^o$	(1%)	2	-290.9147096	380322.81	2.231[4]	-2.365[3]	1.496739
$1s^2 2s2p^3 \ 1D^o$	(99%)			2	-290.4375065	485056.78	8.119[3]	-2.859[2]	0.999841
$1s^2 2s2p^3 \ 3S^o$	(98%)	+ $1s^2 2s2p^3 \ 1P^o$	(1%)	1	-290.4112655	490816.02	-2.067[4]	-3.323	1.991206
$1s^2 2s2p^3 \ 1P^o$	(98%)	+ $1s^2 2s2p^3 \ 3S^o$	(1%)	1	-290.1760976	542429.39	7.602[3]	2.142[2]	1.007965
$1s^2 2p^4 \ 3P$	(97%)	+ $1s^2 2s^2 2p^2 \ 3P$	(1%)	2	-289.2632122	742784.59	3.376[3]	7.257[3]	1.496772
$1s^2 2p^4 \ 3P$	(98%)	+ $1s^2 2s^2 2p^2 \ 3P$	(1%)	1	-289.2340348	749188.29	-1.323[3]	-3.670[3]	1.500161
$1s^2 2p^4 \ 1D$	(97%)	+ $1s^2 2s^2 2p^2 \ 1D$	(1%)	2	-289.0323005	793463.84	8.211[3]	-1.480[4]	1.002207
S XI									
$1s^2 2s^2 2p^2 \ 3P$	(98%)	+ $1s^2 2p^4 \ 3P$	(1%)	1	-336.1013056	5202.55	-2.432[2]	4.871[3]	1.499967
$1s^2 2s^2 2p^2 \ 3P$	(97%)	+ $1s^2 2p^4 \ 3P$	(1%)	2	-336.0685879	12383.25	6.718[3]	-9.511[3]	1.493861
$1s^2 2s^2 2p^2 \ 1D$	(97%)	+ $1s^2 2p^4 \ 1D$	(1%)	2	-335.8184121	67290.49	9.709[3]	1.909[4]	1.004691
$1s^2 2s2p^3 \ 5S^o$	(100%)			2	-335.2772346	186065.22	2.349[4]	-1.202	2.000071
$1s^2 2s2p^3 \ 3D^o$	(98%)	+ $1s^2 2s2p^3 \ 3P^o$	(1%)	2	-334.5068680	355141.13	1.429[4]	3.831[3]	1.170323
$1s^2 2s2p^3 \ 3D^o$	(100%)			3	-334.5056214	355414.74	2.426[4]	-7.710[1]	1.332738
$1s^2 2s2p^3 \ 3P^o$	(99%)	+ $1s^2 2s2p^3 \ 3P^o$	(1%)	1	-334.5055518	355430.00	-1.612[4]	1.934[3]	0.506209
$1s^2 2s2p^3 \ 3P^o$	(99%)	+ $1s^2 2s2p^3 \ 3D^o$	(1%)	1	-334.2242702	417164.19	3.420[4]	-2.022[3]	1.492849
$1s^2 2s2p^3 \ 3P^o$	(98%)	+ $1s^2 2s2p^3 \ 3D^o$	(1%)	2	-334.2223244	417591.23	2.772[4]	-3.758[3]	1.494704
$1s^2 2s2p^3 \ 1D^o$	(99%)			2	-333.7077365	530530.22	1.029[4]	-3.452[2]	1.000166
$1s^2 2s2p^3 \ 3S^o$	(98%)	+ $1s^2 2s2p^3 \ 1P^o$	(1%)	1	-333.6851524	535486.87	-2.534[4]	-4.938	1.985982
$1s^2 2s2p^3 \ 1P^o$	(98%)	+ $1s^2 2s2p^3 \ 3S^o$	(1%)	1	-333.4234398	592926.13	9.307[3]	2.563[2]	1.012298
$1s^2 2p^4 \ 3P$	(97%)	+ $1s^2 2s^2 2p^2 \ 3P$	(1%)	2	-332.4255377	811940.33	4.303[3]	9.106[3]	1.495012
$1s^2 2p^4 \ 3P$	(98%)	+ $1s^2 2s^2 2p^2 \ 3P$	(1%)	1	-332.3853807	820753.77	-1.577[3]	-4.645[3]	1.499991
$1s^2 2p^4 \ 1D$	(97%)	+ $1s^2 2s^2 2p^2 \ 1D$	(1%)	2	-332.1664626	868800.72	1.042[4]	-1.862[4]	1.003593
Cl XII									
$1s^2 2s^2 2p^2 \ 3P$	(98%)	+ $1s^2 2p^4 \ 3P$	(1%)	1	-382.6247038	7221.09	-3.215[2]	6.037[3]	1.499782
$1s^2 2s^2 2p^2 \ 3P$	(97%)	+ $1s^2 2s^2 2p^2 \ 1D$	(2%)	2	-382.5819245	16610.06	8.494[3]	-1.158[4]	1.490471
$1s^2 2s^2 2p^2 \ 1D$	(97%)	+ $1s^2 2s^2 2p^2 \ 3P$	(2%)	2	-382.3128716	75660.34	1.186[4]	2.347[4]	1.007673
$1s^2 2s2p^3 \ 5S^o$	(100%)			2	-381.7193420	205925.02	2.891[4]	-9.637[-1]	1.999480
$1s^2 2s2p^3 \ 3D^o$	(98%)	+ $1s^2 2s2p^3 \ 3P^o$	(2%)	2	-380.8886353	388244.07	1.781[4]	5.812[3]	1.172344
$1s^2 2s2p^3 \ 3D^o$	(98%)	+ $1s^2 2s2p^3 \ 3P^o$	(1%)	1	-380.8868072	388645.28	-1.961[4]	2.958[3]	0.510230
$1s^2 2s2p^3 \ 3D^o$	(100%)			3	-380.8856367	388902.17	2.991[4]	-8.142[1]	1.332524
$1s^2 2s2p^3 \ 3P^o$	(98%)	+ $1s^2 2s2p^3 \ 3D^o$	(1%)	1	-380.5813139	455693.32	4.196[4]	-3.056[3]	1.489190
$1s^2 2s2p^3 \ 3P^o$	(97%)	+ $1s^2 2s2p^3 \ 3D^o$	(2%)	2	-380.5779433	456433.08	3.385[4]	-5.728[3]	1.491913
$1s^2 2s2p^3 \ 1D^o$	(99%)			2	-380.0265010	577460.66	1.285[4]	-4.111[2]	1.000704
$1s^2 2s2p^3 \ 3S^o$	(97%)	+ $1s^2 2s2p^3 \ 1P^o$	(2%)	1	-380.0083781	581438.19	-3.046[4]	-6.340	1.978907
$1s^2 2s2p^3 \ 1P^o$	(97%)	+ $1s^2 2s2p^3 \ 3S^o$	(2%)	1	-379.7185633	645045.17	1.107[4]	3.016[2]	1.018226
$1s^2 2p^4 \ 3P$	(97%)	+ $1s^2 2p^4 \ 1D$	(1%)	2	-378.6355643	882735.99	5.372[3]	1.120[4]	1.492723
$1s^2 2p^4 \ 3P$	(98%)	+ $1s^2 2s^2 2p^2 \ 3P$	(1%)	1	-378.5814390	894615.10	-1.863[3]	-5.778[3]	1.499807
$1s^2 2p^4 \ 1D$	(97%)	+ $1s^2 2p^4 \ 3P$	(1%)	2	-378.3461291	946259.65	1.302[4]	-2.300[4]	1.005478
Ar XIII									
$1s^2 2s^2 2p^2 \ 3P$	(99%)	+ $1s^2 2p^4 \ 3P$	(1%)	1	-432.2083036	9853.80	-4.194[2]	7.378[3]	1.499583
$1s^2 2s^2 2p^2 \ 3P$	(96%)	+ $1s^2 2s^2 2p^2 \ 1D$	(3%)	2	-432.1536681	21844.91	1.063[4]	-1.378[4]	1.485757
$1s^2 2s^2 2p^2 \ 1D$	(96%)	+ $1s^2 2s^2 2p^2 \ 3P$	(3%)	2	-431.8651603	85165.03	1.424[4]	2.833[4]	1.011948
$1s^2 2s2p^3 \ 5S^o$	(100%)			2	-431.2174215	227327.28	3.514[4]	6.830[-1]	1.998731
$1s^2 2s2p^3 \ 3D^o$	(97%)	+ $1s^2 2s2p^3 \ 3P^o$	(3%)	2	-430.3270767	422735.36	2.196[4]	8.514[3]	1.175102
$1s^2 2s2p^3 \ 3D^o$	(98%)	+ $1s^2 2s2p^3 \ 3P^o$	(2%)	1	-430.3245980	423279.37	-2.351[4]	4.375[3]	0.515779
$1s^2 2s2p^3 \ 3D^o$	(100%)			3	-430.3212742	424008.88	3.640[4]	-8.576[1]	1.332294
$1s^2 2s2p^3 \ 3P^o$	(98%)	+ $1s^2 2s2p^3 \ 3D^o$	(2%)	1	-429.9934990	495947.20	5.070[4]	-4.484[3]	1.484275
$1s^2 2s2p^3 \ 3P^o$	(96%)	+ $1s^2 2s2p^3 \ 3D^o$	(3%)	2	-429.9879770	497159.15	4.068[4]	-8.415[3]	1.488194
$1s^2 2s2p^3 \ 1D^o$	(99%)	+ $1s^2 2s2p^3 \ 3P^o$	(1%)	2	-429.4003600	626126.16	1.586[4]	-4.860[2]	1.001531
$1s^2 2s2p^3 \ 3S^o$	(96%)	+ $1s^2 2s2p^3 \ 1P^o$	(3%)	1	-429.3878426	628873.41	-3.592[4]	-6.215	1.969617
$1s^2 2s2p^3 \ 1P^o$	(96%)	+ $1s^2 2s2p^3 \ 3S^o$	(3%)	1	-429.0677621	699122.95	1.277[4]	3.490[2]	1.026041
$1s^2 2p^4 \ 3P$	(96%)	+ $1s^2 2p^4 \ 1D$	(2%)	2	-427.8999369	955430.96	6.591[3]	1.351[4]	1.489831
$1s^2 2p^4 \ 3P$	(98%)	+ $1s^2 2s^2 2p^2 \ 3P$	(1%)	1	-427.8282900	971155.64	-2.183[3]	-7.083[3]	1.499611
$1s^2 2p^4 \ 1D$	(96%)	+ $1s^2 2p^4 \ 3P$	(2%)	2	-427.5773860	1026222.69	1.603[4]	-2.795[4]	1.007937
K XIV									
$1s^2 2s^2 2p^2 \ 3P$	(99%)	+ $1s^2 2p^4 \ 3P$	(1%)	1	-484.8601418	13242.12	-5.408[2]	8.904[3]	1.499371
$1s^2 2s^2 2p^2 \ 3P$	(95%)	+ $1s^2 2s^2 2p^2 \ 1D$	(4%)	2	-484.7918504	28230.36	1.318[4]	-1.601[4]	1.479373
$1s^2 2s^2 2p^2 \ 1D$	(95%)	+ $1s^2 2s^2 2p^2 \ 3P$	(4%)	2	-484.4827031	96080.34	1.684[4]	3.358[4]	1.017865
$1s^2 2s2p^3 \ 5S^o$	(99%)			2	-483.7790199	250520.95	4.223[4]	5.623	1.997779
$1s^2 2s2p^3 \ 3D^o$	(96%)	+ $1s^2 2s2p^3 \ 3P^o$	(4%)	2	-482.8299330	458821.44	2.687[4]	1.208[4]	1.178707
$1s^2 2s2p^3 \ 3D^o$	(97%)	+ $1s^2 2s2p^3 \ 3P^o$	(2%)	1	-482.8266691	459537.78	-2.781[4]	6.281[3]	0.523190
$1s^2 2s2p^3 \ 3D^o$	(100%)			3	-482.8198953	461024.45	4.380[4]	-9.015[1]	1.332049
$1s^2 2s2p^3 \ 3P^o$	(97%)	+ $1s^2 2s2p^3 \ 3D^o$	(2%)	1	-482.4680408	538247.61	6.044[4]	-6.402[3]	1.477859
$1s^2 2s2p^3 \ 3P^o$	(95%)	+ $1s^2 2s2p^3 \ 3D^o$	(4%)	2	-482.4593991	540144.23	4.818[4]	-1.196[4]	1.483386
$1s^2 2s2p^3 \ 1D^o$	(99%)	+ $1s^2 2s2p^3 \ 3P^o$	(1%)	2	-481.8364563	676864.37	1.938[4]	-5.743[2]	1.002744

Table 8 (continued)

Level composition in LSJ coupling			J	Energy (E_h)	ΔE cm $^{-1}$	$A_J(I/\mu_I)$	B_J/Q	g_J	
$1s^2 2s 2p^3 \ ^3S^o$	(95%)	$+ 1s^2 2s 2p^3 \ ^1P^o$	(4%)	1	-481.8311139	678036.89	-4.155[4]	-1.842	1.957797
$1s^2 2s 2p^3 \ ^1P^o$	(95%)	$+ 1s^2 2s 2p^3 \ ^3S^o$	(4%)	1	-481.4778603	755567.10	1.425[4]	3.962[2]	1.035967
$1s^2 2p^4 \ ^3P$	(96%)	$+ 1s^2 2p^4 \ ^1D$	(3%)	2	-480.2259517	1030329.26	7.970[3]	1.602[4]	1.486283
	(98%)	$+ 1s^2 2s^2 2p^2 \ ^3P$	(1%)	1	-480.1325978	1050818.07	-2.542[3]	-8.572[3]	1.499401
$1s^2 2p^4 \ ^1D$	(96%)	$+ 1s^2 2p^4 \ ^3P$	(3%)	2	-479.8668887	1109134.47	1.950[4]	-3.347[4]	1.011024
Ca XV									
$1s^2 2s^2 2p^2 \ ^3P$	(99%)	$+ 1s^2 2p^4 \ ^3P$	(1%)	1	-540.5886442	17547.29	-6.901[2]	1.063[4]	1.499146
	(93%)	$+ 1s^2 2s^2 2p^2 \ ^1D$	(5%)	2	-540.5049737	35910.83	1.622[4]	-1.812[4]	1.470979
$1s^2 2s^2 2p^2 \ ^1D$	(93%)	$+ 1s^2 2s^2 2p^2 \ ^3P$	(5%)	2	-540.1731873	108729.53	1.961[4]	3.911[4]	1.025764
$1s^2 2s 2p^3 \ ^5S^o$	(99%)	$+ 1s^2 2s 2p^3 \ ^3P^o$	(1%)	2	-539.4120963	275769.69	5.027[4]	1.742[1]	1.996569
$1s^2 2s 2p^3 \ ^3D^o$	(94%)	$+ 1s^2 2s 2p^3 \ ^3P^o$	(5%)	2	-538.4053697	496720.65	3.264[4]	1.663[4]	1.183229
	(96%)	$+ 1s^2 2s 2p^3 \ ^3P^o$	(3%)	1	-538.4012286	497629.50	-3.248[4]	8.773[3]	0.532777
	(100%)			3	-538.3892241	500264.19	5.215[4]	-9.444[1]	1.331788
$1s^2 2s 2p^3 \ ^3P^o$	(96%)	$+ 1s^2 2s 2p^3 \ ^3D^o$	(3%)	1	-538.0124929	582947.14	7.110[4]	-8.907[3]	1.469731
	(93%)	$+ 1s^2 2s 2p^3 \ ^3D^o$	(5%)	2	-537.9994897	585801.00	5.624[4]	-1.648[4]	1.477354
$1s^2 2s 2p^3 \ ^5S^o$	(94%)	$+ 1s^2 2s 2p^3 \ ^1P^o$	(5%)	1	-537.3461566	729191.04	-4.710[4]	1.177[1]	1.943232
$1s^2 2s 2p^3 \ ^1D^o$	(98%)	$+ 1s^2 2s 2p^3 \ ^3P^o$	(1%)	2	-537.3422404	730050.55	2.352[4]	-6.849[2]	1.004462
$1s^2 2s 2p^3 \ ^1P^o$	(94%)	$+ 1s^2 2s 2p^3 \ ^3S^o$	(5%)	1	-536.9559392	814833.85	1.527[4]	4.389[2]	1.048117
$1s^2 2p^4 \ ^3P$	(95%)	$+ 1s^2 2p^4 \ ^1D$	(3%)	2	-535.6212980	1107753.74	9.520[3]	1.870[4]	1.482051
	(99%)	$+ 1s^2 2s^2 2p^2 \ ^3P$	(1%)	1	-535.5013531	1134078.59	-2.946[3]	-1.026[4]	1.499178
$1s^2 2p^4 \ ^1D$	(95%)	$+ 1s^2 2p^4 \ ^3P$	(3%)	2	-535.2215973	1195477.90	2.344[4]	-3.955[4]	1.014763
Sc XVI									
$1s^2 2s^2 2p^2 \ ^3P$	(99%)	$+ 1s^2 2p^4 \ ^3P$	(1%)	1	-599.4028147	22949.47	-8.724[2]	1.257[4]	1.498908
	(91%)	$+ 1s^2 2s^2 2p^2 \ ^1D$	(8%)	2	-599.3022067	45030.37	1.983[4]	-1.990[4]	1.460307
$1s^2 2s^2 2p^2 \ ^1D$	(91%)	$+ 1s^2 2s^2 2p^2 \ ^3P$	(7%)	2	-598.9447447	123484.21	2.254[4]	4.474[4]	1.035910
$1s^2 2s 2p^3 \ ^5S^o$	(99%)	$+ 1s^2 2s 2p^3 \ ^3P^o$	(1%)	2	-598.1251844	303356.91	5.930[4]	4.239[1]	1.995033
$1s^2 2s 2p^3 \ ^3D^o$	(93%)	$+ 1s^2 2s 2p^3 \ ^3P^o$	(7%)	2	-597.0621058	536675.69	3.943[4]	2.226[4]	1.188683
	(95%)	$+ 1s^2 2s 2p^3 \ ^3P^o$	(4%)	1	-597.0570992	537774.50	-3.749[4]	1.194[4]	0.544800
	(100%)			3	-597.0374924	542077.70	6.154[4]	-9.942[1]	1.331511
$1s^2 2s 2p^3 \ ^3P^o$	(94%)	$+ 1s^2 2s 2p^3 \ ^3D^o$	(4%)	1	-596.6348983	630436.90	8.261[4]	-1.209[4]	1.459752
	(90%)	$+ 1s^2 2s 2p^3 \ ^3D^o$	(7%)	2	-596.6160017	634584.22	6.474[4]	-2.206[4]	1.470005
$1s^2 2s 2p^3 \ ^3S^o$	(92%)	$+ 1s^2 2s 2p^3 \ ^1P^o$	(7%)	1	-595.9414657	782627.75	-5.226[4]	4.291[1]	1.925855
$1s^2 2s 2p^3 \ ^1D^o$	(98%)	$+ 1s^2 2s 2p^3 \ ^3P^o$	(2%)	2	-595.9255960	786110.74	2.840[4]	-8.304[2]	1.006831
$1s^2 2s 2p^3 \ ^1P^o$	(92%)	$+ 1s^2 2s 2p^3 \ ^3S^o$	(7%)	1	-595.5094821	877437.18	1.560[4]	4.692[2]	1.062439
$1s^2 2p^4 \ ^3P$	(94%)	$+ 1s^2 2p^4 \ ^1D$	(4%)	2	-594.0942210	1188051.08	1.125[4]	2.149[4]	1.477148
	(99%)	$+ 1s^2 2s^2 2p^2 \ ^3P$	(1%)	1	-593.9420373	1221451.55	-3.398[3]	-1.215[4]	1.498942
$1s^2 2p^4 \ ^1D$	(94%)	$+ 1s^2 2p^4 \ ^3P$	(4%)	2	-593.6489435	1285778.20	2.790[4]	-4.617[4]	1.019145
Ti XVII									
$1s^2 2s^2 2p^2 \ ^3P$	(99%)	$+ 1s^2 2p^4 \ ^3P$	(1%)	1	-661.3123823	29646.22	-1.093[3]	1.473[4]	1.498656
	(89%)	$+ 1s^2 2s^2 2p^2 \ ^1D$	(10%)	2	-661.1935264	55732.07	2.408[4]	-2.112[4]	1.447244
$1s^2 2s^2 2p^2 \ ^1D$	(89%)	$+ 1s^2 2s^2 2p^2 \ ^3P$	(10%)	2	-660.8061017	140761.97	2.559[4]	5.025[4]	1.048418
$1s^2 2s 2p^3 \ ^5S^o$	(99%)	$+ 1s^2 2s 2p^3 \ ^3P^o$	(1%)	2	-659.9276364	333562.80	6.944[4]	9.145[1]	1.993088
$1s^2 2s 2p^3 \ ^3D^o$	(91%)	$+ 1s^2 2s 2p^3 \ ^3P^o$	(9%)	2	-658.8096422	578934.16	4.736[4]	2.902[4]	1.195026
	(93%)	$+ 1s^2 2s 2p^3 \ ^3P^o$	(6%)	1	-658.8039804	580176.77	-4.281[4]	1.586[4]	0.559419
	(100%)			3	-658.7736882	586825.16	7.203[4]	-1.032[2]	1.331219
$1s^2 2s 2p^3 \ ^3P^o$	(93%)	$+ 1s^2 2s 2p^3 \ ^3D^o$	(6%)	1	-658.3440501	681119.81	9.485[4]	-1.604[4]	1.447892
	(88%)	$+ 1s^2 2s 2p^3 \ ^3D^o$	(9%)	2	-658.3174391	686960.25	7.353[4]	-2.873[4]	1.461288
$1s^2 2s 2p^3 \ ^3S^o$	(90%)	$+ 1s^2 2s 2p^3 \ ^1P^o$	(8%)	1	-657.6263094	838645.67	-5.666[4]	1.047[2]	1.905771
$1s^2 2s 2p^3 \ ^1D^o$	(97%)	$+ 1s^2 2s 2p^3 \ ^3P^o$	(2%)	2	-657.5950890	845497.77	3.418[4]	-1.042[3]	1.010028
$1s^2 2s 2p^3 \ ^1P^o$	(90%)	$+ 1s^2 2s 2p^3 \ ^3S^o$	(8%)	1	-657.1466412	943920.67	1.494[4]	4.789[2]	1.078695
$1s^2 2p^4 \ ^3P$	(93%)	$+ 1s^2 2p^4 \ ^1D$	(5%)	2	-655.6536446	1271595.55	1.319[4]	2.436[4]	1.471619
	(99%)	$+ 1s^2 2s^2 2p^2 \ ^3P$	(1%)	1	-655.4627479	1313492.53	-3.905[3]	-1.427[4]	1.498693
$1s^2 2p^4 \ ^1D$	(93%)	$+ 1s^2 2p^4 \ ^3P$	(5%)	2	-655.1569614	1380604.91	3.290[4]	-5.330[4]	1.024122
V XVIII									
$1s^2 2s^2 2p^2 \ ^3P$	(99%)	$+ 1s^2 2p^4 \ ^3P$	(1%)	1	-726.3274350	37850.42	-1.359[3]	1.713[4]	1.498391
	(86%)	$+ 1s^2 2s^2 2p^2 \ ^1D$	(13%)	2	-726.1893339	68160.10	2.904[4]	-2.152[4]	1.431901
$1s^2 2s^2 2p^2 \ ^1D$	(86%)	$+ 1s^2 2s^2 2p^2 \ ^3P$	(13%)	2	-725.7662308	161020.50	2.875[4]	5.542[4]	1.063176
$1s^2 2s 2p^3 \ ^5S^o$	(98%)	$+ 1s^2 2s 2p^3 \ ^3P^o$	(2%)	2	-724.8290842	366700.41	8.074[4]	1.821[2]	1.990630
$1s^2 2s 2p^3 \ ^3D^o$	(89%)	$+ 1s^2 2s 2p^3 \ ^3P^o$	(11%)	2	-723.6576261	623805.74	5.657[4]	3.691[4]	1.202165
	(91%)	$+ 1s^2 2s 2p^3 \ ^3P^o$	(7%)	1	-723.6518398	625075.68	-4.839[4]	2.060[4]	0.576663
	(100%)			3	-723.6069553	634926.68	8.370[4]	-1.099[2]	1.330911
$1s^2 2s 2p^3 \ ^3P^o$	(91%)	$+ 1s^2 2s 2p^3 \ ^3D^o$	(7%)	1	-723.1488813	735462.30	1.077[5]	-2.080[4]	1.434265
	(85%)	$+ 1s^2 2s 2p^3 \ ^3D^o$	(11%)	2	-723.1124762	743452.31	8.238[4]	-3.648[4]	1.451187
$1s^2 2s 2p^3 \ ^3S^o$	(87%)	$+ 1s^2 2s 2p^3 \ ^1P^o$	(10%)	1	-722.4100626	897614.26	-5.987[4]	2.157[2]	1.883264
$1s^2 2s 2p^3 \ ^1D^o$	(96%)	$+ 1s^2 2s 2p^3 \ ^3P^o$	(3%)	2	-722.3592942	908756.65	4.106[4]	-1.349[3]	1.014265
$1s^2 2s 2p^3 \ ^1P^o$	(88%)	$+ 1s^2 2s 2p^3 \ ^3S^o$	(10%)	1	-721.8755851	1014918.51	1.301[4]	4.467[2]	1.096459
$1s^2 2p^4 \ ^3P$	(92%)	$+ 1s^2 2p^4 \ ^1D$	(6%)	2	-720.3088388	1358779.58	1.534[4]	2.724[4]	1.465547
	(99%)	$+ 1s^2 2s^2 2p^2 \ ^3P$	(1%)	1	-720.0718709	1410788.01	-4.474[3]	-1.662[4]	1.498430

Table 8 (continued)

Level composition in LSJ coupling			J	Energy (E_h)	ΔE cm $^{-1}$	$A_J(I/\mu_I)$	B_J/Q	g_J	
$1s^2 2p^4$ 1D	(92%)	$+ 1s^2 2p^4$ 3P	(6%)	2	-719.7539632	1480560.69	3.848[4]	-6.092[4]	1.029613
Cr XIX									
$1s^2 2s^2 2p^2$ 3P	(99%)	$+ 1s^2 2p^4$ 3P	(1%)	1	-794.4588560	47788.01	-1.677[3]	1.977[4]	1.498114
	(82%)	$+ 1s^2 2s^2 2p^2$ 1D	(16%)	2	-794.3008594	82464.24	3.475[4]	-2.089[4]	1.414644
$1s^2 2s^2 2p^2$ 1D	(82%)	$+ 1s^2 2s^2 2p^2$ 3P	(16%)	2	-793.8348168	184748.77	3.200[4]	6.006[4]	1.079818
$1s^2 2s 2p^3$ $^5S^o$	(98%)	$+ 1s^2 2s 2p^3$ $^3P^o$	(2%)	2	-792.8402107	403039.57	9.333[4]	3.423[2]	1.987534
$1s^2 2s 2p^3$ $^3D^o$	(87%)	$+ 1s^2 2s 2p^3$ $^3P^o$	(12%)	2	-791.6166651	671576.78	6.718[4]	4.586[4]	1.209983
	(89%)	$+ 1s^2 2s 2p^3$ $^3P^o$	(9%)	1	-791.6117716	672650.79	-5.426[4]	2.616[4]	0.596407
	(100%)			3	-791.5474338	686771.29	9.662[4]	-1.120[2]	1.330587
$1s^2 2s 2p^3$ $^3P^o$	(88%)	$+ 1s^2 2s 2p^3$ $^3D^o$	(9%)	1	-791.0593561	793891.97	1.209[5]	-2.641[4]	1.419139
	(81%)	$+ 1s^2 2s 2p^3$ $^3D^o$	(13%)	2	-791.0108689	804533.68	9.107[4]	-4.520[4]	1.439695
$1s^2 2s 2p^3$ $^3S^o$	(85%)	$+ 1s^2 2s 2p^3$ $^1P^o$	(12%)	1	-790.3031079	959869.25	-6.145[4]	4.029[2]	1.858752
$1s^2 2s 2p^3$ $^1D^o$	(95%)	$+ 1s^2 2s 2p^3$ $^3P^o$	(4%)	2	-790.2277060	976418.06	4.930[4]	-1.838[3]	1.019793
$1s^2 2s 2p^3$ $^1P^o$	(86%)	$+ 1s^2 2s 2p^3$ $^3S^o$	(12%)	1	-789.7054589	1091038.06	9.523[3]	3.620[2]	1.115170
$1s^2 2p^4$ 3P	(91%)	$+ 1s^2 2p^4$ 1D	(8%)	2	-788.0698004	1450023.59	1.773[4]	3.008[4]	1.459039
	(99%)	$+ 1s^2 2s^2 2p^2$ 3P	(1%)	1	-787.7784654	1513964.23	-5.113[3]	-1.922[4]	1.498155
$1s^2 2p^4$ 1D	(91%)	$+ 1s^2 2p^4$ 3P	(8%)	2	-787.4489302	1586288.84	4.465[4]	-6.901[4]	1.035510
Mn XX									
$1s^2 2s^2 2p^2$ 3P	(99%)			1	-865.7178502	59695.88	-2.056[3]	2.269[4]	1.497822
	(79%)	$+ 1s^2 2s^2 2p^2$ 1D	(20%)	2	-865.5396518	98805.91	4.127[4]	-1.906[4]	1.396056
$1s^2 2s^2 2p^2$ 1D	(79%)	$+ 1s^2 2s^2 2p^2$ 3P	(20%)	2	-865.0218197	212456.91	3.537[4]	6.402[4]	1.097763
$1s^2 2s 2p^3$ $^5S^o$	(97%)	$+ 1s^2 2s 2p^3$ $^3P^o$	(3%)	2	-863.9718899	442889.87	1.073[5]	6.142[2]	1.983650
$1s^2 2s 2p^3$ $^3D^o$	(84%)	$+ 1s^2 2s 2p^3$ $^3P^o$	(14%)	2	-862.6972820	722633.95	7.929[4]	5.580[4]	1.218376
	(87%)	$+ 1s^2 2s 2p^3$ $^3P^o$	(11%)	1	-862.6949638	723142.75	-6.046[4]	3.254[4]	0.618385
	(100%)			3	-862.6052582	742830.85	1.109[5]	-1.165[2]	1.330247
$1s^2 2s 2p^3$ $^3P^o$	(86%)	$+ 1s^2 2s 2p^3$ $^3D^o$	(11%)	1	-862.0854368	856918.45	1.343[5]	-3.286[4]	1.402921
	(77%)	$+ 1s^2 2s 2p^3$ $^3D^o$	(15%)	2	-862.0224608	870740.08	9.928[4]	-5.476[4]	1.426785
$1s^2 2s 2p^3$ $^3S^o$	(82%)	$+ 1s^2 2s 2p^3$ $^1P^o$	(14%)	1	-861.3157026	1025855.57	-6.089[4]	6.999[2]	1.832739
$1s^2 2s 2p^3$ $^1D^o$	(94%)	$+ 1s^2 2s 2p^3$ $^3P^o$	(6%)	2	-861.2095744	1049148.02	5.925[4]	-2.586[3]	1.026893
$1s^2 2s 2p^3$ $^1P^o$	(83%)	$+ 1s^2 2s 2p^3$ $^3S^o$	(14%)	1	-860.6452468	1173003.62	4.243[3]	1.881[2]	1.134181
$1s^2 2p^4$ 3P	(90%)	$+ 1s^2 2p^4$ 1D	(9%)	2	-858.9468307	1545762.84	2.037[4]	3.286[4]	1.452220
	(99%)	$+ 1s^2 2s^2 2p^2$ 3P	(1%)	1	-858.5918451	1623673.19	-5.829[3]	-2.209[4]	1.497866
$1s^2 2p^4$ 1D	(90%)	$+ 1s^2 2p^4$ 3P	(9%)	2	-858.2510988	1698458.35	5.146[4]	-7.755[4]	1.041689
Fe XXI									
$1s^2 2s^2 2p^2$ 3P	(99%)			1	-940.1164436	73820.06	-2.503[3]	2.588[4]	1.497518
	(75%)	$+ 1s^2 2s^2 2p^2$ 1D	(24%)	2	-939.9180433	117363.88	4.859[4]	-1.592[4]	1.376837
$1s^2 2s^2 2p^2$ 1D	(75%)	$+ 1s^2 2s^2 2p^2$ 3P	(24%)	2	-939.3380064	244667.27	3.888[4]	6.723[4]	1.116309
$1s^2 2s 2p^3$ $^5S^o$	(96%)	$+ 1s^2 2s 2p^3$ $^3P^o$	(3%)	2	-938.2360392	486521.11	1.227[5]	1.060[3]	1.978799
$1s^2 2s 2p^3$ $^3D^o$	(84%)	$+ 1s^2 2s 2p^3$ $^3P^o$	(12%)	1	-936.9136551	776750.85	-6.708[4]	3.969[4]	0.642215
	(82%)	$+ 1s^2 2s 2p^3$ $^3P^o$	(16%)	2	-936.9108304	777370.81	9.296[4]	6.658[4]	1.227281
	(100%)			3	-936.7914959	803561.69	1.265[5]	-1.211[2]	1.329892
$1s^2 2s 2p^3$ $^3P^o$	(83%)	$+ 1s^2 2s 2p^3$ $^3D^o$	(13%)	1	-936.2380745	925023.66	1.478[5]	-4.011[4]	1.386120
	(73%)	$+ 1s^2 2s 2p^3$ $^3D^o$	(17%)	2	-936.1581921	942555.81	1.067[5]	-6.493[4]	1.412392
$1s^2 2s 2p^3$ $^3S^o$	(79%)	$+ 1s^2 2s 2p^3$ $^1P^o$	(16%)	1	-935.4589964	1096011.52	-5.770[4]	1.150[3]	1.805746
$1s^2 2s 2p^3$ $^1D^o$	(92%)	$+ 1s^2 2s 2p^3$ $^3P^o$	(8%)	2	-935.3149284	1127630.80	7.128[4]	-3.740[3]	1.035868
$1s^2 2s 2p^3$ $^1P^o$	(81%)	$+ 1s^2 2s 2p^3$ $^3S^o$	(16%)	1	-934.7048425	1261529.17	-3.032[3]	-1.053[2]	1.152848
$1s^2 2p^4$ 3P	(88%)	$+ 1s^2 2p^4$ 1D	(10%)	2	-932.9509614	1646461.57	2.329[4]	3.552[4]	1.445217
	(99%)	$+ 1s^2 2s^2 2p^2$ 3P	(1%)	1	-932.5220075	1740606.07	-6.633[3]	-2.523[4]	1.497564
$1s^2 2p^4$ 1D	(89%)	$+ 1s^2 2p^4$ 3P	(10%)	2	-932.1703941	1817776.29	5.893[4]	-8.654[4]	1.048021
Co XXII									
$1s^2 2s^2 2p^2$ 3P	(99%)			1	-1017.6671163	90414.67	-3.029[3]	2.937[4]	1.497201
	(72%)	$+ 1s^2 2s^2 2p^2$ 1D	(27%)	2	-1017.4487608	138338.16	5.674[4]	-1.148[4]	1.357680
$1s^2 2s^2 2p^2$ 1D	(71%)	$+ 1s^2 2s^2 2p^2$ 3P	(27%)	2	-1016.7946054	281908.67	4.257[4]	6.972[4]	1.134763
$1s^2 2s 2p^3$ $^5S^o$	(95%)	$+ 1s^2 2s 2p^3$ $^3P^o$	(4%)	2	-1015.6451465	534185.74	1.398[5]	1.767[3]	1.972777
$1s^2 2s 2p^3$ $^3D^o$	(82%)	$+ 1s^2 2s 2p^3$ $^3P^o$	(14%)	1	-1014.2805689	833675.90	-7.430[4]	4.756[4]	0.667440
	(80%)	$+ 1s^2 2s 2p^3$ $^3P^o$	(18%)	2	-1014.2689159	836233.42	1.082[5]	7.805[4]	1.236706
	(100%)			3	-1014.1176006	869443.31	1.437[5]	-1.257[2]	1.329521
$1s^2 2s 2p^3$ $^3P^o$	(80%)	$+ 1s^2 2s 2p^3$ $^3D^o$	(15%)	1	-1013.5286534	998702.27	1.610[5]	-4.812[4]	1.369292
	(68%)	$+ 1s^2 2s 2p^3$ $^3D^o$	(19%)	2	-1013.4295743	1020447.62	1.129[5]	-7.545[4]	1.396415
$1s^2 2s 2p^3$ $^3S^o$	(76%)	$+ 1s^2 2s 2p^3$ $^1P^o$	(18%)	1	-1012.7444302	1170819.36	-5.134[4]	1.804[3]	1.778256
$1s^2 2s 2p^3$ $^1D^o$	(89%)	$+ 1s^2 2s 2p^3$ $^3P^o$	(10%)	2	-1012.5539418	1212626.72	8.587[4]	-5.496[3]	1.047019
$1s^2 2s 2p^3$ $^1P^o$	(78%)	$+ 1s^2 2s 2p^3$ $^3S^o$	(18%)	1	-1011.8944485	1357368.78	-1.245[4]	-5.574[2]	1.170587
$1s^2 2p^4$ 3P	(87%)	$+ 1s^2 2p^4$ 1D	(11%)	2	-1010.0936576	1752596.67	2.650[4]	3.806[4]	1.438155
	(99%)	$+ 1s^2 2s^2 2p^2$ 3P	(1%)	1	-1009.5793390	1865476.56	-7.533[3]	-2.866[4]	1.497248
$1s^2 2p^4$ 1D	(87%)	$+ 1s^2 2p^4$ 3P	(12%)	2	-1009.2171377	1944970.55	6.708[4]	-9.597[4]	1.054383
Ni XXIII									
$1s^2 2s^2 2p^2$ 3P	(99%)			1	-1098.3830194	109741.08	-3.645[3]	3.316[4]	1.496870
	(68%)	$+ 1s^2 2s^2 2p^2$ 1D	(31%)	2	-1098.1451334	161951.02	6.571[4]	-5.768[3]	1.339171

Table 8 (continued)

Level composition in LSJ coupling			J	Energy (E_h)	$\Delta E \text{ cm}^{-1}$	$A_J(I/\mu_I)$	B_J/Q	g_J	
$1s^2 2s^2 2p^2 {}^1D$	(68%)	$+ 1s^2 2s^2 2p^2 {}^3P$	(31%)	2	-1097.4035318	324713.74	4.650[4]	7.155[4]	1.152540
$1s^2 2s^2 p^3 {}^5S^o$	(94%)	$+ 1s^2 2s^2 p^3 {}^3P^o$	(5%)	2	-1096.2124762	586120.24	1.587[5]	2.857[3]	1.965357
$1s^2 2s^2 p^3 {}^3D^o$	(79%)	$+ 1s^2 2s^2 p^3 {}^3P^o$	(16%)	1	-1094.8091024	894125.16	-8.234[4]	5.604[4]	0.693583
	(78%)	$+ 1s^2 2s^2 p^3 {}^3P^o$	(19%)	2	-1094.7835694	899729.01	1.252[5]	9.002[4]	1.246732
	(100%)			3	-1094.5956060	940982.21	1.624[5]	-1.304[2]	1.329134
$1s^2 2s^2 p^3 {}^3P^o$	(77%)	$+ 1s^2 2s^2 p^3 {}^3D^o$	(17%)	1	-1093.9691946	1078463.62	1.737[5]	-5.679[4]	1.352974
	(64%)	$+ 1s^2 2s^2 p^3 {}^3D^o$	(21%)	2	-1093.8489125	1104862.49	1.176[5]	-8.600[4]	1.378748
$1s^2 2s^2 p^3 {}^3S^o$	(73%)	$+ 1s^2 2s^2 p^3 {}^1P^o$	(20%)	1	-1093.1839384	1250807.44	-4.127[4]	2.721[3]	1.750681
$1s^2 2s^2 p^3 {}^1D^o$	(87%)	$+ 1s^2 2s^2 p^3 {}^3P^o$	(12%)	2	-1092.9371159	1304978.71	1.035[5]	-8.102[3]	1.060599
$1s^2 2s^2 p^3 {}^1P^o$	(76%)	$+ 1s^2 2s^2 p^3 {}^3S^o$	(20%)	1	-1092.2247859	1461317.07	-2.411[4]	-1.213[3]	1.186924
$1s^2 2p^4 {}^3P$	(86%)	$+ 1s^2 2p^4 {}^1D$	(13%)	2	-1090.3869559	1864674.11	3.003[4]	4.044[4]	1.431142
	(99%)	$+ 1s^2 2s^2 2p^2 {}^3P$	(1%)	1	-1089.7747529	1999037.13	-8.542[3]	-3.240[4]	1.496920
$1s^2 2p^4 {}^1D$	(86%)	$+ 1s^2 2p^4 {}^3P$	(13%)	2	-1089.4021877	2080805.75	7.596[4]	-1.059[5]	1.060665

Table 9

Hyperfine magnetic dipole constants $A_J(I/\mu_I)$ (MHz per unit of μ_N) and electric quadrupole constants B_J/Q (MHz/barn) in O III. Comparison of values from RCI and MCHF calculations.

Level	RCI (this work)		MCHF (this work)	
	$A_J(I/\mu_I)$	B_J/Q	$A_J(I/\mu_I)$	B_J/Q
$1s^2 2s^2 2p^2 \ ^3P_1$	-7.847	3.188[2]	-3.426	3.193[2]
	4.251[2]	-6.392[2]	4.242[2]	-6.387[2]
$1s^2 2s^2 2p^2 \ ^1D_2$	6.709[2]	1.249[3]	6.694[2]	1.270[3]
$1s^2 2s2p^3 \ ^5S_2^o$	1.906[3]	-1.052[-2]	1.897[3]	0.0
$1s^2 2s2p^3 \ ^3D_3^o$	1.856[3]	-4.271[1]	1.851[3]	-4.396[1]
	1.047[3]	-3.447	1.045[3]	-2.198[1]
	-1.487[3]	-6.019	-1.483[3]	-1.539[1]
$1s^2 2s2p^3 \ ^3P_2^o$	2.240[3]	1.720[1]	2.227[3]	3.422[1]
	2.660[3]	-2.673[1]	2.650[3]	-1.711[1]
$1s^2 2s2p^3 \ ^1D_2^o$	6.577[2]	-1.635[1]	6.547[2]	-1.854[1]
$1s^2 2s2p^3 \ ^3S_1^o$	-2.304[3]	-8.427[-3]	-2.291[3]	0.0
$1s^2 2s2p^3 \ ^1P_1^o$	6.739[2]	2.581[1]	6.763[2]	3.201[1]
$1s^2 2p^4 \ ^3P_2$	2.102[2]	5.451[2]	2.228[2]	5.378[2]
	-1.854[2]	-2.721[2]	-1.726[2]	-2.689[2]
$1s^2 2p^4 \ ^1D_2$	6.513[2]	-1.178[3]	6.478[2]	-1.205[3]

Table 10

Total energies (in E_h), excitation energies (in cm^{-1}), hyperfine magnetic dipole constants $A_J(I/\mu_I)$ (MHz per unit of μ_N), electric quadrupole constants B_J/Q (MHz/barn), and Landé g_J -factors for levels in the nitrogen isoelectronic sequence ($7 \leq Z \leq 36$ and $Z = 42, 74$). For each of the many-electron wave functions, the leading components are given in the LSJ coupling scheme. The number in square brackets is the power of 10. See page 18 for Explanation of Tables.

Level composition in LSJ coupling			J	Energy (E_h)	$\Delta E \text{ cm}^{-1}$	$A_J(I/\mu_I)$	B_J/Q	g_J
N I								
$2s^2 2p^3 \ ^4S^o$	(96%)	$+ 1s^2 2s 2p^3 3d \ ^4S^o$	(2%)	3/2	-54.6073794	0.00	1.385[1]	-1.496[-3]
$2s^2 2p^3 \ ^2D^o$	(96%)	$+ 1s^2 2s 2p^3 3d \ ^2D^o$	(1%)	5/2	-54.5185543	19494.84	2.825[2]	-2.134[1]
	(96%)	$+ 1s^2 2s 2p^3 3d \ ^2D^o$	(1%)	3/2	-54.5185222	19501.91	1.670[2]	-9.281
$2s^2 2p^3 \ ^2P^o$	(93%)	$+ 2p^5 \ ^2P^o$	(3%)	3/2	-54.4735477	29372.66	1.534[2]	5.870
	(93%)	$+ 2p^5 \ ^2P^o$	(3%)	1/2	-54.4735265	29377.32	7.955[2]	0.0
$2s2p^4 \ ^4P$	(91%)	$+ 1s^2 2s^2 2p^2 3d \ ^4P$	(3%)	5/2	-54.2058086	88134.61	9.117[2]	2.156[2]
	(91%)	$+ 1s^2 2s^2 2p^2 3d \ ^4P$	(3%)	3/2	-54.2055167	88198.66	9.491[2]	-1.721[2]
	(91%)	$+ 1s^2 2s^2 2p^2 3d \ ^4P$	(3%)	1/2	-54.2053304	88239.55	2.104[3]	0.0
O II								
$2s^2 2p^3 \ ^4S^o$	(97%)	$+ 1s^2 2s 2p^3 3d \ ^4S^o$	(1%)	3/2	-74.6062512	0.00	2.192[1]	-5.134[-3]
$2s^2 2p^3 \ ^2D^o$	(97%)	$+ 1s^2 2s 2p^3 3d \ ^2D^o$	(1%)	5/2	-74.4831059	27027.27	5.549[2]	-2.767[1]
	(97%)	$+ 1s^2 2s 2p^3 3d \ ^2D^o$	(1%)	3/2	-74.4830197	27046.19	3.362[2]	1.153
$2s^2 2p^3 \ ^2P^o$	(95%)	$+ 2p^5 \ ^2P^o$	(3%)	3/2	-74.4202118	40830.92	3.022[2]	-8.363
	(95%)	$+ 2p^5 \ ^2P^o$	(3%)	1/2	-74.4201846	40836.89	1.559[3]	0.0
$2s2p^4 \ ^4P$	(96%)	$+ 1s^2 2s^2 2p^2 3d \ ^4P$	(2%)	5/2	-74.0588300	120145.06	1.643[3]	4.832[2]
	(96%)	$+ 1s^2 2s^2 2p^2 3d \ ^4P$	(2%)	3/2	-74.0580811	120309.43	1.666[3]	-3.857[2]
	(96%)	$+ 1s^2 2s^2 2p^2 3d \ ^4P$	(2%)	1/2	-74.0576760	120398.33	3.646[3]	0.0
$2s2p^4 \ ^2D$	(93%)	$+ 1s^2 2s^2 2p^2 3d \ ^2D$	(3%)	5/2	-73.8469156	166654.88	1.878[3]	-1.041[3]
	(93%)	$+ 1s^2 2s^2 2p^2 3d \ ^2D$	(3%)	3/2	-73.8468823	166662.20	-7.650[2]	-7.287[2]
$2s2p^4 \ ^2S$	(93%)	$+ 1s^2 2s^2 2p^2 3d \ ^2S$	(2%)	1/2	-73.7069689	197369.64	6.993[3]	0.0
F III								
$2s^2 2p^3 \ ^4S^o$	(98%)	$+ 1s^2 2s 2p^3 3d \ ^4S^o$	(1%)	3/2	-97.8791584	0.00	2.622[1]	-1.296[-2]
$2s^2 2p^3 \ ^2D^o$	(98%)			5/2	-97.7228884	34297.31	9.530[2]	-3.562[1]
	(98%)			3/2	-97.7227397	34329.92	5.872[2]	3.309[1]
$2s^2 2p^3 \ ^2P^o$	(96%)	$+ 2p^5 \ ^2P^o$	(3%)	3/2	-97.6427889	51877.10	5.191[2]	-4.581[1]
	(96%)	$+ 2p^5 \ ^2P^o$	(3%)	1/2	-97.6427648	51882.40	2.679[3]	0.0
$2s2p^4 \ ^4P$	(97%)	$+ 1s^2 2s^2 2p^2 3d \ ^4P$	(1%)	5/2	-97.1862603	152073.55	2.667[3]	8.674[2]
	(97%)	$+ 1s^2 2s^2 2p^2 3d \ ^4P$	(1%)	3/2	-97.1847236	152410.82	2.656[3]	-6.919[2]
	(97%)	$+ 1s^2 2s^2 2p^2 3d \ ^4P$	(1%)	1/2	-97.1839059	152590.29	5.768[3]	0.0
$2s2p^4 \ ^2D$	(96%)	$+ 1s^2 2s^2 2p^2 3d \ ^2D$	(2%)	5/2	-96.9191468	210698.18	3.073[3]	-1.816[3]
	(96%)	$+ 1s^2 2s^2 2p^2 3d \ ^2D$	(2%)	3/2	-96.9190754	210713.85	-1.149[3]	-1.271[3]
$2s2p^4 \ ^2S$	(96%)	$+ 1s^2 2s^2 2p^2 3d \ ^2S$	(1%)	1/2	-96.7437767	249187.47	1.145[4]	0.0
$2s2p^4 \ ^2P$	(95%)	$+ 1s^2 2s^2 2p^2 3d \ ^2P$	(2%)	3/2	-96.6603346	267500.89	-6.529[2]	8.717[2]
	(95%)	$+ 1s^2 2s^2 2p^2 3d \ ^2P$	(2%)	1/2	-96.6585348	267895.90	1.746[3]	0.0
Ne IV								
$2s^2 2p^3 \ ^4S^o$	(98%)	$+ 1s^2 2s 2p^3 3d \ ^4S^o$	(1%)	3/2	-124.4241779	0.00	2.735[1]	-3.420[-2]
$2s^2 2p^3 \ ^2D^o$	(98%)			5/2	-124.2353345	41446.34	1.501[3]	-4.492[1]
	(98%)			3/2	-124.2351338	41490.39	9.349[2]	1.083[2]
$2s^2 2p^3 \ ^2P^o$	(96%)	$+ 2p^5 \ ^2P^o$	(3%)	1/2	-124.1383198	62738.60	4.222[3]	0.0
	(96%)	$+ 2p^5 \ ^2P^o$	(3%)	3/2	-124.1383032	62742.26	8.174[2]	-1.287[2]
$2s2p^4 \ ^4P$	(98%)	$+ 1s^2 2s^2 2p^2 3d \ ^4P$	(1%)	5/2	-123.5858394	183994.04	4.041[3]	1.400[3]
	(98%)	$+ 1s^2 2s^2 2p^2 3d \ ^4P$	(1%)	3/2	-123.5830378	184608.91	3.973[3]	-1.116[3]
	(98%)	$+ 1s^2 2s^2 2p^2 3d \ ^4P$	(1%)	1/2	-123.5815480	184935.88	8.586[3]	0.0
$2s2p^4 \ ^2D$	(97%)	$+ 1s^2 2s^2 2p^2 3d \ ^2D$	(1%)	5/2	-123.2646630	254484.10	4.668[3]	-2.886[3]
	(97%)	$+ 1s^2 2s^2 2p^2 3d \ ^2D$	(1%)	3/2	-123.2645505	254508.79	-1.627[3]	-2.021[3]
$2s2p^4 \ ^2S$	(97%)	$+ 1s^2 2s^2 2p^2 3d \ ^2S$	(1%)	1/2	-123.0555597	300376.97	1.721[4]	0.0
$2s2p^4 \ ^2P$	(97%)	$+ 1s^2 2s^2 2p^2 3d \ ^2P$	(1%)	3/2	-122.9632230	320642.53	-9.208[2]	1.402[3]
	(97%)	$+ 1s^2 2s^2 2p^2 3d \ ^2P$	(1%)	1/2	-122.9599401	321363.04	2.678[3]	0.0
$2p^5 \ ^2P^o$	(92%)	$+ 2s^2 2p^3 \ ^2P^o$	(2%)	3/2	-122.2118055	485559.61	5.684[2]	-1.346[3]
	(92%)	$+ 2s^2 2p^3 \ ^2P^o$	(2%)	1/2	-122.2073660	486533.97	4.237[3]	0.0
Na V								
$2s^2 2p^3 \ ^4S^o$	(99%)	$+ 1s^2 2s 2p^3 3d \ ^4S^o$	(1%)	3/2	-154.42425695	0.00	2.572[1]	-7.907[-2]
$2s^2 2p^3 \ ^2D^o$	(99%)			5/2	-154.0214506	48529.98	2.222[3]	-5.551[1]
	(98%)			3/2	-154.0212512	48573.76	1.394[3]	2.604[2]
$2s^2 2p^3 \ ^2P^o$	(97%)	$+ 2p^5 \ ^2P^o$	(2%)	1/2	-153.9076866	73498.31	6.256[3]	0.0
	(96%)	$+ 2p^5 \ ^2P^o$	(2%)	3/2	-153.9075339	73531.81	1.210[3]	-2.910[2]
$2s2p^4 \ ^4P$	(99%)			5/2	-153.2585529	215966.69	5.819[3]	2.107[3]
	(99%)			3/2	-153.2538432	217000.33	5.666[3]	-1.679[3]
	(99%)			1/2	-153.2513363	217550.55	1.220[4]	0.0
$2s2p^4 \ ^2D$	(98%)	$+ 1s^2 2s^2 2p^2 3d \ ^2D$	(1%)	5/2	-152.8836571	298246.80	6.734[3]	-4.303[3]
	(98%)	$+ 1s^2 2s^2 2p^2 3d \ ^2D$	(1%)	3/2	-152.8835013	298281.00	-2.219[3]	-3.013[3]
$2s2p^4 \ ^2S$	(98%)	$+ 1s^2 2s^2 2p^2 3d \ ^2S$	(1%)	1/2	-152.6414537	351404.30	2.456[4]	0.0

Table 10 (continued)

Level composition in LSJ coupling			J	Energy (E_h)	ΔE cm $^{-1}$	$A_J(I/\mu_I)$	B_J/Q	g_J	
$2s2p^4 \ 2P$	(98%)	+ $1s^2 2s^2 2p^2 3d \ 2P$	(1%)	3/2	-152.5419009	373253.60	-1.225[3]	2.099[3]	1.333599
	(97%)	+ $1s^2 2s^2 2p^2 3d \ 2P$	(1%)	1/2	-152.5363478	374472.37	3.894[3]	0.0	0.667829
$2p^5 \ 2P^o$	(94%)	+ $2s^2 2p^3 \ 2P^o$	(2%)	3/2	-151.6504252	568909.90	8.675[2]	-2.023[3]	1.333670
	(94%)	+ $2s^2 2p^3 \ 2P^o$	(2%)	1/2	-151.6429405	570552.60	6.296[3]	0.0	0.665380
Mg VI									
$2s^2 2p^3 \ 4S^o$	(99%)	+ $1s^2 2s^2 2p^3 3d \ 4S^o$	(1%)	3/2	-187.3372524	0.00	2.148[1]	-1.453[-1]	2.001273
	(99%)			5/2	-187.0840241	55577.20	3.141[3]	-6.737[1]	1.199872
$2s^2 2p^3 \ 2D^o$	(98%)			3/2	-187.0839565	55592.04	1.978[3]	5.385[2]	0.801865
	(97%)	+ $2p^5 \ 2P^o$	(2%)	1/2	-186.9535534	84212.21	8.848[3]	0.0	0.665210
$2s^2 2p^3 \ 2P^o$	(96%)	+ $2p^5 \ 2P^o$	(2%)	3/2	-186.9530688	84318.56	1.711[3]	-5.822[2]	1.331143
	(99%)			5/2	-186.2070645	248047.57	8.052[3]	3.011[3]	1.600658
$2s2p^4 \ 4P$	(99%)			3/2	-186.1996155	249682.44	7.780[3]	-2.398[3]	1.734368
	(99%)			1/2	-186.1956529	250552.13	1.671[4]	0.0	2.669474
$2s2p^4 \ 2D$	(98%)	+ $1s^2 2s^2 2p^2 3d \ 2D$	(1%)	5/2	-185.7783916	342130.39	9.333[3]	-6.115[3]	1.199962
	(98%)	+ $1s^2 2s^2 2p^2 3d \ 2D$	(1%)	3/2	-185.7782064	342171.06	-2.939[3]	-4.281[3]	0.799202
$2s2p^4 \ 2S$	(98%)			1/2	-185.5034466	402473.85	3.368[4]	0.0	1.997073
	(98%)	+ $1s^2 2s^2 2p^2 3d \ 2P$	(1%)	3/2	-185.3975248	425720.99	-1.570[3]	2.991[3]	1.333424
$2s2p^4 \ 2P$	(98%)	+ $1s^2 2s^2 2p^2 3d \ 2P$	(1%)	1/2	-185.3886476	427669.31	5.475[3]	0.0	0.670194
	(95%)	+ $2s^2 2p^3 \ 2P^o$	(2%)	3/2	-184.3644856	652446.90	1.266[3]	-2.892[3]	1.333551
$2p^5 \ 2P^o$	(95%)	+ $2s^2 2p^3 \ 2P^o$	(2%)	1/2	-184.3526008	655055.30	8.913[3]	0.0	0.665232
Al VII									
$2s^2 2p^3 \ 4S^o$	(99%)			3/2	-223.7122500	0.00	1.534[1]	-1.744[-1]	2.000846
	(98%)	+ $2s^2 2p^3 \ 2P^o$	(1%)	3/2	-223.4272969	62539.95	2.701[3]	1.009[3]	0.803883
$2s^2 2p^3 \ 2D^o$	(99%)			5/2	-223.4269773	62610.11	4.282[3]	-8.052[1]	1.199730
	(97%)	+ $2p^5 \ 2P^o$	(2%)	1/2	-223.2797752	94917.23	1.207[4]	0.0	0.665042
$2s^2 2p^3 \ 2P^o$	(96%)	+ $2p^5 \ 2P^o$	(2%)	3/2	-223.2786013	95174.87	2.335[3]	-1.069[3]	1.329152
	(99%)			5/2	-222.4351706	280286.51	1.080[4]	4.139[3]	1.600445
$2s2p^4 \ 4P$	(99%)			3/2	-222.4239363	282752.16	1.036[4]	-3.294[3]	1.734190
	(99%)			1/2	-222.4179871	284057.85	2.222[4]	0.0	2.669150
$2s2p^4 \ 2D$	(99%)			5/2	-221.9523541	386252.47	1.253[4]	-8.370[3]	1.199883
	(99%)			3/2	-221.9521788	386290.96	-3.805[3]	-5.860[3]	0.799204
$2s2p^4 \ 2S$	(98%)	+ $2s2p^4 \ 2P$	(1%)	1/2	-221.6451215	453682.24	4.473[4]	0.0	1.992735
	(98%)			3/2	-221.5333241	478218.94	-1.949[3]	4.103[3]	1.333197
$2s2p^4 \ 2P$	(98%)	+ $2s2p^4 \ 2S$	(1%)	1/2	-221.5197565	481196.69	7.526[3]	0.0	0.674396
	(96%)	+ $2s^2 2p^3 \ 2P^o$	(2%)	3/2	-220.3573568	736313.92	1.775[3]	-3.976[3]	1.333418
$2p^5 \ 2P^o$	(96%)	+ $2s^2 2p^3 \ 2P^o$	(2%)	1/2	-220.3393610	740263.54	1.216[4]	0.0	0.665067
Si VIII									
$2s^2 2p^3 \ 4S^o$	(99%)			3/2	-263.3723635	0.00	1.295[1]	5.988[-2]	2.000247
	(98%)	+ $2s^2 2p^3 \ 2P^o$	(1%)	3/2	-263.0561084	69409.98	3.572[3]	1.754[3]	0.807033
$2s^2 2p^3 \ 2D^o$	(99%)			5/2	-263.0549606	69661.88	5.670[3]	-9.546[1]	1.199573
	(97%)	+ $2p^5 \ 2P^o$	(2%)	1/2	-262.8909573	105656.45	1.599[4]	0.0	0.664857
$2s^2 2p^3 \ 2P^o$	(96%)	+ $2p^5 \ 2P^o$	(2%)	3/2	-262.8884965	106196.53	3.097[3]	-1.834[3]	1.326158
	(99%)			5/2	-261.9474839	312724.91	1.410[4]	5.513[3]	1.600182
$2s2p^4 \ 4P$	(99%)			3/2	-261.9311743	316304.46	1.345[4]	-4.387[3]	1.733976
	(99%)			1/2	-261.9226059	318185.01	2.882[4]	0.0	2.668736
$2s2p^4 \ 2D$	(99%)			5/2	-261.4098852	430714.79	1.639[4]	-1.112[4]	1.199823
	(99%)			3/2	-261.4097979	430733.34	-4.834[3]	-7.782[3]	0.799269
$2s2p^4 \ 2S$	(98%)	+ $2s2p^4 \ 2P$	(1%)	1/2	-261.0706507	505167.55	5.782[4]	0.0	1.985803
	(98%)			3/2	-260.9533876	530903.82	-2.359[3]	5.460[3]	1.332898
$2s2p^4 \ 2P$	(98%)	+ $2s2p^4 \ 2S$	(1%)	1/2	-260.9333781	535295.40	1.021[4]	0.0	0.681235
	(96%)	+ $2s^2 2p^3 \ 2P^o$	(2%)	3/2	-259.6329967	820696.13	2.407[3]	-5.298[3]	1.333270
$2p^5 \ 2P^o$	(96%)	+ $2s^2 2p^3 \ 2P^o$	(2%)	1/2	-259.6067916	826447.48	1.611[4]	0.0	0.664884
P IX									
$2s^2 2p^3 \ 4S^o$	(99%)			3/2	-306.3233443	0.00	5.461	1.170	1.999407
	(97%)	+ $2s^2 2p^3 \ 2P^o$	(2%)	3/2	-305.9764445	76135.70	4.603[3]	2.872[3]	0.811656
$2s^2 2p^3 \ 2D^o$	(99%)			5/2	-305.9737674	76723.25	7.329[3]	-1.111[2]	1.199402
	(97%)	+ $2p^5 \ 2P^o$	(2%)	1/2	-305.7928394	116432.36	2.069[4]	0.0	0.664653
$2s^2 2p^3 \ 2P^o$	(95%)	+ $2s^2 2p^3 \ 2D^o$	(2%)	3/2	-305.7881477	117462.06	4.011[3]	-2.976[3]	1.321892
	(99%)			5/2	-304.7493600	345449.60	1.803[4]	7.156[3]	1.599856
$2s2p^4 \ 4P$	(99%)			3/2	-304.7264121	350486.08	1.709[4]	-5.695[3]	1.733717
	(99%)			1/2	-304.7144958	353101.41	3.662[4]	0.0	2.668200
$2s2p^4 \ 2D$	(99%)			3/2	-304.1562024	475632.64	-6.047[3]	-1.008[4]	0.799435
	(99%)			5/2	-304.1560527	475665.51	2.099[4]	-1.440[4]	1.199796
$2s2p^4 \ 2S$	(97%)	+ $2s2p^4 \ 2P$	(2%)	1/2	-303.7853073	557034.71	7.298[4]	0.0	1.975513
	(99%)			3/2	-303.6628159	583918.46	-2.789[3]	7.083[3]	1.332500
$2s2p^4 \ 2P$	(97%)	+ $2s2p^4 \ 2S$	(2%)	1/2	-303.6341659	590206.42	1.377[4]	0.0	0.691506
	(96%)	+ $2s^2 2p^3 \ 2P^o$	(2%)	3/2	-302.1962762	905786.72	3.176[3]	-6.883[3]	1.333108

Table 10 (continued)

Level composition in LSJ coupling			J	Energy (E_h)	ΔE cm $^{-1}$	$A_J(I/\mu_I)$	B_J/Q	g_J
(96%)	$+ 2s^2 2p^3 \ ^2P^o$	(2%)	1/2	-302.1593267	913896.20	2.082[4]	0.0	0.664683
S X								
$2s^2 2p^3 \ ^4S^o$	(99%)		3/2	-352.5714336	0.00	1.320	4.642	1.998232
$2s^2 2p^3 \ ^2D^o$	(96%)	$+ 2s^2 2p^3 \ ^2P^o$	(3%)	3/2	-352.1946773	82688.45	5.800[3]	4.462[3]
	(99%)			5/2	-352.1894333	83839.38	9.284[3]	-1.281[2]
$2s^2 2p^3 \ ^2P^o$	(98%)	$+ 2p^5 \ ^2P^o$	(2%)	1/2	-351.9914264	127296.88	2.623[4]	0.0
	(94%)	$+ 2s^2 2p^3 \ ^2D^o$	(4%)	3/2	-351.9831074	129122.67	5.095[3]	-4.597[3]
$2s2p^4 \ ^4P$	(99%)			5/2	-350.8468052	378512.17	2.262[4]	9.092[3]
	(99%)			3/2	-350.8153514	385415.49	2.131[4]	-7.239[3]
	(99%)			1/2	-350.7992707	388944.80	4.572[4]	0.0
$2s2p^4 \ ^2D$	(99%)			3/2	-350.1971832	521087.72	-7.464[3]	-1.279[4]
	(99%)			5/2	-350.1965663	521223.12	2.639[4]	-1.827[4]
$2s2p^4 \ ^2S$	(96%)	$+ 2s2p^4 \ ^2P$	(3%)	1/2	-349.7949620	609365.07	9.017[4]	0.0
$2s2p^4 \ ^2P$	(99%)			3/2	-349.6673249	637378.17	-3.220[3]	8.995[3]
	(96%)	$+ 2s2p^4 \ ^2S$	(3%)	1/2	-349.6273205	646158.14	1.851[4]	0.0
$2p^5 \ ^2P^o$	(97%)	$+ 2s^2 2p^3 \ ^2P^o$	(2%)	3/2	-348.0526940	991748.69	4.092[3]	-8.755[3]
	(97%)	$+ 2s^2 2p^3 \ ^2P^o$	(2%)	1/2	-348.0019880	1002877.36	2.639[4]	0.0
Cl XI								
$2s^2 2p^3 \ ^4S^o$	(99%)	$+ 2s^2 2p^3 \ ^2P^o$	(1%)	3/2	-402.1236145	0.00	6.064	1.367[1]
$2s^2 2p^3 \ ^2D^o$	(94%)	$+ 2s^2 2p^3 \ ^2P^o$	(5%)	3/2	-401.7180182	89018.09	7.163[3]	6.615[3]
	(100%)			5/2	-401.7087611	91049.80	1.156[4]	-1.464[2]
$2s^2 2p^3 \ ^2P^o$	(98%)	$+ 2p^5 \ ^2P^o$	(2%)	1/2	-401.4934863	138297.14	3.270[4]	0.0
	(92%)	$+ 2s^2 2p^3 \ ^2D^o$	(5%)	3/2	-401.4795713	141351.12	6.369[3]	-6.791[3]
$2s2p^4 \ ^4P$	(99%)			5/2	-400.2464490	411990.19	2.794[4]	1.134[4]
	(100%)			3/2	-400.2042838	421244.38	2.616[4]	-9.038[3]
	(99%)			1/2	-400.1831488	425882.97	5.624[4]	0.0
$2s2p^4 \ ^2D$	(99%)			3/2	-399.5391514	567224.07	-9.107[3]	-1.593[4]
	(99%)			5/2	-399.5377104	567540.32	3.267[4]	-2.277[4]
$2s2p^4 \ ^2S$	(95%)	$+ 2s2p^4 \ ^2P$	(4%)	1/2	-399.1061172	662264.08	1.093[5]	0.0
$2s2p^4 \ ^2P$	(99%)			3/2	-398.9732423	691426.76	-3.632[3]	1.122[4]
	(95%)	$+ 2s2p^4 \ ^2S$	(4%)	1/2	-398.9185937	703420.74	2.484[4]	0.0
$2p^5 \ ^2P^o$	(97%)	$+ 2s^2 2p^3 \ ^2P^o$	(2%)	3/2	-397.2083511	1078775.59	5.168[3]	-1.094[4]
	(97%)	$+ 2s^2 2p^3 \ ^2P^o$	(2%)	1/2	-397.1403561	1093698.76	3.289[4]	0.0
Ar XII								
$2s^2 2p^3 \ ^4S^o$	(99%)	$+ 2s^2 2p^3 \ ^2P^o$	(1%)	3/2	-454.9874713	0.00	2.912[1]	3.463[1]
$2s^2 2p^3 \ ^2D^o$	(93%)	$+ 2s^2 2p^3 \ ^2P^o$	(7%)	3/2	-454.5542874	95072.87	8.692[3]	9.398[3]
	(100%)			5/2	-454.5391102	98403.88	1.419[4]	-1.660[2]
$2s^2 2p^3 \ ^2P^o$	(98%)	$+ 2p^5 \ ^2P^o$	(2%)	1/2	-454.3063480	149489.28	4.016[4]	0.0
	(90%)	$+ 2s^2 2p^3 \ ^2D^o$	(7%)	3/2	-454.2841828	154353.97	7.851[3]	-9.630[3]
$2s2p^4 \ ^4P$	(99%)			5/2	-452.9554994	445966.28	3.404[4]	1.392[4]
	(100%)			3/2	-452.9000452	458137.06	3.165[4]	-1.111[4]
	(99%)			1/2	-452.8729153	464091.39	6.829[4]	0.0
$2s2p^4 \ ^2D$	(99%)			3/2	-452.1890899	614173.70	-1.100[4]	-1.953[4]
	(99%)			5/2	-452.1863022	614785.55	3.990[4]	-2.794[4]
$2s2p^4 \ ^2S$	(93%)	$+ 2s2p^4 \ ^2P$	(6%)	1/2	-451.7258357	715846.25	1.301[5]	0.0
$2s2p^4 \ ^2P$	(99%)			3/2	-451.5874387	746220.89	-3.998[3]	1.376[4]
	(93%)	$+ 2s2p^4 \ ^2S$	(6%)	1/2	-451.5142313	762288.04	3.321[4]	0.0
$2p^5 \ ^2P^o$	(97%)	$+ 2s^2 2p^3 \ ^2P^o$	(2%)	3/2	-449.6698921	1167073.71	6.417[3]	-1.346[4]
	(97%)	$+ 2s^2 2p^3 \ ^2P^o$	(2%)	1/2	-449.5805115	1186690.47	4.039[4]	0.0
K XIII								
$2s^2 2p^3 \ ^4S^o$	(98%)	$+ 2s^2 2p^3 \ ^2P^o$	(1%)	3/2	-511.1713736	0.00	8.554[1]	7.954[1]
$2s^2 2p^3 \ ^2D^o$	(91%)	$+ 2s^2 2p^3 \ ^2P^o$	(9%)	3/2	-510.7120286	100814.56	1.038[4]	1.284[4]
	(100%)			5/2	-510.6885474	105968.09	1.719[4]	-1.869[2]
$2s^2 2p^3 \ ^2P^o$	(98%)	$+ 2p^5 \ ^2P^o$	(2%)	1/2	-510.4380486	160946.24	4.872[4]	0.0
	(88%)	$+ 2s^2 2p^3 \ ^2D^o$	(9%)	3/2	-510.4042008	168374.96	9.560[3]	-1.316[4]
$2s2p^4 \ ^4P$	(99%)			5/2	-508.9818728	480539.86	4.098[4]	1.684[4]
	(100%)			3/2	-508.9101451	496282.27	3.781[4]	-1.348[4]
	(99%)	$+ 2s2p^4 \ ^2S$	(1%)	1/2	-508.8760601	503763.05	8.205[4]	0.0
$2s2p^4 \ ^2D$	(99%)	$+ 2s2p^4 \ ^2P$	(1%)	3/2	-508.1546814	662087.38	-1.316[4]	-2.361[4]
	(99%)			5/2	-508.1498074	663157.11	4.816[4]	-3.383[4]
$2s2p^4 \ ^2S$	(91%)	$+ 2s2p^4 \ ^2P$	(8%)	1/2	-507.6618420	770253.12	1.523[5]	0.0
$2s2p^4 \ ^2P$	(99%)	$+ 2s2p^4 \ ^2D$	(1%)	3/2	-507.5174373	801946.29	-4.285[3]	1.663[4]
	(91%)	$+ 2s2p^4 \ ^2S$	(8%)	1/2	-507.4210970	823090.55	4.414[4]	0.0
$2p^5 \ ^2P^o$	(97%)	$+ 2s^2 2p^3 \ ^2P^o$	(2%)	3/2	-505.4446215	1256876.76	7.853[3]	-1.634[4]
	(97%)	$+ 2s^2 2p^3 \ ^2P^o$	(2%)	1/2	-505.3291503	1282219.77	4.898[4]	0.0
Ca XIV								
$2s^2 2p^3 \ ^4S^o$	(98%)	$+ 2s^2 2p^3 \ ^2P^o$	(2%)	3/2	-570.6842094	0.00	1.985[2]	1.699[2]
$2s^2 2p^3 \ ^2D^o$	(88%)	$+ 2s^2 2p^3 \ ^2P^o$	(11%)	3/2	-570.2001784	106232.52	1.220[4]	1.693[4]

Table 10 (continued)

Level composition in LSJ coupling		J	Energy (E_h)	ΔE cm $^{-1}$	$A_J(I/\mu_I)$	B_J/Q	g_J
(100%)		5/2	-570.1655613	113830.09	2.059[4]	-2.092[2]	1.198318
2s 2 2p 3 2P o	(98%) + 2p 5 2P o	(2%) 1/2	-569.8970487	172761.78	5.843[4]	0.0	0.663361
(85%) + 2s 2 2p 3 2D o	(11%) 3/2	-569.8472394	183693.66	1.152[4]	-1.738[4]	1.279936	
2s2p 4 4P	(99%) + 2s2p 4 2D	(1%) 5/2	-568.3339309	515826.48	4.882[4]	2.011[4]	1.596563
(99%)		3/2	-568.2425039	535892.38	4.464[4]	-1.617[4]	1.731079
(99%) + 2s2p 4 2S	(1%) 1/2	-568.2005260	545105.46	9.769[4]	0.0	2.661823	
2s2p 4 2D	(99%) + 2s2p 4 2P	(1%) 3/2	-567.4440425	711134.41	-1.560[4]	-2.818[4]	0.804131
(99%) + 2s2p 4 4P	(1%) 5/2	-567.4360677	712884.68	5.754[4]	-4.046[4]	1.200859	
2s2p 4 2S	(89%) + 2s2p 4 2P	(10%) 1/2	-566.9222314	825658.70	1.758[5]	0.0	1.866457
2s2p 4 2P	(99%) + 2s2p 4 2D	(1%) 3/2	-566.7711328	858821.01	-4.452[3]	1.984[4]	1.327347
(89%) + 2s2p 4 2S	(10%) 1/2	-566.6464043	886195.75	5.813[4]	0.0	0.803443	
2p 5 2P o	(97%) + 2s 2 2p 3 2P o	(2%) 3/2	-564.5402424	1348444.85	9.488[3]	-1.961[4]	1.332084
(97%) + 2s 2 2p 3 2P o	(2%) 1/2	-564.3933216	1380690.23	5.874[4]	0.0	0.663405	
Sc XV							
2s 2 2p 3 4S o	(97%) + 2s 2 2p 3 2P o	(2%) 3/2	-633.5355879	0.00	4.024[2]	3.421[2]	1.981026
2s 2 2p 3 2D o	(86%) + 2s 2 2p 3 2P o	(13%) 3/2	-633.0281954	111359.80	1.414[4]	2.160[4]	0.878515
(100%)		5/2	-632.9792406	122104.13	2.442[4]	-2.329[2]	1.198056
2s 2 2p 3 2P o	(98%) + 2p 5 2P o	(2%) 1/2	-632.6924108	185055.98	6.941[4]	0.0	0.663048
(83%) + 2s 2 2p 3 2D o	(14%) 3/2	-632.6214704	200625.62	1.373[4]	-2.227[4]	1.269637	
2s2p 4 4P	(99%) + 2s2p 4 2D	(1%) 5/2	-631.0206520	551964.61	5.761[4]	2.374[4]	1.595390
(99%)		3/2	-630.9056266	577209.79	5.214[4]	-1.919[4]	1.730038
(99%) + 2s2p 4 2S	(1%) 1/2	-630.8548933	588344.45	1.154[5]	0.0	2.659219	
2s2p 4 2D	(98%) + 2s2p 4 2P	(1%) 3/2	-630.0658944	761509.69	-1.833[4]	-3.323[4]	0.806612
(99%) + 2s2p 4 4P	(1%) 5/2	-630.0534638	764237.89	6.810[4]	-4.786[4]	1.201493	
2s2p 4 2S	(86%) + 2s2p 4 2P	(13%) 1/2	-629.5156181	882281.38	2.002[5]	0.0	1.836866
2s2p 4 2P	(98%) + 2s2p 4 2D	(1%) 3/2	-629.3569469	917105.67	-4.452[3]	2.337[4]	1.325159
(87%) + 2s2p 4 2S	(12%) 1/2	-629.1978828	952016.21	7.573[4]	0.0	0.834794	
2p 5 2P o	(97%) + 2s 2 2p 3 2P o	(2%) 3/2	-626.9650160	1442073.81	1.134[4]	-2.328[4]	1.331837
(98%) + 2s 2 2p 3 2P o	(2%) 1/2	-626.7805872	1482551.25	6.975[4]	0.0	0.663095	
Ti XVI							
2s 2 2p 3 4S o	(96%) + 2s 2 2p 3 2P o	(3%) 3/2	-699.7360107	0.00	7.464[2]	6.556[2]	1.973038
2s 2 2p 3 2D o	(83%) + 2s 2 2p 3 2P o	(15%) 3/2	-699.2061560	116289.66	1.615[4]	2.678[4]	0.895396
(100%)		5/2	-699.1394159	130937.41	2.872[4]	-2.579[2]	1.197779
2s 2 2p 3 2P o	(98%) + 2p 5 2P o	(2%) 1/2	-698.8339401	197981.61	8.172[4]	0.0	0.662716
(80%) + 2s 2 2p 3 2D o	(16%) 3/2	-698.7357808	219525.07	1.623[4]	-2.782[4]	1.259968	
2s2p 4 4P	(99%) + 2s2p 4 2D	(1%) 5/2	-697.0517704	589122.63	6.742[4]	2.772[4]	1.593977
(99%)		3/2	-696.9087463	620512.79	6.027[4]	-2.257[4]	1.728682
(98%) + 2s2p 4 2S	(2%) 1/2	-696.8485356	633727.51	1.356[5]	0.0	2.655884	
2s2p 4 2D	(98%) + 2s2p 4 2P	(2%) 3/2	-696.0296995	813441.24	-2.133[4]	-3.876[4]	0.809993
(99%) + 2s2p 4 4P	(1%) 5/2	-696.0110472	817534.97	7.995[4]	-5.605[4]	1.202336	
2s2p 4 2S	(84%) + 2s2p 4 2P	(15%) 1/2	-695.4512530	940395.59	2.250[5]	0.0	1.806837
2s2p 4 2P	(98%) + 2s2p 4 2D	(2%) 3/2	-695.2839519	977113.93	-4.238[3]	2.719[4]	1.322343
(85%) + 2s2p 4 2S	(15%) 1/2	-695.0839064	1021018.84	9.745[4]	0.0	0.867266	
2p 5 2P o	(98%) + 2s 2 2p 3 2P o	(2%) 3/2	-692.7278341	1538116.91	1.341[4]	-2.740[4]	1.331575
(98%) + 2s 2 2p 3 2P o	(2%) 1/2	-692.4990939	1588319.60	8.211[4]	0.0	0.662766	
V XVII							
2s 2 2p 3 4S o	(95%) + 2s 2 2p 3 2P o	(4%) 3/2	-769.2965442	0.00	1.298[3]	1.202[3]	1.962268
2s 2 2p 3 2D o	(81%) + 2s 2 2p 3 2P o	(16%) 3/2	-768.7443559	121191.32	1.819[4]	3.234[4]	0.913937
(100%)		5/2	-768.6563006	140517.22	3.350[4]	-2.844[2]	1.197487
2s 2 2p 3 2P o	(98%) + 2p 5 2P o	(2%) 1/2	-768.3318257	211731.24	9.547[4]	0.0	0.662366
(77%) + 2s 2 2p 3 2D o	(18%) 3/2	-768.1994218	240790.53	1.901[4]	-3.397[4]	1.251380	
2s2p 4 4P	(98%) + 2s2p 4 2D	(1%) 5/2	-766.4374314	627502.71	7.830[4]	3.204[4]	1.592297
(99%)		3/2	-766.2614879	666117.85	6.897[4]	-2.632[4]	1.726907
(98%) + 2s2p 4 2S	(2%) 1/2	-766.1912951	681523.39	1.585[5]	0.0	2.651645	
2s2p 4 2D	(97%) + 2s2p 4 2P	(2%) 3/2	-765.3453124	867195.12	-2.457[4]	-4.473[4]	0.814508
(98%) + 2s2p 4 4P	(1%) 5/2	-765.3181896	873147.89	9.317[4]	-6.506[4]	1.203416	
2s2p 4 2S	(81%) + 2s2p 4 2P	(17%) 1/2	-764.7386612	1000339.67	2.499[5]	0.0	1.777151
2s2p 4 2P	(97%) + 2s2p 4 2D	(2%) 3/2	-764.5615137	1039219.05	-3.756[3]	3.125[4]	1.318769
(82%) + 2s2p 4 2S	(17%) 1/2	-764.3131369	1093731.45	1.239[5]	0.0	0.900250	
2p 5 2P o	(98%) + 2s 2 2p 3 2P o	(2%) 3/2	-761.8381248	1636933.80	1.572[4]	-3.198[4]	1.331299
(98%) + 2s 2 2p 3 2P o	(2%) 1/2	-761.5574730	1698529.76	9.591[4]	0.0	0.662418	
Cr XVIII							
2s 2 2p 3 4S o	(93%) + 2s 2 2p 3 2P o	(6%) 3/2	-842.2293076	0.00	2.145[3]	2.113[3]	1.947933
2s 2 2p 3 2D o	(79%) + 2s 2 2p 3 2P o	(17%) 3/2	-841.6537254	126325.70	2.016[4]	3.811[4]	0.934631
(100%)		5/2	-841.5409414	151078.91	3.880[4]	-3.124[2]	1.197180
2s 2 2p 3 2P o	(98%) + 2p 5 2P o	(2%) 1/2	-841.1970964	226544.16	1.108[5]	0.0	0.661998
(75%) + 2s 2 2p 3 2D o	(20%) 3/2	-841.0224727	264869.63	2.209[4]	-4.071[4]	1.244159	
2s2p 4 4P	(98%) + 2s2p 4 2D	(2%) 5/2	-839.1885970	667358.82	9.034[4]	3.668[4]	1.590325

Table 10 (continued)

Level composition in LSJ coupling		J	Energy (E_h)	ΔE cm $^{-1}$	$A_J(I/\mu_I)$	B_J/Q	g_J
2s $2p^4$ 2D	(99%) + 2s $2p^4$ 2D	(1%)	3/2 -838.9742847	714394.94	7.814[4]	-3.046[4]	1.724573
	(97%) + 2s $2p^4$ 2S	(3%)	1/2 -838.8939099	732035.16	1.848[5]	0.0	2.646303
	(96%) + 2s $2p^4$ 2P	(3%)	3/2 -838.0233759	923095.29	-2.796[4]	-5.108[4]	0.820424
	(98%) + 2s $2p^4$ 4P	(2%)	5/2 -837.9849846	931521.21	1.079[5]	-7.487[4]	1.204755
	2s $2p^4$ 2S (78%) + 2s $2p^4$ 2P (20%)	1/2 -837.3880299	1062537.61	2.743[5]	0.0	1.748388	
	2s $2p^4$ 2P (96%) + 2s $2p^4$ 2D (3%)	3/2 -837.1996856	1103874.41	-2.959[3]	3.550[4]	1.314309	
	(80%) + 2s $2p^4$ 2S (19%)	1/2 -836.8949149	1170763.84	1.555[5]	0.0	0.933365	
	2p 5 2Po (98%) + 2s $2p^3$ 2Po (2%)	3/2 -834.3058495	1738998.00	1.829[4]	-3.705[4]	1.331009	
	(98%) + 2s $2p^3$ 2Po (2%)	1/2 -833.9648440	1813840.05	1.112[5]	0.0	0.662053	
Mn XIX							
2s $2p^3$ 4So (91%) + 2s $2p^3$ 2Po (8%)	3/2 -918.5468980	0.00	3.393[3]	3.570[3]	1.929216		
2s $2p^3$ 2Do (76%) + 2s $2p^3$ 2Po (18%)	3/2 -917.9452447	132047.62	2.200[4]	4.391[4]	0.958158		
(100%)	5/2 -917.8046399	162906.80	4.464[4]	-3.418[2]	1.196858		
2s $2p^3$ 2Po (98%) + 2p 5 2Po (2%)	1/2 -917.4410244	242711.18	1.277[5]	0.0	0.661611		
(73%) + 2s $2p^3$ 2Do (22%)	3/2 -917.2152049	292272.83	2.548[4]	-4.802[4]	1.238448		
2s $2p^4$ 4P (97%) + 2s $2p^4$ 2D (2%)	5/2 -915.3166077	708966.73	1.036[5]	4.161[4]	1.588044		
(99%) + 2s $2p^4$ 2D (1%)	3/2 -915.0579585	765733.67	8.763[4]	-3.502[4]	1.721495		
(96%) + 2s $2p^4$ 2S (4%)	1/2 -914.9676014	785564.76	2.149[5]	0.0	2.639633		
2s $2p^4$ 2D (95%) + 2s $2p^4$ 2P (4%)	3/2 -914.0748693	981496.81	-3.136[4]	-5.773[4]	0.828049		
(97%) + 2s $2p^4$ 4P (2%)	5/2 -914.0218080	993142.42	1.241[5]	-8.550[4]	1.206373		
2s $2p^4$ 2S (75%) + 2s $2p^4$ 2P (22%)	1/2 -913.4097548	1127472.57	2.973[5]	0.0	1.720949		
2s $2p^4$ 2P (95%) + 2s $2p^4$ 2D (4%)	3/2 -913.2087651	1171584.70	-1.799[3]	3.984[4]	1.308843		
(78%) + 2s $2p^4$ 2S (21%)	1/2 -912.8388100	1252780.45	1.931[5]	0.0	0.966436		
2p 5 2Po (98%) + 2s $2p^3$ 2Po (2%)	3/2 -910.1413649	1844801.22	2.112[4]	-4.263[4]	1.330704		
(98%) + 2s $2p^3$ 2Po (2%)	1/2 -909.7306708	1934938.14	1.282[5]	0.0	0.661668		
Fe XX							
2s $2p^3$ 4So (88%) + 2s $2p^3$ 2Po (10%)	3/2 -998.2630537	0.00	5.162[3]	5.794[3]	1.905430		
2s $2p^3$ 2Do (74%) + 2s $2p^3$ 2Po (18%)	3/2 -997.6305533	138817.79	2.359[4]	4.949[4]	0.985200		
(100%)	5/2 -997.4595788	176342.35	5.107[4]	-3.728[2]	1.196520		
2s $2p^3$ 2Po (98%) + 2p 5 2Po (2%)	1/2 -997.0757770	260577.10	1.463[5]	0.0	0.661205		
(71%) + 2s $2p^3$ 2Do (23%)	3/2 -996.7887765	323566.43	2.918[4]	-5.589[4]	1.234249		
2s $2p^4$ 4P (97%) + 2s $2p^4$ 2D (3%)	5/2 -994.8336381	752669.70	1.181[5]	4.678[4]	1.585443		
(98%) + 2s $2p^4$ 2D (1%)	3/2 -994.5241994	820583.63	9.722[4]	-4.000[4]	1.717426		
(95%) + 2s $2p^4$ 2S (5%)	1/2 -994.4245542	842453.24	2.499[5]	0.0	2.631387		
2s $2p^4$ 2D (93%) + 2s $2p^4$ 2P (5%)	3/2 -993.5115405	1042836.57	-3.454[4]	-6.459[4]	0.837725		
(97%) + 2s $2p^4$ 4P (3%)	5/2 -993.4397742	1058587.45	1.420[5]	-9.692[4]	1.208280		
2s $2p^4$ 2S (72%) + 2s $2p^4$ 2P (24%)	1/2 -992.8148798	1195735.93	3.181[5]	0.0	1.695101		
2s $2p^4$ 2P (94%) + 2s $2p^4$ 2D (5%)	3/2 -992.5997475	1242952.00	-2.460[2]	4.415[4]	1.302271		
(75%) + 2s $2p^4$ 2S (23%)	1/2 -992.1550647	1340548.59	2.371[5]	0.0	0.999443		
2p 5 2Po (98%) + 2s $2p^3$ 2Po (2%)	3/2 -989.3557776	1954921.08	2.422[4]	-4.876[4]	1.330385		
(98%) + 2s $2p^3$ 2Po (2%)	1/2 -988.8651166	2062608.71	1.469[5]	0.0	0.661265		
Co XXI							
2s $2p^3$ 4So (84%) + 2s $2p^3$ 2Po (12%)	3/2 -1081.3922195	0.00	7.567[3]	9.030[3]	1.876252		
2s $2p^3$ 2Do (72%) + 2s $2p^3$ 2Po (17%)	3/2 -1080.7216053	147182.80	2.483[4]	5.463[4]	1.016165		
(100%)	5/2 -1080.5184342	191773.70	5.810[4]	-4.053[2]	1.196167		
2s $2p^3$ 2Po (98%) + 2p 5 2Po (1%)	1/2 -1080.1140134	280533.79	1.668[5]	0.0	0.660780		
(69%) + 2s $2p^3$ 2Do (25%)	3/2 -1079.7547930	359373.57	3.321[4]	-6.433[4]	1.231476		
2s $2p^4$ 4P (96%) + 2s $2p^4$ 2D (4%)	5/2 -1077.7523819	798851.99	1.340[5]	5.216[4]	1.582520		
(97%) + 2s $2p^4$ 2D (2%)	3/2 -1077.3852838	879420.70	1.066[5]	-4.542[4]	1.712044		
(93%) + 2s $2p^4$ 2S (6%)	1/2 -1077.2776240	903049.29	2.907[5]	0.0	2.621303		
2s $2p^4$ 2D (91%) + 2s $2p^4$ 2P (6%)	3/2 -1076.3455565	1107614.46	-3.716[4]	-7.155[4]	0.849835		
(96%) + 2s $2p^4$ 4P (4%)	5/2 -1076.2504237	1128493.69	1.616[5]	-1.091[5]	1.210477		
2s $2p^4$ 2S (69%) + 2s $2p^4$ 2P (27%)	1/2 -1075.6147692	1268003.72	3.355[5]	0.0	1.671030		
2s $2p^4$ 2P (93%) + 2s $2p^4$ 2D (7%)	3/2 -1075.3840156	1318648.30	1.718[3]	4.831[4]	1.294537		
(73%) + 2s $2p^4$ 2S (25%)	1/2 -1074.8542716	1434913.66	2.883[5]	0.0	1.032462		
2p 5 2Po (98%) + 2s $2p^3$ 2Po (2%)	3/2 -1071.9606492	2069990.35	2.762[4]	-5.547[4]	1.330051		
(98%) + 2s $2p^3$ 2Po (1%)	1/2 -1071.3787472	2197703.06	1.674[5]	0.0	0.660842		
Ni XXII							
2s $2p^3$ 4So (80%) + 2s $2p^3$ 2Po (15%)	3/2 -1167.9496295	0.00	1.070[4]	1.350[4]	1.841964		
2s $2p^3$ 2Do (70%) + 2s $2p^3$ 2Po (16%)	3/2 -1167.2308798	157747.33	2.564[4]	5.910[4]	1.050915		
(100%)	5/2 -1166.9945180	209622.73	6.579[4]	-4.393[2]	1.195799		
2s $2p^3$ 2Po (98%) + 2p 5 2Po (1%)	1/2 -1166.5690300	303006.56	1.892[5]	0.0	0.660337		
(67%) + 2s $2p^3$ 2Do (26%)	3/2 -1166.1254521	400360.66	3.758[4]	-7.333[4]	1.229986		
2s $2p^4$ 4P (96%) + 2s $2p^4$ 2D (4%)	5/2 -1164.0864174	847877.02	1.514[5]	5.768[4]	1.579286		
(96%) + 2s $2p^4$ 2D (2%)	3/2 -1163.6544850	942675.23	1.152[5]	-5.126[4]	1.704937		
(92%) + 2s $2p^4$ 2S (8%)	1/2 -1163.5407280	967642.00	3.385[5]	0.0	2.609125		
2s $2p^4$ 2D (89%) + 2s $2p^4$ 2P (8%)	3/2 -1162.5897286	1176362.24	-3.873[4]	-7.847[4]	0.864791		
(96%) + 2s $2p^4$ 4P (4%)	5/2 -1162.4659969	1203518.20	1.831[5]	-1.221[5]	1.212954		

Table 10 (continued)

Level composition in LSJ coupling			J	Energy (E_h)	ΔE cm $^{-1}$	$A_J(I/\mu_I)$	B_J/Q	g_J	
$2s2p^4 \ ^2S$ (65%)	$+ 2s2p^4 \ ^2P$	(29%)	1/2	-1161.8214180	1344986.92	3.483[5]	0.0	1.648953	
$2s2p^4 \ ^2P$ (91%)	$+ 2s2p^4 \ ^2D$	(8%)	3/2	-1161.5735799	1399381.10	4.100[3]	5.215[4]	1.285638	
	$+ 2s2p^4 \ ^2S$	(27%)	1/2	-1160.9476140	1536764.72	3.473[5]	0.0	1.065532	
$2p^5 \ ^2P^o$ (98%)	$+ 2s^22p^3 \ ^2P^o$	(2%)	3/2	-1157.9681296	2190685.95	3.133[4]	-6.277[4]	1.329703	
	$+ 2s^22p^3 \ ^2P^o$	(1%)	1/2	-1157.2826641	2341128.24	1.900[5]	0.0	0.660401	
Cu XXIII									
$2s^22p^3 \ ^4S^o$ (76%)	$+ 2s^22p^3 \ ^2P^o$	(18%)	3/2	-1257.9512168	0.00	1.460[4]	1.938[4]	1.803565	
$2s^22p^3 \ ^2D^o$ (67%)	$+ 2s^22p^3 \ ^4S^o$	(18%)	3/2	-1257.1714840	171131.56	2.600[4]	6.276[4]	1.088623	
	(100%)		5/2	-1256.9017827	230324.15	7.415[4]	-4.750[2]	1.195416	
$2s^22p^3 \ ^2P^o$ (99%)	$+ 2p^5 \ ^2P^o$	(1%)	1/2	-1256.4547654	328433.10	2.137[5]	0.0	0.659874	
	(66%)	$+ 2s^22p^3 \ ^2D^o$	(27%)	3/2	-1255.9135458	447217.08	4.229[4]	-8.293[4]	1.229608
$2s2p^4 \ ^4P$ (95%)	$+ 2s2p^4 \ ^2D$	(5%)	5/2	-1253.8490764	900315.73	1.703[5]	6.331[4]	1.575752	
	(95%)	$+ 2s2p^4 \ ^2D$	(3%)	3/2	-1253.3449811	1010951.85	1.225[5]	-5.755[4]	1.695567
$2s2p^4 \ ^2D$ (87%)	$+ 2s2p^4 \ ^2P$	(9%)	3/2	-1252.2567891	1249782.39	-3.857[4]	-8.530[4]	0.883084	
	(95%)	$+ 2s2p^4 \ ^4P$	(5%)	5/2	-1252.0987989	1284457.23	2.066[5]	-1.357[5]	1.215699
$2s2p^4 \ ^2S$ (61%)	$+ 2s2p^4 \ ^2P$	(31%)	1/2	-1251.4465708	1427604.75	3.549[5]	0.0	1.628743	
$2s2p^4 \ ^2P$ (89%)	$+ 2s2p^4 \ ^2D$	(10%)	3/2	-1251.1806555	1485966.41	6.848[3]	5.553[4]	1.275621	
	(69%)	$+ 2s2p^4 \ ^2S$	(28%)	1/2	-1250.4463441	1647129.12	4.150[5]	0.0	1.099014
$2p^5 \ ^2P^o$ (98%)	$+ 2s^22p^3 \ ^2P^o$	(2%)	3/2	-1247.3909501	2317710.59	3.535[4]	-7.069[4]	1.329341	
	(98%)	$+ 2s^22p^3 \ ^2P^o$	(1%)	1/2	-1246.5884954	2493829.02	2.145[5]	0.0	0.659941
Zn XXIV									
$2s^22p^3 \ ^4S^o$ (71%)	$+ 2s^22p^3 \ ^2P^o$	(21%)	3/2	-1351.4135051	0.00	1.926[4]	2.672[4]	1.762650	
$2s^22p^3 \ ^2D^o$ (65%)	$+ 2s^22p^3 \ ^4S^o$	(22%)	3/2	-1350.5572532	187925.56	2.592[4]	6.556[4]	1.127871	
	(100%)		5/2	-1350.2548152	254303.01	8.323[4]	-5.122[2]	1.195018	
$2s^22p^3 \ ^2P^o$ (99%)	$+ 2p^5 \ ^2P^o$	(1%)	1/2	-1349.7857948	357241.10	2.404[5]	0.0	0.659393	
	(64%)	$+ 2s^22p^3 \ ^2D^o$	(27%)	3/2	-1349.1324519	500633.29	4.735[4]	-9.312[4]	1.230163
$2s2p^4 \ ^4P$ (94%)	$+ 2s2p^4 \ ^2D$	(6%)	5/2	-1347.0556898	956429.87	1.908[5]	6.898[4]	1.571952	
	(94%)	$+ 2s2p^4 \ ^2D$	(4%)	3/2	-1346.4721917	1084492.90	1.278[5]	-6.422[4]	1.683318
	(87%)	$+ 2s2p^4 \ ^2S$	(13%)	1/2	-1346.3545120	1110320.60	4.604[5]	0.0	2.577612
$2s2p^4 \ ^2D$ (84%)	$+ 2s2p^4 \ ^2P$	(11%)	3/2	-1345.3606251	1328453.56	-3.581[4]	-9.190[4]	0.905200	
	(94%)	$+ 2s2p^4 \ ^4P$	(6%)	5/2	-1345.1624722	1371943.10	2.321[5]	-1.501[5]	1.218679
$2s2p^4 \ ^2S$ (58%)	$+ 2s2p^4 \ ^2P$	(33%)	1/2	-1344.5034836	1516574.36	3.540[5]	0.0	1.610722	
$2s2p^4 \ ^2P$ (87%)	$+ 2s2p^4 \ ^2D$	(12%)	3/2	-1344.2185454	1579111.09	9.948[3]	5.831[4]	1.264619	
	(66%)	$+ 2s2p^4 \ ^2S$	(30%)	1/2	-1343.3628095	1766923.39	4.918[5]	0.0	1.132755
$2p^5 \ ^2P^o$ (98%)	$+ 2s^22p^3 \ ^2P^o$	(2%)	3/2	-1340.2424212	2451769.44	3.971[4]	-7.928[4]	1.328965	
	(98%)	$+ 2s^22p^3 \ ^2P^o$	(1%)	1/2	-1339.3083936	2656764.79	2.413[5]	0.0	0.659461
Ga XXV									
$2s^22p^3 \ ^4S^o$ (66%)	$+ 2s^22p^3 \ ^2P^o$	(24%)	3/2	-1448.3533909	0.00	2.462[4]	3.550[4]	1.721085	
$2s^22p^3 \ ^2D^o$ (62%)	$+ 2s^22p^3 \ ^4S^o$	(26%)	3/2	-1447.4026894	208654.85	2.546[4]	6.754[4]	1.166973	
	(100%)		5/2	-1447.0686964	281957.83	9.306[4]	-5.511[2]	1.194604	
$2s^22p^3 \ ^2P^o$ (99%)	$+ 2p^5 \ ^2P^o$	(1%)	1/2	-1446.5771895	389831.14	2.694[5]	0.0	0.658892	
	(63%)	$+ 2s^22p^3 \ ^2D^o$	(28%)	3/2	-1445.7959914	561284.29	5.277[4]	-1.040[5]	1.231473
$2s2p^4 \ ^4P$ (93%)	$+ 2s2p^4 \ ^2D$	(7%)	5/2	-1443.7211811	1016652.50	2.130[5]	7.463[4]	1.567918	
	(92%)	$+ 2s2p^4 \ ^2D$	(5%)	3/2	-1443.0514079	1163650.72	1.298[5]	-7.124[4]	1.667477
	(85%)	$+ 2s2p^4 \ ^2S$	(15%)	1/2	-1442.9369466	1188772.06	5.373[5]	0.0	2.558039
$2s2p^4 \ ^2D$ (80%)	$+ 2s2p^4 \ ^2P$	(12%)	3/2	-1441.9147341	1413121.77	-2.935[4]	-9.826[4]	0.931674	
	(93%)	$+ 2s2p^4 \ ^4P$	(7%)	5/2	-1441.6705799	1466707.42	2.598[5]	-1.652[5]	1.221862
$2s2p^4 \ ^2S$ (54%)	$+ 2s2p^4 \ ^2P$	(35%)	1/2	-1441.0050493	1612774.51	3.443[5]	0.0	1.594844	
$2s2p^4 \ ^2P$ (85%)	$+ 2s2p^4 \ ^2D$	(14%)	3/2	-1440.7006415	1679584.30	1.334[4]	6.036[4]	1.252806	
	(64%)	$+ 2s2p^4 \ ^2S$	(31%)	1/2	-1439.7092770	1897163.65	5.784[5]	0.0	1.166872
$2p^5 \ ^2P^o$ (98%)	$+ 2s^22p^3 \ ^2P^o$	(2%)	3/2	-1436.5363164	2593547.99	4.441[4]	-8.854[4]	1.328574	
	(99%)	$+ 2s^22p^3 \ ^2P^o$	(1%)	1/2	-1435.4549165	2830887.82	2.704[5]	0.0	0.658963
Ge XXVI									
$2s^22p^3 \ ^4S^o$ (62%)	$+ 2s^22p^3 \ ^2P^o$	(26%)	3/2	-1548.7885785	0.00	3.061[4]	4.561[4]	1.680602	
$2s^22p^3 \ ^2D^o$ (60%)	$+ 2s^22p^3 \ ^4S^o$	(29%)	3/2	-1547.7234602	233766.44	2.472[4]	6.885[4]	1.204357	
	(100%)		5/2	-1547.3594671	313653.68	1.037[5]	-5.918[2]	1.194175	
$2s^22p^3 \ ^2P^o$ (99%)	$+ 2p^5 \ ^2P^o$	(1%)	1/2	-1546.8449816	426570.19	3.008[5]	0.0	0.658371	
	(62%)	$+ 2s^22p^3 \ ^2D^o$	(28%)	3/2	-1545.9188916	629823.44	5.856[4]	-1.154[5]	1.233377
$2s2p^4 \ ^4P$ (92%)	$+ 2s2p^4 \ ^2D$	(8%)	5/2	-1543.8616581	1081333.99	2.370[5]	8.021[4]	1.563690	
	(89%)	$+ 2s2p^4 \ ^2D$	(7%)	3/2	-1543.0994578	1248617.63	1.277[5]	-7.851[4]	1.647343
	(81%)	$+ 2s2p^4 \ ^2S$	(18%)	1/2	-1542.9919980	1272202.33	6.265[5]	0.0	2.535961
$2s2p^4 \ ^2D$ (76%)	$+ 2s2p^4 \ ^2P$	(13%)	3/2	-1541.9332756	1504565.03	-1.795[4]	-1.044[5]	0.962985	
	(92%)	$+ 2s2p^4 \ ^4P$	(8%)	5/2	-1541.6377123	1569433.66	2.897[5]	-1.809[5]	1.225206
$2s2p^4 \ ^2S$ (49%)	$+ 2s2p^4 \ ^2P$	(37%)	1/2	-1540.9651827	1717036.85	3.246[5]	0.0	1.581071	
$2s2p^4 \ ^2P$ (82%)	$+ 2s2p^4 \ ^2D$	(17%)	3/2	-1540.6413421	1788111.65	1.694[4]	6.160[4]	1.240405	
	(62%)	$+ 2s2p^4 \ ^2S$	(32%)	1/2	-1539.4989184	2038844.66	6.753[5]	0.0	1.201339
$2p^5 \ ^2P^o$ (98%)	$+ 2s^22p^3 \ ^2P^o$	(1%)	3/2	-1536.2872662	2743720.81	4.948[4]	-9.852[4]	1.328168	

Table 10 (continued)

Level composition in LSJ coupling			J	Energy (E_h)	ΔE cm $^{-1}$	$A_J(I/\mu_I)$	B_J/Q	g_J
(99%)	$+ 2s^2 2p^3 \ ^2P^o$	(1%)	1/2	-1535.0414215	3017152.13	3.019[5]	0.0	0.658444
As XXVII								
$2s^2 2p^3 \ ^4S^o$	(58%)	$+ 2s^2 2p^3 \ ^2P^o$	(29%)	3/2	-1652.7374195	0.00	3.715[4]	5.693[4]
$2s^2 2p^3 \ ^2D^o$	(58%)	$+ 2s^2 2p^3 \ ^4S^o$	(33%)	3/2	-1651.5362097	263635.08	2.378[4]	6.963[4]
	(100%)			5/2	-1651.1439525	349725.59	1.151[5]	-6.341[2]
$2s^2 2p^3 \ ^2P^o$	(99%)	$+ 2p^5 \ ^2P^o$	(1%)	1/2	-1650.6059901	467794.68	3.348[5]	0.0
	(61%)	$+ 2s^2 2p^3 \ ^2D^o$	(29%)	3/2	-1649.5166099	706885.99	6.474[4]	-1.276[5]
$2s2p^4 \ ^4P$	(91%)	$+ 2s2p^4 \ ^2D$	(9%)	5/2	-1647.4940031	1150796.86	2.630[5]	8.568[4]
	(85%)	$+ 2s2p^4 \ ^2D$	(9%)	3/2	-1646.6343239	1339474.62	1.200[5]	-8.589[4]
	(78%)	$+ 2s2p^4 \ ^2S$	(21%)	1/2	-1646.5374846	1360728.40	7.290[5]	0.0
$2s2p^4 \ ^2D$	(72%)	$+ 2s2p^4 \ ^2P$	(14%)	3/2	-1645.4307191	1603635.35	-3.032[2]	-1.105[5]
	(91%)	$+ 2s2p^4 \ ^4P$	(9%)	5/2	-1645.0791832	1680788.55	3.221[5]	-1.972[5]
$2s2p^4 \ ^2S$	(45%)	$+ 2s2p^4 \ ^2P$	(39%)	1/2	-1644.3985213	1830176.56	2.944[5]	0.0
$2s2p^4 \ ^2P$	(80%)	$+ 2s2p^4 \ ^2D$	(19%)	3/2	-1644.0558002	1905395.16	2.070[4]	6.197[4]
	(60%)	$+ 2s2p^4 \ ^2S$	(33%)	1/2	-1642.7455364	2192964.82	7.830[5]	0.0
$2p^5 \ ^2P^o$	(98%)	$+ 2s^2 2p^3 \ ^2P^o$	(1%)	3/2	-1639.5106290	2902944.89	5.491[4]	-1.092[5]
	(99%)	$+ 2s^2 2p^3 \ ^2P^o$	(1%)	1/2	-1638.0819331	3216507.39	3.361[5]	0.0
Se XXVIII								
$2s^2 2p^3 \ ^4S^o$	(54%)	$+ 2s^2 2p^3 \ ^2P^o$	(31%)	3/2	-1760.2184909	0.00	4.417[4]	6.933[4]
$2s^2 2p^3 \ ^2D^o$	(56%)	$+ 2s^2 2p^3 \ ^4S^o$	(36%)	3/2	-1758.8580496	298582.34	2.271[4]	7.005[4]
	(100%)			5/2	-1758.4392957	390488.19	1.275[5]	-6.781[2]
$2s^2 2p^3 \ ^2P^o$	(99%)	$+ 2p^5 \ ^2P^o$	(1%)	1/2	-1757.8773535	513820.25	3.716[5]	0.0
	(60%)	$+ 2s^2 2p^3 \ ^2D^o$	(29%)	3/2	-1756.6048653	793099.12	7.131[4]	-1.405[5]
$2s2p^4 \ ^4P$	(90%)	$+ 2s2p^4 \ ^2D$	(10%)	5/2	-1754.6354142	1225343.66	2.910[5]	9.101[4]
	(81%)	$+ 2s2p^4 \ ^2D$	(11%)	3/2	-1753.6746587	1436205.13	1.058[5]	-9.322[4]
	(75%)	$+ 2s2p^4 \ ^2S$	(25%)	1/2	-1753.5915046	1454455.33	8.452[5]	0.0
$2s2p^4 \ ^2D$	(67%)	$+ 2s2p^4 \ ^4P$	(18%)	3/2	-1752.4214052	1711262.46	2.471[4]	-1.166[5]
	(90%)	$+ 2s2p^4 \ ^4P$	(10%)	5/2	-1752.0105758	1801429.09	3.570[5]	-2.141[5]
$2s2p^4 \ ^2P$	(41%)	$+ 2s2p^4 \ ^2S$	(41%)	1/2	-1751.3200272	1952987.00	2.533[5]	0.0
	(78%)	$+ 2s2p^4 \ ^2D$	(21%)	3/2	-1750.9594740	2032119.27	2.453[4]	6.144[4]
	(58%)	$+ 2s2p^4 \ ^2S$	(34%)	1/2	-1749.4631177	2360531.51	9.019[5]	0.0
$2p^5 \ ^2P^o$	(98%)	$+ 2s^2 2p^3 \ ^2P^o$	(1%)	3/2	-1746.2220466	3071864.37	6.074[4]	-1.207[5]
	(99%)	$+ 2s^2 2p^3 \ ^2P^o$	(1%)	1/2	-1744.5906993	3429903.71	3.730[5]	0.0
Br XXIX								
$2s^2 2p^3 \ ^4S^o$	(50%)	$+ 2s^2 2p^3 \ ^2P^o$	(33%)	3/2	-1871.2512225	0.00	5.162[4]	8.271[4]
$2s^2 2p^3 \ ^2D^o$	(55%)	$+ 2s^2 2p^3 \ ^4S^o$	(39%)	3/2	-1869.7070847	338899.07	2.156[4]	7.023[4]
	(100%)			5/2	-1869.2635338	436247.23	1.407[5]	-7.240[2]
$2s^2 2p^3 \ ^2P^o$	(99%)	$+ 2p^5 \ ^2P^o$	(1%)	1/2	-1868.6771056	564953.36	4.113[5]	0.0
	(59%)	$+ 2s^2 2p^3 \ ^2D^o$	(29%)	3/2	-1867.2002122	889093.97	7.829[4]	-1.541[5]
$2s2p^4 \ ^4P$	(89%)	$+ 2s2p^4 \ ^2D$	(11%)	5/2	-1865.3039913	1305266.35	3.212[5]	9.616[4]
	(77%)	$+ 2s2p^4 \ ^2D$	(14%)	3/2	-1864.2402661	1538727.05	8.459[4]	-1.003[5]
	(71%)	$+ 2s2p^4 \ ^2S$	(28%)	1/2	-1864.1729603	1553498.95	9.754[5]	0.0
$2s2p^4 \ ^2D$	(62%)	$+ 2s2p^4 \ ^4P$	(23%)	3/2	-1862.9202368	1828439.98	5.776[4]	-1.231[5]
	(89%)	$+ 2s2p^4 \ ^4P$	(11%)	5/2	-1862.4483300	1932011.54	3.946[5]	-2.317[5]
$2s2p^4 \ ^2P$	(43%)	$+ 2s2p^4 \ ^2S$	(37%)	1/2	-1861.7456241	2086237.65	2.017[5]	0.0
	(75%)	$+ 2s2p^4 \ ^2D$	(24%)	3/2	-1861.3687164	2168959.33	2.841[4]	6.000[4]
	(56%)	$+ 2s2p^4 \ ^2S$	(35%)	1/2	-1859.6664257	2542568.95	1.032[6]	0.0
$2p^5 \ ^2P^o$	(98%)	$+ 2s^2 2p^3 \ ^2P^o$	(1%)	3/2	-1856.4379861	3251129.52	6.697[4]	-1.330[5]
	(99%)	$+ 2s^2 2p^3 \ ^2P^o$	(1%)	1/2	-1854.5827297	3658311.22	4.128[5]	0.0
Kr XXX								
$2s^2 2p^3 \ ^4S^o$	(47%)	$+ 2s^2 2p^3 \ ^2P^o$	(35%)	3/2	-1985.8542911	0.00	5.948[4]	9.700[4]
$2s^2 2p^3 \ ^2D^o$	(53%)	$+ 2s^2 2p^3 \ ^4S^o$	(41%)	3/2	-1984.1007161	384865.22	2.036[4]	7.028[4]
	(100%)			5/2	-1983.6339451	487309.61	1.549[5]	-7.717[2]
$2s^2 2p^3 \ ^2P^o$	(99%)			1/2	-1983.0225237	621501.10	4.540[5]	0.0
	(59%)	$+ 2s^2 2p^3 \ ^2D^o$	(29%)	3/2	-1981.3183873	995515.79	8.569[4]	-1.685[5]
$2s2p^4 \ ^4P$	(88%)	$+ 2s2p^4 \ ^2D$	(12%)	5/2	-1979.5171106	1390850.31	3.536[5]	1.011[5]
	(71%)	$+ 2s2p^4 \ ^2D$	(17%)	3/2	-1978.3502903	1646937.77	5.633[4]	-1.069[5]
	(68%)	$+ 2s2p^4 \ ^2S$	(31%)	1/2	-1978.2998867	1658000.08	1.119[6]	0.0
$2s2p^4 \ ^2D$	(57%)	$+ 2s2p^4 \ ^4P$	(28%)	3/2	-1976.9412418	1956188.16	9.884[4]	-1.302[5]
	(88%)	$+ 2s2p^4 \ ^4P$	(12%)	5/2	-1976.4081218	2073194.48	4.350[5]	-2.499[5]
$2s2p^4 \ ^2P$	(45%)	$+ 2s2p^4 \ ^2S$	(33%)	1/2	-1975.6906122	2230669.62	1.403[5]	0.0
	(73%)	$+ 2s2p^4 \ ^2D$	(26%)	3/2	-1975.2991518	2316585.26	3.228[4]	5.770[4]
	(54%)	$+ 2s2p^4 \ ^2S$	(36%)	1/2	-1973.3693913	2740118.71	1.175[6]	0.0
$2p^5 \ ^2P^o$	(98%)	$+ 2s^2 2p^3 \ ^2P^o$	(1%)	3/2	-1970.1742211	3441377.49	7.361[4]	-1.462[5]
	(99%)	$+ 2s^2 2p^3 \ ^2P^o$	(1%)	1/2	-1968.0722776	3902700.75	4.556[5]	0.0
Mo XXXVI								
$2s^2 2p^3 \ ^2P^o$	(41%)	$+ 2s^2 2p^3 \ ^4S^o$	(36%)	3/2	-2749.7273173	0.00	1.154[5]	2.013[5]
$2s^2 2p^3 \ ^4S^o$	(50%)	$+ 2s^2 2p^3 \ ^2D^o$	(48%)	3/2	-2746.0988862	796348.57	1.169[4]	7.020[4]

Table 10 (continued)

Level composition in LSJ coupling			J	Energy (E_h)	ΔE cm $^{-1}$	$A_J(I/\mu_I)$	B_J/Q	g_J	
$2s^2 2p^3 \ ^2D^o$	(100%)		5/2	-2745.5180675	923823.52	2.628[5]	-1.099[3]	1.189031	
$2s^2 2p^3 \ ^2P^o$	(99%)		1/2	-2744.7460262	1093266.99	7.843[5]	0.0	0.652076	
	(55%)	+ $2s^2 2p^3 \ ^2D^o$	(29%)	3/2	-2741.1042042	1892554.51	1.397[5]	-2.730[5]	1.261933
$2s2p^4 \ ^4P$	(83%)	+ $2s2p^4 \ ^2D$	(17%)	5/2	-2740.4215834	2042372.47	6.031[5]	1.262[5]	1.519616
	(49%)	+ $2s2p^4 \ ^2S$	(47%)	1/2	-2738.7235517	2415047.34	2.260[6]	0.0	2.270806
$2s2p^4 \ ^2D$	(83%)	+ $2s2p^4 \ ^4P$	(17%)	5/2	-2735.2190483	3184196.90	7.451[5]	-3.739[5]	1.258679
$2s2p^4 \ ^2P$	(53%)	+ $2s2p^4 \ ^4P$	(32%)	1/2	-2734.3534636	3374170.78	-3.858[5]	0.0	1.502205
	(44%)	+ $2s2p^4 \ ^2S$	(38%)	1/2	-2730.0641923	4315556.98	2.294[6]	0.0	1.528728
$2p^5 \ ^2P^o$	(99%)	+ $2s^2 2p^3 \ ^2P^o$	(1%)	3/2	-2727.6045428	4855387.65	1.230[5]	-2.443[5]	1.323320
	(99%)	+ $2s^2 2p^3 \ ^2P^o$	(1%)	1/2	-2723.4503387	5767130.03	7.872[5]	0.0	0.652169
W LXVIII									
$2s^2 2p^3 \ ^2P^o$	(49%)	+ $2s^2 2p^3 \ ^2D^o$	(27%)	3/2	-9302.7182563	0.00	8.188[5]	1.608[6]	1.310614
$2s^2 2p^3 \ ^4S^o$	(55%)	+ $2s^2 2p^3 \ ^2D^o$	(45%)	3/2	-9251.0505799	11339743.90	-5.138[5]	7.739[4]	1.432771
$2s^2 2p^3 \ ^2D^o$	(100%)			5/2	-9249.8310483	11607400.14	2.181[6]	-2.932[3]	1.161525
$2s^2 2p^3 \ ^2P^o$	(100%)			1/2	-9248.3654393	11929064.12	7.574[6]	0.0	0.616487
$2s2p^4 \ ^2S$	(65%)	+ $2s2p^4 \ ^4P$	(25%)	1/2	-9235.2148740	14815279.51	2.371[7]	0.0	1.990465
$2s2p^4 \ ^2P$	(52%)	+ $2s2p^4 \ ^2D$	(35%)	3/2	-9234.9227026	14879403.72	-3.764[6]	-1.699[5]	1.168594
$2s^2 2p^3 \ ^2P^o$	(51%)	+ $2s^2 2p^3 \ ^2D^o$	(28%)	3/2	-9196.4732118	23318091.30	8.447[5]	-1.694[6]	1.286261
$2s2p^4 \ ^4P$	(85%)	+ $2s2p^4 \ ^2D$	(10%)	3/2	-9186.2604959	25559523.29	5.532[6]	-1.285[6]	1.585423
$2s2p^4 \ ^2P$	(65%)	+ $2s2p^4 \ ^4P$	(35%)	1/2	-9182.3586975	26415869.03	-9.024[6]	0.0	1.343751
$2s2p^4 \ ^2D$	(55%)	+ $2s2p^4 \ ^2P$	(44%)	3/2	-9181.8460915	26528373.04	4.627[4]	-5.312[5]	1.005084
$2p^5 \ ^2P^o$	(99%)			3/2	-9168.5689588	29442366.76	7.946[5]	-1.644[6]	1.297907
$2s2p^4 \ ^4P$	(40%)	+ $2s2p^4 \ ^2S$	(35%)	1/2	-9130.0438073	37897659.95	2.383[7]	0.0	1.877095
$2p^5 \ ^2P^o$	(100%)			1/2	-9115.7785445	41028523.14	7.613[6]	0.0	0.616544

Table 11

Hyperfine magnetic dipole constants $A_J(I/\mu_I)$ (MHz per unit of μ_N) and electric quadrupole constants B_J/Q (MHz/barn) in Ne IV. Comparison of values from RCI and MCHF calculations.

Level	RCI (this work)		MCHF (this work)	
	$A_J(I/\mu_I)$	B_J/Q	$A_J(I/\mu_I)$	B_J/Q
$2s^22p^3\ ^4S_{3/2}^o$	2.735[1]	-3.420[-2]	2.093[1]	0.0
$2s^22p^3\ ^2D_{5/2}^o$	1.501[3]	-4.492[1]	1.501[3]	-4.486[1]
	9.349[2]	1.083[2]	9.157[2]	-3.141[1]
$2s^22p^3\ ^2P_{1/2}^o$	4.222[3]	0.0	4.187[3]	0.0
	8.174[2]	-1.287[2]	8.195[2]	1.458[1]
$2s2p^4\ ^4P_{5/2}$	4.041[3]	1.400[3]	4.016[3]	1.330[3]
	3.973[3]	-1.116[3]	3.957[3]	-1.117[3]
	8.586[3]	0.0	8.532[3]	0.0
$2s2p^4\ ^2D_{5/2}$	4.668[3]	-2.886[3]	4.630[3]	-2.877[3]
	-1.627[3]	-2.021[3]	-1.598[3]	-2.014[3]
$2s2p^4\ ^2S_{1/2}$	1.721[4]	0.0	1.704[4]	0.0
$2s2p^4\ ^2P_{3/2}$	-9.208[2]	1.402[3]	-9.124[2]	1.392[3]
	2.678[3]	0.0	2.616[3]	0.0
$2p^5\ ^2P_{3/2}^o$	5.684[2]	-1.346[3]	5.680[2]	-1.342[3]
	4.237[3]	0.0	4.197[3]	0.0